HIGGS-PORTAL AND Z'-PORTAL DARK MATTERS IN BRANE-WORLD COSMOLOGIES

by

TAOLI LIU

NOBUCHIKA OKADA, COMMITTEE CHAIR
PAOLO RUMERIO
DEAN TOWNSLEY
RYAN WANG
DESMOND VILLALBA

A DISSERTATION

Submitted in partial fulfillment of the requirements
for the degree of Doctor of Philosophy
in the Department of Department of Physics and Astronomy
in the Graduate School of
The University of Alabama

TUSCALOOSA, ALABAMA

2023

ABSTRACT

According to various astrophysical and cosmological observations, Dark Matter (DM) accounts for approximately 27% of the Universe's total energy density. However, no viable DM particle candidate exists within the framework of the Standard Model (SM) of particle physics. An electrically neutral, weakly interacting massive particle (WIMP) from physics beyond the SM emerges as an appealing candidate for DM.

In this dissertation research, we consider the WIMP DM model within the framework of 5-dimensional brane-world cosmology. In this setup, our familiar 3-dimensional space is realized as a hyper-surface embedded in a 4-dimensional space. Within this context, all SM and DM fields are confined to the hyper-surface, while the graviton resides in the bulk. We explore two well-established brane-world cosmologies: the Randall-Sundrum (RS) and the Gauss-Bonnet (GB) brane-world cosmologies. These models reproduce the standard Big Bang cosmology (BBC) at temperatures below the so-called transition temperature T_t. However, at higher temperatures, they introduce significant modifications to the universe's expansion dynamics. This non-standard expansion law directly influences the predictions related to WIMP DM physics.

In our investigation, we consider two well-founded WIMP DM models: the Higgs-portal scalar DM model and the Z'-portal DM model. We analyze the effects of brane-world cosmologies and identify the allowed parameter space by incorporating constraints from the observed DM relic density, as well as data from direct and indirect DM detection experiments. It is worth noting that for both DM models, the allowed parameter regions are severely restricted within the conventional BBC framework.

Our findings reveal that these allowed parameter regions face even more stringent limitations in the RS cosmology, and in some cases, they may even disappear entirely. Conversely,

the GB cosmological effects significantly expand the regions of parameter space that are allowed. Furthermore, the discovery of Higgs-portal or Z'-portal DM within the GB brane-world cosmology would enable us to determine the transition temperature.

DEDICATION

I dedicate my dissertation work to two of my teachers, Mr. Liu, Baoyi, and Professor Nobuchika Okada. Mr. Liu taught us physics in middle school, he was the one who led me in my physics journey. Professor Nobuchika Okada, as my advisor, helped me to change from an amateur to a professional.

LIST OF ABBREVIATIONS AND SYMBOLS

BBC	Big Bang Cosmology
BBN	Big Bang Nucleosynthesis
CMB	Cosmic Microwave Background
C.O.M	Center-of-Mass
D	Dimensional
DM	Dark Matter
$D^i_\mu, D^{i\mu}$	Covariant derivative of particle i.
$\epsilon^\mu_\alpha, \epsilon_{\alpha\mu}$	Wave functions of bosons.
g_x	Number of degrees of freedom of particle x.
GB	Gauss-Bonnet
H_{st}	Hubble parameter in the standard Big Bang cosmology.
m_D	The mass of a DM particle.
n_x	Number density of particle x.
Ω_x	Density parameter of particle x, $\Omega_x = \rho_x/\rho_c$.
P_x	Pressure produced by particle x.
ρ_c	Critical density.
ρ_x	Energy density of particle x, $\Omega_x = \rho_x/\rho_c$.
RS	Randall-Sundrum
SM	Standard Model
T_t	Transition temperature
u_f, v_f	Wave functions of fermions.
VEV	Vacuum Expectation Value

WIMP	Weakly Interacting Massive Particle
X_0	The quantity X at present time.
X_B	The quantity X of Boson.
X_F	The quantity X of Fermion.
X_m	The quantity X at the dust (non-relativistic matter) dominated era.
X_R	The quantity X at the radiation dominated era.
X_{rad}	The quantity X in the radiation-dominated era.
x_t	$x_t = \frac{m_D}{T_t}$.
X_y^0	The quantity X_y at present.
X	The quantity X at the cosmological constant dominated era.

ACKNOWLEDGMENTS

First, I would like to thank my advisor professor Nobuchika Okada for his work. He is diligent at work, and part of his work is for me. He is always nice and patient, I appreciate that. His wife, Satomi Okada, also gave me a lot of help. Part of my thesis was checked, revised, and furbished by her. She also joined to help me with my preparation of the dissertation defense. I also want to show my appreciation to Digesh Raut, my classmate, and my friend, who helped so much in preparing the paper to publish and preparing for the defense.

Also, I appreciate my defense committee members' spending time on my work. Thank you, Dr. Rumerio, Dr. Townsley, Dr. Wang, and Dr. Villalba. And I want to show my sorrow for Dr. Harms, may he rest in peace.

I also appreciate the help from my friend Mahmud Ashraf Shamim, who gave me a lecture on some topics I felt puzzled.

CONTENTS

LIST OF TABLES

LIST OF FIGURES

CHAPTER 1

INTRODUCTION

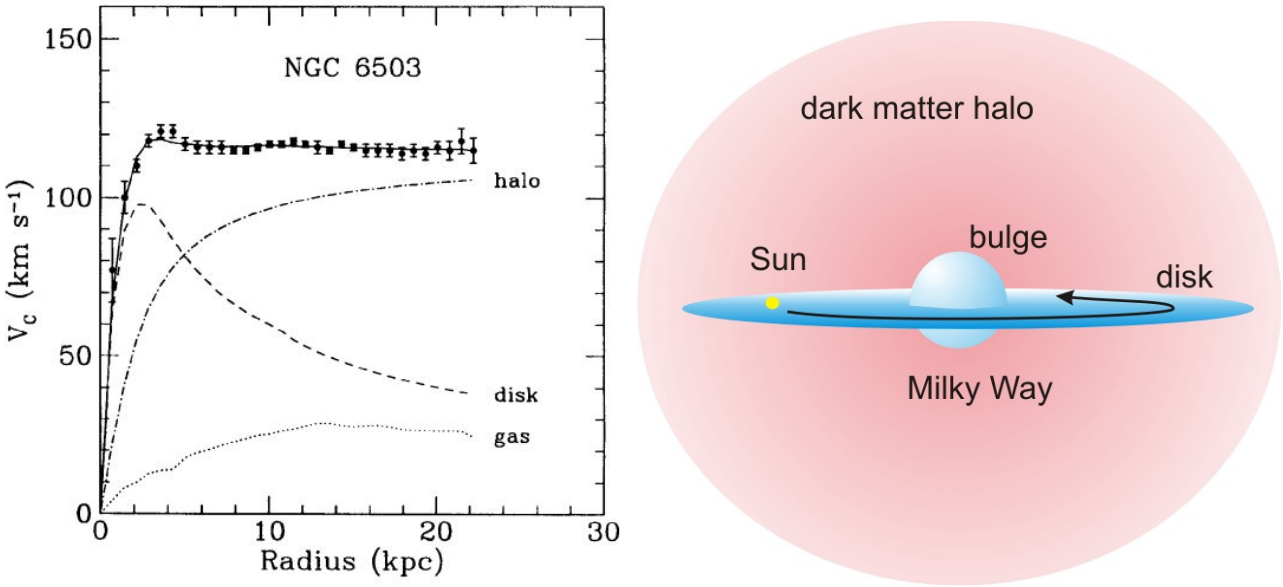

Figure 1.1: Galaxy rotation curve and DM halo

The notion of dark matter (DM) was first introduced to solve a problem as shown in Fig. 1.1 [1]. What people now find when they observe the disk galaxy is just the bulge and the disk, so a Sun should show a circular velocity, $v_c = \sqrt{\frac{GM(r)}{r}}$, with radius r to the center of the Milky Way and $M(r)$ the total mass enclosed in this radius. If this mass is concentrated in the galactic disk, then $M(r)$ should be constant for r larger than the radius of this disk. In this case, the circular velocity of the Sun should be $v_c \propto r^{-1/2}$. However, the observed velocity is almost constant, as shown in the top curve in the left panel. This suggests that $M(r) \propto r$. So that an

optically unobserved matter exists beyond the radius of the disk. This is named dark matter (DM).

In addition to the astronomical observations, the cosmological observations, in particular, precise measurements of the Cosmic Microwave Background (CMB) anisotropy by Planck 2018 [2], also support the DM existence in our universe, and now it is fixed that DM occupies about 26.8% of the energy density of our Universe. However, there is no suitable candidate for it in the standard model (SM) of particle physics. A hopeful and attractive candidate is the electrically neutral, weakly interacting massive particle (WIMP) from physics beyond the SM.

Among many WIMP DM models, one of the simplest models is the Higgs-portal scalar DM [3], in which an SM gauge-singlet scalar was added to the SM as the candidate for DM. A new Z_2 symmetry was also added to stabilize this DM candidate. This DM particle interacts with the SM particles through the Higgs boson, and only two parameters control this interaction: one is the mixed quartic coupling (λ) between the DM and the Higgs doublet, and the other is the DM mass (m_D). These two parameters are related by the constraint of the observed DM relic density, and λ is described as a function of m_D. Further constraints come from the outcomes of direct and indirect DM detection experiments. In particular, the direct DM detection experiments severely constrain the allowed range of m_D values.

Another simple DM model we consider here is the B L Z'-portal DM model [4, 5, 6, 7]. Here, "B L" means "Baryon number minus Lepton number," and a new $U(1)_{B-L}$ gauge symmetry and the corresponding B L gauge boson Z' are introduced. Along with them, three right-handed neutrinos, an SM-gauge singlet Higgs boson, and a Dirac fermion which is the DM candidate are also included in this model. By $U(1)_{B-L}$ symmetry breaking, the Z' boson gets its mass, while by $SU(2)$ $U(1)_Y$ and $U(1)_{B-L}$ symmetries breaking, neutrino masses are generated by the see-saw mechanism. In this model, the DM particle interacts with the SM particles through the Z' boson, and hence we call this model the Z'-portal DM model.

The above DM models have been studied in the standard BBC with three spatial dimensions. In this thesis, we study the two models in the context of the 5 dimensional brane-world cosmol-

ogy with 4 spatial dimensions. In this setup, the graviton resides in the whole 4 dimensional space ("bulk"), while the SM and DM particles are confined on the 3 dimensional hyper-surface ("3-brane") embedded in the 4 dimensional space. Two brane-world cosmologies are studied in this thesis, the Randall-Sundrum (RS) brane-world cosmology, based on the setup proposed in [8], and the Gauss-Bonnet cosmology [9]. They affected the evolution of the universe in the early times when the temperature was high. Then at the so-called transition temperature T_t, the evolution of the Universe approached to the one of the standard BBC. This process affects the form of the particles' interaction cross-section and the outcomes that we get from the standard Big Bang cosmology. We compare those different outcomes with each other and see what has changed and its implications to future experiments.

CHAPTER 2

BIG BANG COSMOLOGY (BBC) AND DARK MATTER (DM)

2.1 BBC: From Einstein's Equation to the Friedmann Equation

2.1.1 Robertson-Walker (RW) Metric and Einstein's Equation

Our universe is seen as spatially homogeneous and isotropic and continues to expand. This scene is embodied in the maximally-symmetric Robertson-Walker (RW) metric,

$$\mathrm{d}s^2 = \mathrm{d}t^2 \quad a(t)^2 \left(\frac{\mathrm{d}r^2}{1 \quad kr^2} + r^2 \mathrm{d}\theta^2 + r^2 \sin^2\theta d\phi^2 \right). \tag{2.1}$$

Here, $a(t)$ is the cosmic scale factor, and with an appropriate rescaling of the coordinates, k, the spatial curvature, can be chosen as 0, +1, or 1. For example, for one spatial dimension, since $\mathrm{d}l^2 = \frac{1}{1-kx^2}\mathrm{d}x^2$, for $k = 0$, $\mathrm{d}l^2 = \mathrm{d}x^2$, which shows a flat universe; for $k = +1$, $\mathrm{d}l^2 = \frac{\mathrm{d}x}{1-x^2}$, so 0 $x < 1$, which shows a closed universe; while for $k =$ 1, $\mathrm{d}l^2 = \frac{\mathrm{d}x}{1+x^2}$, which shows an open universe. The dynamics of the expanding Universe is shown in the time dependence of the scale factor $a(t)$, which is determined by Einstein's equation in the General Theory of Relativity (GR):

$$R_{\mu\nu} \quad \frac{1}{2} g_{\mu\nu} R = \frac{1}{M_p^2} T_{\mu\nu}. \tag{2.2}$$

Here, $g_{\mu\nu}(x)$ is the metric tensor. In GR, the scalar product of two vectors A_μ and B_μ is defined as $A \quad B \quad g_{\mu\nu} A^\mu B^\nu$. $R_{\mu\nu}$ and R are related to $g_{\mu\nu}$ through the Christoffel symbol Γ, which is defined as $\Gamma_{\alpha\mu\nu} = \frac{1}{2}(g_{\alpha\mu,\nu} + g_{\alpha\nu,\mu} \quad g_{\mu\nu,\alpha})$, where $g_{\mu\nu,\alpha} = \partial g_{\mu\nu}/\partial x^\alpha$. And then, the Riemann tensor is defined as $R^\alpha_{\mu\nu\rho} = \Gamma^\alpha_{\mu\rho,\nu} \quad \Gamma^\alpha_{\mu\nu,\rho} + \Gamma^\beta_{\nu\rho}\Gamma^\alpha_{\beta\nu} \quad \Gamma^\beta_{\mu\nu}\Gamma^\alpha_{\beta\rho}$. Here, "$,\mu$" etc. in the subscripts

mean the derivative with respect to x^μ, and $\Gamma^\alpha_{\mu\nu} = g^{\alpha\beta}\Gamma_{\beta\mu\nu}$. Then we have the Ricci tensor $R_{\mu\nu} = R^\alpha_{\mu\alpha\nu} = g^{\alpha\beta}R_{\beta\mu\alpha\nu}$ and the scalar curvature $R = g^{\mu\nu}R_{\mu\nu}$. $T_{\mu\nu}$ is the energy-momentum tensor of the universe, which is defined from the matter action $S_{matt} = \int d^4x \sqrt{-g}\mathscr{L}_m$, with $g = |g^{\mu\nu}|$, as $\frac{1}{2}\sqrt{-g}T_{\mu\nu} = \frac{\partial(\sqrt{-g}\mathscr{L}_m)}{\partial g^{\mu\nu}} \quad \partial_\rho(\frac{\partial(\sqrt{-g}\mathscr{L}_m)}{\partial g^{\mu\nu}_{,\rho}})$. In addition, $M_p = 2.44 \quad 10^{18}$ GeV is the reduced Planck mass. Einstein's equation shows that the left-hand side of Eq. (2.2) is from the curvature of space-time, or the structure of the universe, while the right-hand side is the source of gravitation from matter.

2.1.2 Solving the Einstein's Equation with RW Metric

For simplicity, we first consider the flat universe ($k = 0$). First, we have

$$\begin{cases} g_{\mu\nu} = diag(1, \quad a(t), \quad a(t), \quad a(t)), \\ g^{\mu\nu} = diag(1, \quad 1/a(t), \quad 1/a(t), \quad 1/a(t)). \end{cases} \tag{2.3}$$

Based on it, non-vanishing components of the Riemann tensor are

$$\begin{cases} R_{00} \quad \frac{1}{2}g_{00}R = 3\left(\frac{\dot{a}}{a}\right)^2, \\ R_{ij} \quad \frac{1}{2}g_{ij}R = (\quad \dot{a}^2 \quad 2a\ddot{a})\delta_{ij}. \end{cases} \tag{2.4}$$

Here, $\dot{a} = \frac{da}{dt}$, and $\ddot{a} = \frac{d^2a}{dt^2}$. For $k \neq 0$, there is

$$\begin{cases} R_{00} \quad \frac{1}{2}g_{00}R = 3\left(\frac{\dot{a}}{a}\right)^2 + 3\frac{k}{a^2}, \\ R_{ij} \quad \frac{1}{2}g_{ij}R = (\quad \dot{a}^2 \quad 2a\ddot{a} \quad k)\delta_{ij}. \end{cases} \tag{2.5}$$

These provide the left-hand side of Einstein's equation.

As for the right-hand side of Einstein's equation, since the universe is homogeneous and isotropic, $T_{\mu\nu}$ must be diagonal. The simplest example of such an energy-momentum tensor is the one gotten by taking the perfect fluid approximation, for $k = 0$, $T^{\mu\nu} = diag(\rho,\ P/a^2,\ P/a^2,\ P/a^2)$,

and $T_{\mu\nu} = g_{\mu\rho}g_{\nu\sigma}T^{\rho\sigma} = diag(\rho,\ a^2P,\ a^2P,\ a^2P)$, with ρ the energy density and P the pressure. Then Einstein's equation becomes

$$\begin{cases} (0,0) \text{ component:} & \left(\frac{\dot{a}}{a}\right)^2 \quad H^2 = \frac{\rho}{3M_p^2}, & (2.6) \\ (i,j) \text{ component:} & 2\left(\frac{\ddot{a}}{a}\right) + \left(\frac{\dot{a}}{a}\right)^2 = \quad \frac{1}{M_p^2}P. & (2.7) \end{cases}$$

Here, eq. (2.6), the Friedmann equation defined the Hubble parameter, H, which represents the expanding rate of the universe. Combining eqs. (2.6) and (2.7), we get a new equation

$$\dot{\rho} + 3H(\rho + P) = 0. \tag{2.8}$$

So, now Einstein's equation is described by eqs. (2.6) and (2.8). In addition, we can find that eq. (2.8) corresponds to the first law of thermodynamics. Since ρ represents the energy density and the volume of the universe $V \propto a^3$, we have $\mathrm{d}E + P\mathrm{d}V = 0 \Rightarrow \mathrm{d}(\rho V) + P\mathrm{d}V = 0 \Rightarrow (\mathrm{d}\rho)V + (\rho + P)\mathrm{d}V = 0 \Rightarrow \frac{\mathrm{d}\rho}{\mathrm{d}t} + (\rho + P)\frac{\mathrm{d}V/\mathrm{d}t}{V} = 0 \Rightarrow \dot{\rho} + 3H(\rho + P) = 0$. Therefore, eq. (2.8) represents energy conservation. In addition, from the fundamental thermodynamic equation $\mathrm{d}E = T\mathrm{d}S \quad P\mathrm{d}V$, we have $\mathrm{d}S = 0$, that is,

$$S = const. \tag{2.9}$$

Eqs. (2.6) (the Friedmann equation), (2.8) (Energy conservation), and (2.9) (Adiabatic evolution of the universe) provide the basis in cosmology for our study here.

2.1.3 Big Bang Solution

By introducing a simple relation $P = w\rho$ with a constant w, eq. (2.8) leads to

$$\rho(t) \propto [a(t)]^{-3(1+w)}. \tag{2.10}$$

Some interesting examples include $w = 1/3,\ 0,$ and $\quad 1$

$$\begin{cases} (i) \text{ Radiation} & w = 1/3 \quad) \quad \rho \ / \ a^{-4}, \qquad (2.11) \\ (ii) \text{ Dust (Non-relativistic matter)} & w = 0 \quad) \quad \rho \ / \ a^{-3}, \qquad (2.12) \\ (iii) \text{ Cosmological Costant} & w = \quad 1 \quad) \quad \rho = \rho_{cc} = \text{constant}. \qquad (2.13) \end{cases}$$

From thermodynamics, we have that the energy density of a box containing radiation is proportional to T^4 (eq. (2.42)), and $T \ / \ a^{-1}$ (eq. (2.41)). Therefore, for radiation, the energy density $\rho \ / \ a^{-4}$, which is eq. (2.11). As for the dust case, it is easy to understand that the mass density, hence the energy density (since $v \quad c$) has the relation of eq. (2.12). In eq. (2.13), the cosmological constant corresponds to the dark energy.

2.1.4 Evolution of the Universe

Providing $a \ / \ t^{\alpha}$, then for the radiation and dust cases, α is fixed. For the cosmological constant case, $H^2 = H_{cc}^2 = \frac{\rho_{cc}}{3M_p^2}$ is a constant, $a(t)$ is an exponential function of time. The outcomes are

$$\begin{cases} (i) \text{ Radiation} & a \ / \ t^{1/2}, \\ (ii) \text{ Dust (Non-relativistic matter)} & a \ / \ t^{2/3}, \\ (iii) \text{ Cosmological Costant} & a \ / \ \mathrm{e}^{H_{cc}t}. \end{cases} \qquad (2.14)$$

The cosmic scale factor is a function of time.

2.1.5 Critical Density and Density Parameter

In general case, $k \neq 0$, the Friedmann equation is

$$H^2 + \frac{k}{a^2} = \frac{\rho}{3M_p^2}. \qquad (2.15)$$

Next, we define the critical density as

$$\rho_c \quad 3M_p^2 H^2, \qquad (2.16)$$

which is just the Friedmann equation with $k = 0$. We also define the density parameter of particle x as

$$\Omega_x \quad \frac{\rho_x}{\rho_c}, \tag{2.17}$$

where ρ_x is the energy density of this kind of particle. Hence, the Friedmann equation is rewritten as

$$\Omega_{tot} \quad 1 = \frac{k}{H^2 a^2}, \tag{2.18}$$

or equivalently,

$$\Omega_R + \Omega_m + \Omega \quad + \Omega_k = 1, \tag{2.19}$$

where $\rho_{tot} = \rho_R + \rho_m + \rho$ and $\Omega_{tot} = \rho_{tot}/\rho_c$, with the energy densities of radiation (ρ_R), matter (ρ_m) and cosmological constant (ρ), and Ω_k $\frac{k}{H^2 a^2}$.

We use sub-script or sup-script 0 to represent a quantity that is at present. For example, Ω_x^0 is the density parameter of particle x at present, a_0 is the scale factor at present, H_0 is the Hubble parameter at present (the so-called Hubble constant), and ρ_c^0 is the critical density at present. Then we have

$$\Omega_x(t) = \Omega_x^0 \left(\frac{a_0}{a(t)}\right)^{3(1+w_x)} \left(\frac{H_0}{H(t)}\right)^2, \tag{2.20}$$

where $H_0 = 100 h_0 \ km \ s^{-1} Mpc^{-1}$, with $h_0 \ ' \ 0.68$, $pc(parsec) \ ' \ 3.086 \quad 10^{16} \ m$ and $\rho_c^0 = 1.05 \quad 10^{-5} h_0^2 \ GeV/cm^3$.

Now Planck 2018 result [2] has set the energy budget of the Universe as

$$\begin{cases} \Omega_R^0 = \frac{\rho_{rad}^0}{\rho_c^0} = \Omega_\gamma^0 \ ' \ 4.8 \quad 10^{-5}, & (2.21) \\ \Omega_m^0 = \frac{\rho_m}{\rho_c^0} = \Omega_{DM}^0 + \Omega_b^0 \ ' \ 0.32, & (2.22) \\ \Omega^0 = \frac{\rho_\lambda^0}{\rho_c^0} \ ' \ 0.68. & (2.23) \end{cases}$$

In them, eq. (2.21) means that now the radiation is composed mainly of photons, so we just consider Ω_γ. In eq. (2.22), we decompose ρ_m as $\rho_m = \rho_{DM} + \rho_b$ with the energy density of dark matter (ρ_{DM}) and baryon (ρ_b), since matter includes both of them. Because the universe

is flat, we have $\Omega_{tot}^0 = 1$, that is, $k = 0$ for eq. (2.19) . Then by eqs. (2.21), (2.22) and (2.23), the explicit form of eq. (2.20) is

$$\begin{cases} \Omega_R = \Omega_R^0 \left(\frac{a_0}{a(t)}\right)^4 \left(\frac{H_0}{H(t)}\right)^2 & (w = 1/3), \quad (2.24) \\ \Omega_m = \Omega_m^0 \left(\frac{a_0}{a(t)}\right)^3 \left(\frac{H_0}{H(t)}\right)^2 & (w = 0), \quad (2.25) \\ \Omega \ = \Omega^0 \left(\frac{H_0}{H(t)}\right)^2 & (w = \ \ 1). \quad (2.26) \end{cases}$$

Now we can express the Hubble parameter as a function of energy densities by the deformation of the Friedmann equation. In order to do this, we need an expression of the energy density as a function of some familiar quantities, this process is from the quantum statistics.

2.2 Quantum Statistical Mechanics

2.2.1 Number Density, Energy Density and Pressure

Quantum statistical mechanics starts from the phase space distribution function,

$$f(\vec{p}) = \frac{1}{\mathrm{e}^{\frac{E-\mu}{T}} \quad 1}. \tag{2.27}$$

Here $\ 1$ corresponds to Fermi-Dirac and Bose-Einstein statistics, respectively, and μ is the chemical potential. With the phase space distribution function, we can calculate the number density, energy density, and pressure of a thermal equilibrium state.

For the number density,

$$n_x = \frac{g_x}{(2\pi)^3} \int \mathrm{d}^3p \ f(\vec{p}), \tag{2.28}$$

where g_x is the number of degrees of freedom of a particle x. For example, for a photon, $g_x = 2$, for Dirac fermion, $g_x = 4$, while for a real scalar particle, $g_x = 1$.

For the energy density, we have

$$\rho_x = \frac{g_x}{(2\pi)^3} \int \mathrm{d}^3p \ E(\vec{p}) f(\vec{p}), \tag{2.29}$$

with $E(\vec{p})^2 = m^2 + \vec{p}^2$.

As for pressure,

$$P_x = \frac{g_x}{(2\pi)^3} \int \mathrm{d}^3 p \, \frac{|\vec{p}|^2}{3E} f(\vec{p}), \tag{2.30}$$

where P_x is the pressure and is expressed as a function of momentum $\vec{p}$ and energy E, which is derived from the kinetic theory of gases, as shown in Fig. 2.1. Here, consider a box of gas, suppose there are N particles hit on a surface in time Δt, and they generate a pressure P_x. Each particle has momentum p_x and therefore generates a force F_x by the hitting.

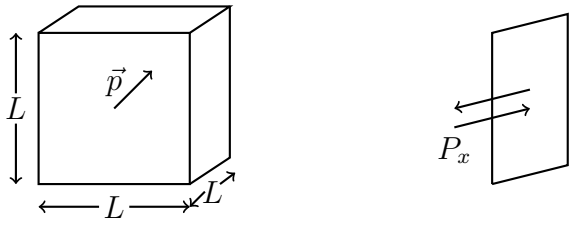

Figure 2.1: Kinetic theory of gases

First, there is a common relation between a particle's momentum $\vec{p}$, energy E, and velocity $\vec{v}$. Consider a 4-velocity $u^\mu = \mathrm{d}x^\mu/\mathrm{d}s$, with $\mathrm{d}s^2 = \eta_{\mu\nu}\mathrm{d}x^\mu \mathrm{d}x^\nu$. In non-relativistic limit, $\mathrm{d}s \simeq \mathrm{d}x^0$, so $u^0 = \mathrm{d}x^0/\mathrm{d}s \simeq 1$ and $\vec{u} = \mathrm{d}\vec{x}/\mathrm{d}s \simeq \mathrm{d}\vec{x}/\mathrm{d}t$. Therefore, $E = mu^0 \approx m$ and $\vec{p} = m\vec{u} \approx m\vec{v}$. Hence, in the non-relativistic limit,

$$\vec{v} = \frac{\mathrm{d}\vec{x}}{\mathrm{d}t} = \frac{\mathrm{d}\vec{x}/\mathrm{d}s}{\mathrm{d}x^0/\mathrm{d}s} = \frac{\vec{u}}{u^0} = \frac{\vec{p}}{E}. \tag{2.31}$$

Then we have $F_x \Delta t = \Delta p_x = 2p_x$, and $\Delta t = \frac{2L}{v_x} = \frac{2L}{(p_x/E)}$. Therefore, the pressure P_x is

$$P_x = \frac{F_x}{L^2} \quad N = \frac{N}{L^2} \quad \frac{2p_x}{\Delta t} = \frac{N}{L^2} \quad 2p_x \quad \frac{1}{2L}(\frac{p_x}{E}) = \frac{N}{V}\frac{p_x^2}{E} = n\frac{|\vec{p}|^2}{3E}. \tag{2.32}$$

By the use of $|\vec{p}|^2 = p_x^2 + p_y^2 + p_z^2 = 3p_x^2$, we get eq. (2.30).

Since $\mathrm{d}^3 p = p^2 \mathrm{d}p \mathrm{d}\Omega$, it gives $4\pi p^2 \mathrm{d}p$ by integrating over $\mathrm{d}\Omega$. By using the relation, $E^2 =$

$p^2 + m^2 \;\; ! \;\; 2E\mathrm{d}E = 2p\mathrm{d}p$, $p^2\mathrm{d}p = pE\mathrm{d}E = \;\; p\overline{E^2 \quad m^2}E\mathrm{d}E$, and hence

$$\begin{cases} n_x = \frac{g_x}{2\pi^2}\int_m^\infty \frac{\sqrt{E^2-m^2}}{e^{\frac{E-\mu}{T}}\pm 1}EdE, \\ \rho_x = \frac{g_x}{2\pi^2}\int_m^\infty \frac{\sqrt{E^2-m^2}}{e^{\frac{E-\mu}{T}}\pm 1}E^2dE, \\ P_x = \frac{g_x}{6\pi^2}\int_m^\infty \frac{(E^2-m^2)^{3/2}}{e^{\frac{E-\mu}{T}}\pm 1}dE. \end{cases} \tag{2.33}$$

2.2.2 Relativistic and Non-Relativistic limits

Relativistic Limit ($T \quad m$)

In the early Universe, T is very high, that is, $T \quad m$ and $T \quad \mu$. In this limit, we neglect μ, the chemical potential. For the number density, we find the following approximation formulas:

$$n_x = \begin{cases} \frac{\xi(3)}{\pi^2}g_xT^3 \qquad \text{(Bose)}, \\ \frac{3}{4}\frac{\xi(3)}{\pi^2}g_xT^3 \qquad \text{(Fermi)}, \end{cases} \tag{2.34}$$

where $\xi(3) = \frac{1}{2}\int_0^\infty \frac{x^2}{e^x-1} \;\; ' \;\; 1.20206$ is the Riemann zeta function.

The energy density is approximately given by

$$\rho_x = \begin{cases} \frac{\pi^2}{30}g_xT^4 \qquad \text{(Bose)}, \\ \frac{7}{8}\frac{\pi^2}{30}g_xT^4 \qquad \text{(Fermi)}. \end{cases} \tag{2.35}$$

As for the pressure,

$$P_x = \frac{1}{3}\rho_x, \tag{2.36}$$

which is the Stefan-Boltzmann law. In addition, we have the average energy per particle,

$$hEi = \frac{\rho}{n} = \begin{cases} \frac{pi^4}{30\xi(3)}T \;\; ' \;\; 2.07T \qquad \text{(Bose)}, \\ \frac{7\pi^4}{180\xi(3)} \;\; ' \;\; 3.115T \qquad \text{(Fermi)}. \end{cases} \tag{2.37}$$

Non-Relativistic Limit ($m \quad T$)

In this case, we have

$$\begin{cases} n_x = g_x(\frac{mT}{2\pi})^{3/2}\mathrm{e}^{-m/T}, \\ \rho_x = m_x n_x, \\ P_x = n_x T. \end{cases} \tag{2.38}$$

2.2.3 Entropy Conservation and Adiabatic Expansion of Universe

In thermodynamics, $S = \frac{(\rho+P)V}{T}$ with S the total entropy, and then the entropy density is

$$s = S/V = \frac{\rho + P}{T} = \frac{2\pi^2}{45} g_* T^3, \tag{2.39}$$

where

$$g_* = \sum_i g_B^i + \frac{7}{8}\sum_i g_F^i \tag{2.40}$$

is the total degree of freedom. In it, g_B is the degree of freedom of bosons, g_F is the degree of freedom of fermions, and the coefficient of $\frac{7}{8}$ is from statistical dynamics, see eq. (2.35). When all the SM particles are relativistic, $g_* = 106.75$.

Because the total entropy is conserved, that is, $S = sV \ / \ sa^3 = const.$, there is

$$T^3 a^3 = const. \ ) \ T \ / \ a^{-1}. \tag{2.41}$$

Then, in the radiation-dominated era,

$$\rho_{rad} = \frac{\pi^2}{30} g_* T^4. \tag{2.42}$$

In order to study the decoupling of the DM in the early Universe, where the Universe was in

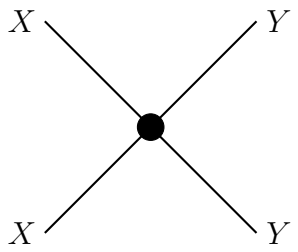

Figure 2.2: Particles X/Y annihilate and create particles Y/X.

the radiation-dominated era, we take $\rho_{tot} = \rho_{rad}$, and the Friedmann equation (2.6) is

$$H^2 = \frac{\rho_{rad}}{3M_p^2} = \frac{1}{3M_p^2}(\frac{\pi^2}{30}g_*T^4) \quad) \quad H \quad ' \quad 0.33 \quad p\overline{g_*}\frac{T^2}{M_p}. \tag{2.43}$$

2.3 Decoupling (Freeze-out)

2.3.1 The Process of Decoupling

In the early universe, ρ and T were very high, so all particles were in thermal equilibrium (chemical equilibrium). However, according to the expansion of the universe, both ρ and T went down and some particles started to decouple from the equilibrium system. This process is called "decoupling" or "freeze-out". The Boltzmann equation describes the number density of a particle during this process.

The chemical equilibrium between particles X and Y is a process shown as (see Fig. 2.2)

$$X\bar{X} \quad (\quad) \quad Y\bar{Y}, \tag{2.44}$$

which means particles X annihilate with each other to create particles Y and vice versa, and the two inverse processes have the same annihilation/creation rates, and therefore the number of each kind of particle remains the same. However, due to the expansion of the Universe, the number densities of both particles decreased, and accordingly, the annihilation rate of those particles also decreased until at last $X(Y)$ can not annihilate into $Y(X)$. This process is called decoupling.

Let us derive the condition at which decoupling happens. For the process of annihilation, the annihilation rate is $\Gamma_x = n_x \langle \sigma v_{rel} \rangle$, where n_x is the number density of particle X, σ is the annihilation cross section between particle X and its anti-particle $\bar{X}$, v_{rel} is the relative velocity between particles X and $\bar{X}$, and $\langle \sigma v_{rel} \rangle$ is the thermal average of σv_{rel}. Once the DM mode is specified, σ is calculated as we will discuss later.

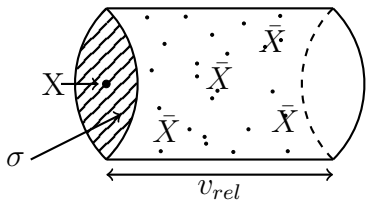

Figure 2.3: Annihilation Cross Section

As shown in Fig. 2.3, the possibility of a particle X to annihilate with its anti-particle $\bar{X}$ per unit time equals the number of particle $\bar{X}$ in a volume with bottom σ and length v_{rel}. So, for a time period t, the number of annihilation that happens to X is $\Gamma_x t$. If $\Gamma_x t \quad 1$, decoupling happens. Since $a(t) \ / \ t^{\frac{1}{2}}$ in the radiation dominated era, we have $H = \frac{\dot{a}}{a} = \frac{1}{2t}$, so the decoupling happens when $\frac{1}{t} \quad H$. Therefore,

$$\begin{cases} \Gamma_x > H, \ X \text{ is in thermal equilibrium,} \\ \Gamma_x = H, \ X \text{ is decoupling,} \\ \Gamma_x < H, \ X \text{ has decoupled.} \end{cases} \tag{2.45}$$

The (photon) temperature of the Universe when the X particle decouples is called "decoupling temperature" (T_D). After the decoupling, the total number of X particles in the Universe is fixed and remains the same if it is stable (DM). The number density of X particle at present is more precisely determined by the Boltzmann equation, that we will discuss in the next subsection.

2.3.2 Thermal Relics (Cold DM Physics) and Boltzmann Equation

A WIMP DM particle X with mass m should decouple from the thermal system in a non-relativistic regime T_D m. To estimate the DM relic density, we need to know $\mathrm{d}N_x/\mathrm{d}t$, where $N_x(t)$ is the total number of particle X. As we discussed, this process is expressed by the Boltzmann equation, and so the resultant $N(t)$ is determined by solving this equation.

The Original Form of Boltzmann Equation

The number of particles X in the Universe changes in time because of its annihilation and creation processes, which can be expressed as

$$\frac{\mathrm{d}N_x}{\mathrm{d}t} = V\Lambda_x \quad \Gamma_x N_x, \tag{2.46}$$

where V is the volume of universe, Λ_x is the creation rate of particle X, and Γ_x is the annihilation rate of particle X.

When X is in equilibrium, the creation process is equivalent to the annihilation process:

$$\begin{aligned} V\Lambda_x \quad \Gamma_x^{eq} N_x^{eq} &= 0 \ \big) \\ \Lambda_x = \Gamma_x^{eq}\tfrac{N_x^{eq}}{V} &= \Gamma_x^{eq} n_x^{eq} = (n_x^{eq})^2 \langle \sigma v_{rel} \rangle . \end{aligned} \tag{2.47}$$

Therefore,

$$\begin{aligned} \tfrac{\mathrm{d}N_x}{\mathrm{d}t} &= \tfrac{\mathrm{d}}{\mathrm{d}t}(n_x V) = \tfrac{\mathrm{d}n_x}{\mathrm{d}t} V + n_x \tfrac{\mathrm{d}V}{\mathrm{d}t} \\ &= (n_x^{eq})^2 \langle \sigma v_{rel} \rangle V \quad n_x \langle \sigma v_{rel} \rangle (n_x V) \ \big) \\ \tfrac{\mathrm{d}n_x}{\mathrm{d}t} + \tfrac{(\mathrm{d}V/\mathrm{d}t)}{V} n_x &= \quad \langle \sigma v_{rel} \rangle (n_x^2 \quad (n_x^{eq})^2) \end{aligned} \tag{2.48}$$

Since we know that $V \propto a^3$, $\frac{dV/dt}{V} = 3H$ and we get the Boltzmann equation as

$$\frac{\mathrm{d}n_x}{\mathrm{d}t} + 3Hn_x = \quad \langle \sigma v_{rel} \rangle (n_x^2 \quad (n_x^{eq})^2), \tag{2.49}$$

with H from eq. (2.43). By finding out the σ from a DM model and solving the Boltzmann

equation we can get n_x.

More Convenient Form of Boltzmann Equation

We introduce two new parameters

$$\begin{cases} Y_x & \frac{n_x}{s} = \frac{n_x V}{sV} = \frac{N_x}{S}, \\ x & \frac{m}{T}. \end{cases} \tag{2.50}$$

Here, Y_x is the yield of particle X, V is the total volume of the Universe, N_x is the total number of particles X, and S is the entropy of the Universe, which is a constant, so Y_x / N_x. In terms of these two parameters, the Boltzmann equation is expressed as

$$\frac{\mathrm{d}Y_x}{\mathrm{d}x} = \frac{s(x)\langle\sigma v_{rel}\rangle}{H(x)x}(Y_x^2 \quad (Y_x^{eq})^2). \tag{2.51}$$

From the view of the BBC, in the early times, our Universe had a very high temperature and expanded very quickly. During this process, the temperature continued to decrease. At first, different particles were in thermal equilibrium. This process is expressed in eq. (2.44) and in Fig. 2.2. But when the Universe expanded, the temperature decreased, and the energy density decreased, the thermal equilibrium of X can no longer keep the balance, that is, the $( )$ started to become $=)$ in eq. (2.44). This process is called decoupling or freezing-out and the temperature at which decoupling happens is defined as the decoupling temperature, T_D.

Decoupling

We now show how particle X decouples from the thermal equilibrium by solving the Boltzmann equation. We suppose that the particle X decouples when it becomes non-relativistic ($x > 1$). For simplicity, we parameterize the annihilation cross-section as

$$\langle\sigma v_{rel}\rangle = \sigma_n x^{-n}, \tag{2.52}$$

where $n = 0, 1,$, then we have

$$\frac{dY_X}{dx} = \frac{\lambda_n}{x^{n+2}}(Y_X^2 \quad (Y_X^{eq})^2), \tag{2.53}$$

with

$$\lambda_n = \frac{s(m_x)}{H(m_x)}\sigma_n. \tag{2.54}$$

In the following, we solve this equation semi-analytically.

When decoupling starts, we parameterize

$$Y_X = Y_X^{eq} + \Delta, \ \Delta \quad Y_X^{eq}. \tag{2.55}$$

Since Y_X^{eq} / e^{-x} for $x > 1$, the left-hand side is roughly

$$\frac{dY_X}{dx} = \frac{d(Y_X^{eq} + \Delta)}{dx} \ , \ \frac{dY_X^{eq}}{dx} \ , \quad Y_X^{eq} \ ) \ \frac{dY_X^{eq}}{dx} \qquad Y_X^{eq}. \tag{2.56}$$

And the right-hand side gives

$$\frac{\lambda_n}{x^{n+2}}(Y_X^2 \quad (Y_X^{eq})^2) \ , \quad 2\frac{\lambda_n}{x^{n+2}}Y_X^{eq}\Delta. \tag{2.57}$$

Therefore, there is

$$\Delta \ , \ \frac{x^{n+2}}{2\lambda_n}. \tag{2.58}$$

This means when x increases, or T decreases, Δ increases accordingly. So, when a small deviation is generated, it grows quickly.

We define the decoupling by the condition $\Delta(x_D) \ , \ Y_X^{eq}(x_D)$, where $x_D = m_x/T_D$, so that

$$Y_X^{eq} \ , \ \frac{x_D^{n+2}}{2\lambda_n}. \tag{2.59}$$

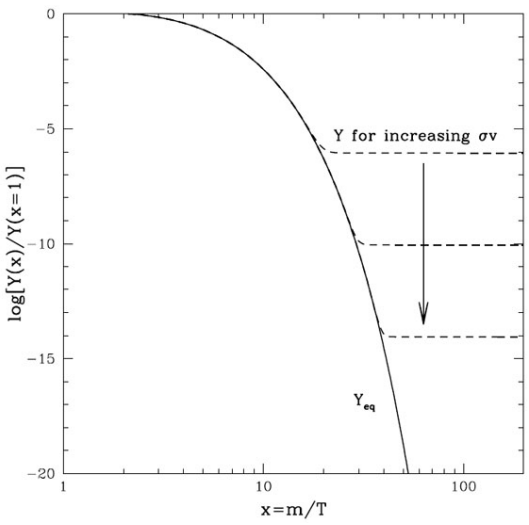

Figure 2.4: Numerical solutions to the Boltzmann equation for different cross-sections σs (dashed lines), along with Y_X^{eq} (solid line).

At last, when $\Delta(x)$ $Y_X^{eq}(x)$, we approximate the Boltzmann equation as

$$\frac{d\Delta}{dx} \quad \frac{\lambda_n}{x^{n+2}}\Delta^2. \tag{2.60}$$

By integrating it, we find for x 1

$$\Delta(x \quad 1) \quad \frac{(n+1)x_D^{n+1}}{\lambda_n}, \tag{2.61}$$

which is a constant. In addition, we can see that since λ_n σ_n, when σ_n increases, Δ will decrease.

Numerical solutions to the Boltzmann equation for different cross sections are shown in Fig. 2.4. Here, the solid line is the yield at thermal equilibrium, while the dotted lines show the yield Y after decoupling for different σs. As the annihilation cross section becomes larger, the resultant yield becomes lower. Note that these three lines become almost constant quickly after decoupling.

DM Relic Density

For DM X, its energy density in the present Universe is given by

$$\rho_x^0 = m_x n_x^0 = m_x Y_x(x \;!\; 1)s_0, \tag{2.62}$$

where $s_0 = 2890$ cm^{-3} is the entropy density of the present universe. Since $x = m/T$, we approximate $x \;!\; 1$ for the present Universe. The DM relic density is defined as

$$\Omega_x h^2 = \frac{\rho_x^0}{\rho_c^0} h^2, \tag{2.63}$$

where $\rho_c^0/h^2 = 1.05 \quad 10^{-5}$ GeV cm^{-3}.

CHAPTER 3

5-DIMENSIONAL COSMOLOGIES

The real world is 4 dimensional, which includes 3 space dimensions and 1 time dimension. However, for a long time, researchers started to study the possibility of higher-dimensional ($(4+N)$ dimensional) world models, and one of this endeavor's aims is to solve the hierarchy problem. What we discussed in the last chapter should have a new view in a higher-dimensional world. We will study it in two 5 dimensional models, the Randall-Sundrum (RS) model ([10, 11, 12, 13, 14]), and the Gauss-Bonnet (GB) model ([15, 16, 17, 18, 19]). One additional space dimension is added in these modes, and our 3 dimensional space is realized as a brane (hyper-surface) embedded into 4-dimensional space.

3.1 Randall-Sundrum (RS) Models (RS I and RS II) and Gauss-Bonnet Model

3.1.1 Solutions to RS I Model

The RS I model setup is shown in Fig. 3.1. The new space direction is marked as y, and the periodic boundary condition is imposed to this y dimension by compactifying it on an S^1/Z_2

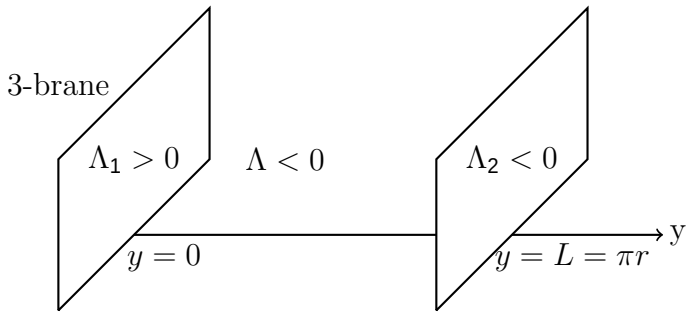

Figure 3.1: The setup of the RS brane-world scenario.

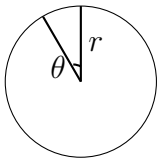

Figure 3.2: S^1/Z_2 orbifold.

orbifold, as shown in Fig. 3.2. The circle with radius r of S^1 shows the distance along y, here a periodic condition with period $2\pi r$ was introduced, and so the points on y are marked by an angle θ. In addition, two points at $y = r\theta$ and $y = r(\ \ \theta)$ are identified. Thus, the points $y = 0$ and $y = L = \pi r$ are turning points in traveling along y, and we consider the region $L \quad y \quad L$. As shown in Fig. 3.1, two 3-branes are set up at $y = 0$ and $y = L = \pi r$, respectively. The Λs are cosmic constants in different places. The SM particles reside on the 3-brane at $y = L$.

The action of this system is given by

$$S = S_H + S_1 + S_2, \tag{3.1}$$

$$S_H = \int d^4x \int_{-L}^{L} dy \sqrt{g}(M^3 R \quad \Lambda), \tag{3.2}$$

$$S_1 = \int d^4x \int_{-L}^{L} dy \sqrt{g}(\mathcal{L}_1 \quad \Lambda_1)\delta(y), \quad S_2 = \int d^4x \int_{-L}^{L} dy \sqrt{g}(\mathcal{L}_2 \quad \Lambda_2)\delta(y \quad L), \tag{3.3}$$

where S_H is the gravity action in the bulk, S_1 is the action on the first brane, and S_2 is the action on the second brane. R is the 5 dimensional Ricci scalar, g is the determinant of the 5-dimensional metric, and M is the Planck mass of the 5-dimensional gravity theory. $\mathcal{L}_1$ and $\mathcal{L}_2$ are the Lagrangians of the two branes, respectively, where matters might reside. Λ, Λ_1, and Λ_2 are cosmological constants between the two branes, on the brane 1 and brane 2, respectively.

We assume the metric in this model has the form of

$$ds^2 = e^{-2A(y)}\eta_{\mu\nu}dx^\mu dx^\nu + dy^2, \tag{3.4}$$

and Randall and Sundrum found the solution [20] by solving the 5 dimensional Einstein's equation derived from the above action

$$A(y) = kjyj, \tag{3.5}$$

under the conditions

$$\Lambda = \quad \frac{\Lambda_1^2}{12M^3}, \; \Lambda_1 = \quad \Lambda_2 = 12kM^3. \tag{3.6}$$

The final solution for the bulk metric is

$$ds^2 = e^{-2kr\theta}\eta_{\mu\nu}dx^\mu dx^\nu + r^2 d\theta^2, \tag{3.7}$$

3.1.2 Solving the Hierarchy Problem

Now that the M, k, and r are 5-dimensional theory parameters. If r is sufficiently small, then the fifth dimension is not detectable in present gravity experiments, and space-time effectively appears 4 dimensional.

We consider fluctuations in the bulk metric of the form,

$$ds^2 = e^{-2kT(x)|\theta|}[\eta_{\mu\nu} + \bar{h}_{\mu\nu}(x)]dx^\mu dx^\nu + T^2(x)d\theta^2, \tag{3.8}$$

where $\bar{h}_{\mu\nu}$ is the tensor fluctuations of the metric in 4-dimensional Minkowski space,

$$\bar{g}_{\mu\nu}(x) \quad \eta_{\mu\nu} + \bar{h}_{\mu\nu}(x), \tag{3.9}$$

and $T(x)$ is locally constant if the fluctuations are smooth. We assume that $T(x)$ has the vacuum expectation value (VEV) r and the extra-dimensional radius is stabilized at this VEV.

So, we replace T just by r. By substituting eq. (3.8) into eq. (3.3), a part of the action is

$$S_{eff} \quad \int d^4x \int_{-\pi}^{\pi} d\theta \; 2M^3 r e^{-2kr|\theta|} \sqrt{\bar{g}}\bar{R}, \tag{3.10}$$

here $\bar{R}$ is the 4 dimensional Ricci scalar made from $\bar{g}_{\mu\nu}(x)$. Integrating out the θ part, we get an effective 4-dimensional action with the 4-dimensional Planck mass given by

$$M_{pl}^2 = M^3 r \int_{-\pi}^{\pi} d\theta \; e^{-2kr|\theta|} = \frac{M^3}{k}[1 \quad e^{-2kr\pi}] \quad \frac{M^3}{k}, \tag{3.11}$$

for $kL > 1$.

The real-world (the world on the second brane) metric has the relation that $g_{\mu\nu} = e^{-2kr\pi}\bar{g}_{\mu\nu}$. We consider the action of the SM Higgs field in the real world:

$$S \quad \int d^4x \; \sqrt{g}\left[g^{\mu\nu} D_\mu H^\dagger D_\nu H \quad \lambda(|H|^2 \quad v_0^2)^2\right] \tag{3.12}$$

$$= \int d^4x \sqrt{\bar{g}} e^{-4kr\pi}\left[\bar{g}^{\mu\nu} e^{2kr\pi} D_\mu H^\dagger D_\nu H \quad \lambda(|H|^2 \quad v_0^2)^2\right] \tag{3.13}$$

$$= \int d^4x \sqrt{\bar{g}}\left[\bar{g}^{\mu\nu} D_\mu H^\dagger D_\nu H \quad \lambda(|H|^2 \quad e^{-2kr\pi} v_0^2)^2\right], \tag{3.14}$$

where v_0 is the VEV of the Higgs doublet in the original action. From eq. (3.13) to eq. (3.14), we canonically normalize the kinetic term by $H \; ! \; e^{kr\pi}H$. Now we can see that the Higgs VEV is given by

$$v \quad e^{-kr\pi} v_0. \tag{3.15}$$

In the same way, any mass in our real world is related to a higher-dimensional mass parameter as

$$m \quad e^{-kr\pi} m_0. \tag{3.16}$$

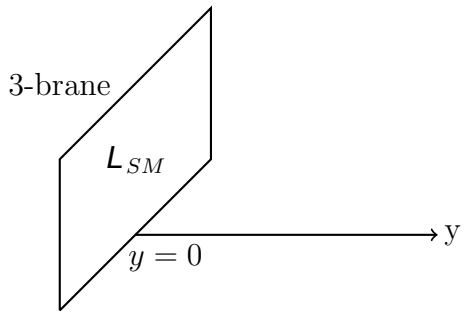

Figure 3.3: The setup of 5-dimensional brane-world cosmology.

For example, if we set $kr\pi$ 50 (a mild hierarchy), $e^{kr\pi}$ 10^{15} and it will produce the TeV mass scales from a fundamental mass scale of about the Planck scale, 10^{19} GeV

3.1.3 The RS II Model and Gauss-Bonnet (GB) Model

The RS II model setup is shown in Fig. 3.3. This setup is effectively realized by pushing r ! 1 in the RS I setup. From eq. (3.11), we see that M_{pl} is also well-defined in this setup. However, the first brane represents our real 4-dimensional world, and $\mathcal{L}_{SM}$ is the SM Lagrangian.

The RS II brane-world cosmology can be extended by adding the Gauss-Bonnet (GB) term to the bulk gravity action. The action of this GB brane-world cosmology is given by

$$\begin{aligned} S &= \int d^4x \int dy \sqrt{g} \left\{ M^3 R + \alpha M \left(R^2 \quad 4R_{MN}R^{MN} + R_{MNPQ}R^{MNPQ} \right) \quad \Lambda \right\} \\ &+ \int d^4x \int dy \sqrt{g} \left(\mathcal{L}_1 \quad \Lambda_1 \right) \delta(y). \end{aligned} \tag{3.17}$$

The first term represents the action in 5 dimensional space-time, if $\alpha = 0$ then it goes to RS II model. The second term is the action on the only brane here. These two models are what we consider in this dissertation.

3.2 A View of the Early Universe Evolution

We suppose that in the early times, the Universe is 5-dimensional, either RS II or GB case, but when the temperature decreased, the 5-dimensional Universe started to effectively evolve into the 4 dimensional Universe that we see today. This transition is characterized by the so-called transition temperature T_t.

As we have discussed in the previous section, we calculate the DM relic density by solving the Boltzmann equation,

$$\frac{\mathrm{d}Y_x}{\mathrm{d}x} = \quad \frac{s\hbar\sigma v i}{Hx}(Y^2 \quad Y_{eq}^2), \tag{3.18}$$

with the the help of Friedmann equation,

$$H^2 = \frac{\rho}{3M_p^2} \tag{3.19}$$

If the early Universe is 5-dimensional, the Friedmann equation should be modified for $T > T_t$. Thus, the evolution of the 5-dimensional Universe affects DM physics if $T_D > T_t$. This is the case we consider in this dissertation.

We parameterize the modified Friedmann equation in 5-dimensional cosmology as

$$H = H_{st}F(x_t/x), \tag{3.20}$$

where H_{st} is the standard Big Bang cosmological Hubble parameter, and the function F denotes the modification of the Friedmann equation in braneworld cosmology, and $x_t = m/T_t$ and $x = m/T$. Since we suppose that at temperature $T < T_t$, 4 dimensional cosmology started to replace the 5 dimensional one, we set $F(x_t/x) = 1$ for $x > x_t$. We assume a simple form for F as [21]

$$F(x_t/x) = \left(\frac{x_t}{x}\right)^{\gamma}, \tag{3.21}$$

for $x_t/x > 1$ with a constant γ. It has been found [21] that this is a good approximation for

Friedmann equations in known brane-world cosmological models: $\gamma = 2$ for the RS brane-world cosmology, while $\gamma = 2/3$ for the GB brane-world cosmology. Then, the Boltzmann equation becomes

$$\frac{dY}{dx} = \frac{s\langle\sigma v\rangle}{xH_{st}F(x_t/x)}(Y^2 - Y_{eq}^2). \tag{3.22}$$

Note that this modification is equivalent to the replacement

$$\langle\sigma v\rangle \to \langle\sigma v\rangle \left(\frac{\langle\sigma v\rangle}{F(x_t/x)}\right) = \langle\sigma v\rangle \left(\frac{x}{x_t}\right)^{\gamma} \tag{3.23}$$

in the standard BBC.

The γs can be found as follows. In the RS model, for a spatially flat universe on the brane, the Friedmann equation was found to be [11, 12, 13, 14]

$$H^2 = \frac{\rho}{3M_P^2}\left(1 + \frac{\rho}{\rho_{RS}}\right), \tag{3.24}$$

where ρ is the energy density on the brane, and

$$\rho_{RS} = 12\frac{M_5^6}{M_P^2}. \tag{3.25}$$

Here, the 4 - dimensional cosmological constant and the dark radiation have been set to vanish [22]. Since at low energies (temperatures), $\rho/\rho_{RS} \ll 1$ and the Friedmann equation of the BBC is reproduced. For high temperatures, $\rho/\rho_{RS} \gg 1$, the Friedmann equation can be approximated by

$$H \simeq H_{st}\sqrt{\frac{\rho}{\rho_{RS}}} = H_{st}\left(\frac{x_t}{x}\right)^2, \tag{3.26}$$

and thus $\gamma = 2$. Note that when the evolution of the Universe is 5-dimensional ($\rho/\rho_{RS} \gg 1$), $H^2 \propto \rho^2/M_5^6$ and the evolution of the Universes controlled by the 5-dimensional Planck mass, as we expected.

In the GB model, the Friedmann equation on the spatially flat brane is found to be [18],[19]

$$\kappa_5^2(\rho + m_\sigma^4) = 2\sqrt{1 + \frac{H^2}{\mu^2}}\left(3 \quad \beta + 2\beta\frac{H^2}{\mu^2}\right), \tag{3.27}$$

with $\beta = 4\alpha\mu^2 = 1 \quad \sqrt{1 + 4\alpha\Lambda_5/3}$. There are four free parameters in this model, $\kappa_5,\ m_\sigma,\ \mu,$ and β. Since at low energies, the Friedmann equation should reproduce the standard BBC one with a vanishing 4 dimensional cosmological constant, we have a relation:

$$\kappa_5^2 m_\sigma^4 = 2\mu(3 \quad \beta),\ \frac{1}{M_P^2} = \frac{\mu}{1+\beta}\kappa_5^2. \tag{3.28}$$

In general, the GB cosmology has three epochs in its evolution [9]: at low energies, the universe obeys the standard expansion law. While at middle energies (RS epoch), the universe expands according to the RS brane cosmology. At high energies (GB epoch), the Friedmann equation is approximately expressed as

$$H \ ' \ \left(\frac{1+\beta}{4\beta}\frac{\mu}{M_P^2}\rho\right)^{1/3}. \tag{3.29}$$

The RS epoch collapses at $\beta = 0.151$ ([9]), which is the solution to $3\beta^3 \quad 12\beta^2 + 15\beta \quad 2 = 0$. To focus on the GB brane-world cosmology, we consider this case. Thus, the Friedmann equation in the GB epoch is

$$H \ ' \ \left(\frac{1+\beta}{4\beta}\frac{\mu}{M_P^2}\rho\right)^{1/3} = H_{st}\left(\frac{\rho}{\rho_{GB}}\right)^{-1/6} = H_{st}\left(\frac{x_t}{x}\right)^{-2/3}, \tag{3.30}$$

with $\rho_{GB} = 3^6\left(\frac{1+\beta}{4\beta}\mu M_P\right)^2$, which means $\gamma = \quad 2/3$ for $T > T_t$.

Before concluding this chapter, we discuss a model-independent lower bound on the transition temperature. The BBC is the standard theory to successfully describe the expansion of the Universe and the existence of the Cosmic Microwave Background (CMB). The Big Bang Nucleosynthesis (BBN), one of the main successes of the BBC, is the theory to explain how

light nuclei were successfully synthesized in the early Universe. The successful BBN began when the temperature of the universe was about T 1 MeV. This means that the Universe's evolution for T . 1 MeV must follow the BBC. Thus, we set the lower bound on the transition temperature to be $T_t > 1$ MeV.

CHAPTER 4

THE STANDARD MODEL (SM)

4.1 SM Contents and Interactions

The SM includes the known fundamental particles in our world and depicts how they interact with each other, although it does not include gravity, which is described by the theory of general relativity. In the SM, there are three kinds of interactions: the strong interaction, the weak interaction, and the electromagnetic interaction. Corresponding gauge bosons mediate these interactions with spin 1. The strong interaction is mediated by gluons, the weak interaction is mediated by $W^{\pm}$ bosons and Z bosons, and the electromagnetic interaction is mediated by photons. The SM is constructed based on the gauge principle, that is, the SM Lagrangian must be gauge invariant. The gauge symmetry based on $SU(3)_C$ corresponds to the strong interaction, and the weak and electromagnetic interactions are unified into the gauge symmetry of $SU(2)_L \quad U(1)_Y$. See Table 4.1.

The SM particle content is shown in Table 4.2. The elementary fermions include quarks and leptons, and they all have spin $\frac{1}{2}$. q_L^i is the left-handed quark doublet with the generation index $i = 1, 2, 3$. The first generation includes up quark (u) and down quark (d), the second generation includes charm quark (c) and strange quark (s), and the third generation includes top quark (t)

Interaction	Gauge Boson	Gauge Symmetry
Strong	gluon	$SU(3)_C$
Weak	$W^{\pm}$, Z bosons	$SU(2)_L \quad U(1)_Y$
Electromagnetic	photon	

Table 4.1: Fundamental interactions in the SM.

	$SU(3)_c$	$SU(2)_L$	$U(1)_Y$
$q_L^i = \begin{pmatrix} u_L^i \\ d_L^i \end{pmatrix}$	**3**	**2**	1/6
u_R^i	**3**	**1**	2/3
d_R^i	**3**	**1**	1/3
$l_L^i = \begin{pmatrix} \nu_L^i \\ e_L^i \end{pmatrix}$	**1**	**2**	1/2
e_R^i	**1**	**1**	1
$H = \begin{pmatrix} H^+ \\ H^0 \end{pmatrix}$	**1**	**2**	1/2

Table 4.2: Particle content of the SM

and bottom quark (b). u_R^i and d_R^i are right-handed up and down quarks, respectively. Leptons (and antileptons) are also fermions, but they have no color charge. l_L^i is a left-handed lepton of i-th generation. l_L^1 includes left-handed electron (e^-) and electron neutrino (ν_e), l_i^2 includes muon (μ^-) and muon neutrino (ν_μ), and l_L^3 includes left-handed tau (τ^-) and tau neutrino (ν_τ). $e_R^{1,2,3}$ are right-handed electrons, muon, and tau, respectively. The Higgs doublet field is a scalar field with spin 0, whose VEV breaks $SU(2)_L \quad U(1)_L$ gauge symmetry and generates W and Z bosons masses as well as quarks and leptons masses.

4.2 SM Particles' Interactions

The behavior and interactions of the SM particles are shown in the SM Lagrangian as

$$\begin{aligned} \mathcal{L}_{SM} = & \quad \frac{1}{2}tr[G^{\mu\nu}G_{\mu\nu}] \quad \frac{1}{2}tr[F^{\mu\nu}F_{\mu\nu}] \quad \frac{1}{4}B^{\mu\nu}B_{\mu\nu} \\ & + \quad \overline{q_L^i}i\gamma^\mu D_\mu^q q_L^i + \overline{l_L^i}i\gamma^\mu D_\mu^l l_L^i \\ & + \quad \overline{u_R^i}i\gamma^\mu D_\mu^u u_R^i + \overline{d_R^i}i\gamma^\mu D_\mu^d d_R^i + \overline{e_R^i}i\gamma^\mu D_m^e u e_R^i \\ & + \quad (D^{H\mu}H)^\dagger(D_\mu^H H) \quad \lambda(H^\dagger H \quad \frac{1}{2}v^2)^2 \\ & \quad \{Y_u^{ij}\overline{q_L^i}\tilde{H}u_R^j + Y_d^{ij}\overline{q_L^i}Hd_R^j + Y_e^{ij}\overline{l_L^i}He_R^j + H.c.\}, \end{aligned} \tag{4.1}$$

where $\tilde{H} = i\sigma_2 H^*$, $D^{i\mu}$ or D^i_μ are covariant derivatives of particle i, and $G_{\mu\nu}$, $F_{\mu\nu}$ and $B_{\mu\nu}$ are field strengths of $SU(3)_C$, $SU(2)_L$ and $U(1)_Y$ gauge bosons, respectively,

$$\begin{aligned} G_{\mu\nu} &= \partial_\mu G_\nu \quad \partial_\nu G_\mu \quad ig_3[G_\mu, G_\nu], \\ F_{\mu\nu} &= \partial_\mu A_\nu \quad \partial_\nu A_\mu \quad ig_2[A_\mu, A_\nu], \\ B_{\mu\nu} &= \partial_\mu B_\nu \quad \partial_\nu B_\mu, \end{aligned} \tag{4.2}$$

with g_3, g_2 and g_1 being $SU(3)_C$, $SU(2)_L$ and $U(1)_Y$ gauge coupling constants, respectively, and Y_f^{ij} are the Yukawa coupling constants with the generation indices $i, j = 1, 2, 3$ and $f = u, d, e$.

4.2.1 Spontaneous Symmetry Breaking and Higgs Mechanism

Spontaneous Global $U(1)$ Symmetry Breaking

For a scalar field Φ with $U(1)$ charge Q, its global $U(1)$ transformation is

$$\Phi' = e^{iQ\theta}\Phi, \tag{4.3}$$

where θ is independent of x^μ. Consider a basic Lagrangian

$$\mathcal{L} = (\partial_\mu \Phi)^\dagger (\partial^\mu \Phi) \quad V(\Phi^\dagger \Phi), \tag{4.4}$$

where the scalar potential V is a function of $(\Phi^\dagger\Phi)$. Here we see that $\mathcal{L}$ is invariant under the $U(1)$ transformation.

Now consider a symmetric potential V,

$$V(\Phi^\dagger\Phi) = \frac{1}{2}m^2(\Phi^\dagger\Phi) + \frac{\lambda}{4}(\Phi^\dagger\Phi)^2, \tag{4.5}$$

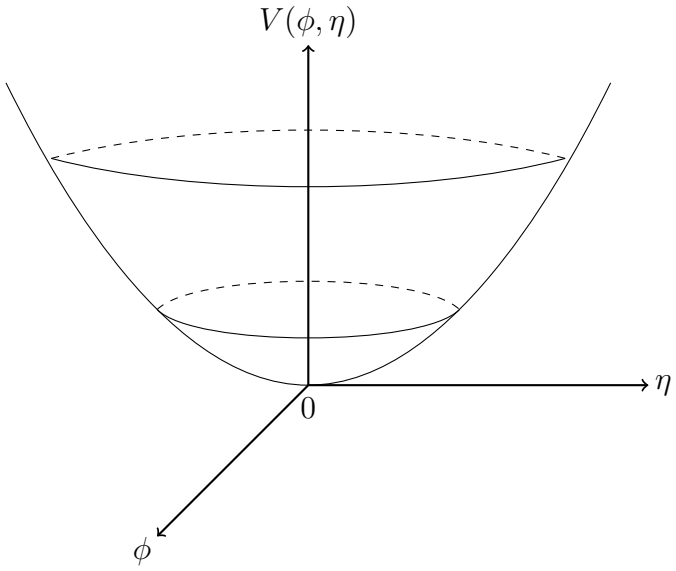

Figure 4.1: Symmetric Scalar Potential V as a function of η and ϕ.

with both m^2 and λ positive. First, find its potential minimum, which is called a vacuum,

$$\frac{\partial V}{\partial \Phi} = 0 \;\;) \;\; \Phi = 0. \tag{4.6}$$

In terms of two real scalars $\Phi = \frac{1}{\sqrt{2}}(\phi + i\eta)$, V goes to

$$V = \frac{1}{2}m^2(\phi^2 + \eta^2) + \frac{\lambda}{16}(\phi^2 + \eta^2)^2, \tag{4.7}$$

as shown in Fig. 4.1. Obviously, the potential minimum is at $\phi = \eta = 0$. In this case, there is no symmetry breaking.

Then, we consider the case that the first term of V is negative,

$$V = \quad m^2(\Phi^\dagger\Phi) + \frac{\lambda}{4}(\Phi^\dagger\Phi)^2 + \frac{m^4}{\lambda}, \tag{4.8}$$

where the last term is added to set the vacuum energy to be 0. We consider the stationary condition:

$$\frac{\partial V}{\partial \Phi} = 0 \;\;) \;\; \phi = \eta = 0 \; or \; \phi^2 + \eta^2 = 4\frac{m^2}{\lambda}. \tag{4.9}$$

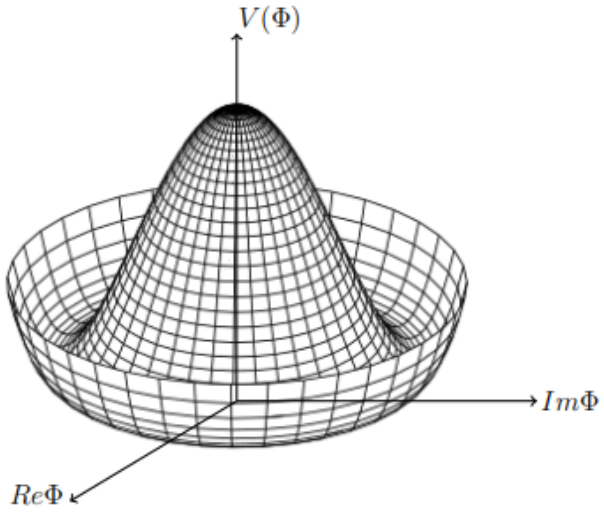

Figure 4.2: $V = \quad m^2(\Phi^\dagger\Phi) + \frac{\lambda}{4}(\Phi^\dagger\Phi)^2 + \frac{m^4}{\lambda}$.

Here, the first one, $\phi = \eta = 0$ sets the potential maximum, and the second one, $\phi^2 + \eta^2 = \frac{4m^2}{\lambda}$, sets the potential minimum. This potential is shown in Fig. 4.2. We can see that $V = 0$ along the circle defined by $\phi^2 + \eta^2 = \frac{4m^2}{\lambda}$ (see Fig. 4.3). On the circle, we select a special point, $(\hbar\phi i = 2\sqrt{\frac{m^2}{\lambda}}, \hbar\eta i = 0)$, which is marked by the black dot, as the vacuum. With this choice, the global $U(1)$ symmetry is spontaneously broken.

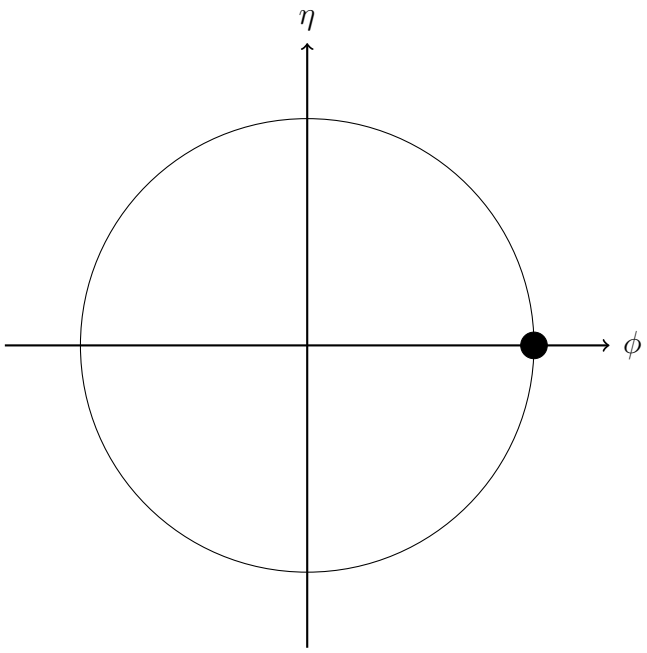

Figure 4.3: Potential Minimum.

The scalar potential V is more conveniently parameterized as

$$V = \frac{\lambda}{4}\left(\Phi^{\dagger}\Phi \quad \frac{v^2}{2}\right)^2, \tag{4.10}$$

with $v = \hbar\phi\imath = 2\sqrt{\frac{m^2}{\lambda}}$. We redefine the physical scalars such as

$$\phi = \hbar\phi\imath + h = v + h, \tag{4.11}$$

$$\eta = \hbar\eta\imath + \eta = 0 + \eta = \eta, \tag{4.12}$$

and express the potential with the physical states,

$$V(h,\eta) = \frac{1}{2}\left(\frac{\lambda}{2}v^2\right)h^2 + \frac{1}{4}vh(h^2+\eta^2) + \frac{\lambda}{16}(h^2+\eta^2)^2. \tag{4.13}$$

We can see that h is massive while η is massless,

$$m_h^2 = \frac{\lambda}{2}v^2 \tag{4.14}$$

$$m_\eta = 0. \tag{4.15}$$

If a continuous symmetry is spontaneously broken by a scalar field VEV, as the global $U(1)$ symmetry broken here, there should be a massless scalar field in the physical spectrum. This is called the Nambu-Goldstone (NG) theorem and the massless state is called the Nambu-Goldstone boson.

Spontaneous $U(1)$ Gauge Symmetry Breaking and Higgs Mechanism.

Now consider a $U(1)$ gauge theory, and the local $U(1)$ transformation,

$$\Phi' = e^{iQ\theta(x)}\Phi, \tag{4.16}$$

where $\theta(x)$ is function of x. The Lagrangian for the scalar Φ is given by

$$\mathcal{L}_{scalar} = (D_\mu\Phi)^\dagger(D^\mu\Phi) \quad \frac{\lambda}{4}\left(\Phi^\dagger\Phi \quad \frac{v^2}{2}\right)^2. \tag{4.17}$$

In the same setting as before,

$$\Phi = \frac{1}{\sqrt{2}}(v + h + i\eta), \tag{4.18}$$

with $D_\mu = \partial_\mu \quad iQgA_\mu$,

$$\begin{aligned}(D_\mu\Phi)^\dagger(D^\mu\Phi) &= \frac{1}{2}(\partial_\mu h)(\partial^\mu h) + \frac{1}{2}(\partial_\mu\eta)(\partial^\mu\eta) \\ &+ Qgv\eta(\partial_\mu A^\mu) + \frac{1}{2}(Qgv)^2 A_\mu A^\mu \\ &+ Qg\eta(\partial_\mu h)A^\mu \quad Qgh(\partial_\mu\eta)A^\mu + Q^2g^2vhA^\mu A_\mu \\ &+ \frac{1}{2}Q^2g^2(h^2+\eta^2)A_\mu A^\mu,\end{aligned} \tag{4.19}$$

up to total derivatives. This includes the following terms quadratic in fields:

$$\frac{1}{2}(\partial_\mu h)(\partial^\mu h) + \frac{1}{2}(\partial_\mu \eta)(\partial^\mu \eta) + \frac{1}{2}(Qgv)^2 A_\mu A^\mu + Qgv\eta(\partial_\mu A^\mu). \tag{4.20}$$

Here, the first two terms are the kinetic terms for h and η, and the third term is the gauge boson mass term generated by the VEV with the gauge boson mass, $m_A^2 = Q^2 g^2 v^2$. The last term is quite unusual, which is neither a kinetic term nor a mass term. In fact, this term can be eliminated by the so-called R_ξ gauge. In the R_ξ gauge, the gauge fixing term is chosen to be

$$\begin{aligned} \mathcal{L}_{GF} &= \frac{1}{2\xi}(\partial_\mu A^\mu + \xi Qgv\eta)^2 \qquad (4.21) \\ &= \frac{1}{2\xi}(\partial_\mu A^\mu)^2 \quad \frac{1}{2}\xi(Qgv)^2\eta^2 \quad Qgv\eta(\partial_\mu A^\mu), \end{aligned}$$

so that $\eta(\partial_\mu A^\mu)$ term is cancelled out. In this way, we get the mass spectrum of the spontaneously broken $U(1)$ gauge theory:

$$\text{gauge boson } A_\mu \text{ mass: } m_A^2 = Q^2 g^2 v^2 \tag{4.22}$$

$$\text{Higgs boson } h \text{ mass: } m_h^2 = \frac{\lambda}{2} v^2 \tag{4.23}$$

$$\text{would-be NG-boson } \eta \text{ mass: } m_\eta^2 = \xi m_A^2. \tag{4.24}$$

The scalar η is called the "would-be NG boson" since it appears as the NG boson if the $U(1)$ symmetry is global. The gauge parameter ξ is not observable, and we may set $\xi \; ! \; 1$. This choice is called "unitary gauge", in which $m_\eta^2 \; ! \; 1$ and thus the would-be NG boson disappears from the theory as a physical state. Here we may check the consistency of the spontaneously broken $U(1)$ gauge theory in terms of physical degrees of freedom. Before the $U(1)$ gauge symmetry breaking, the gauge boson is massless and it has two degrees of freedom. The complex scalar $\Phi = \phi + i\eta$ also has two degrees of freedom. Thus, the total degrees of freedom of the fields is four. After the $U(1)$ gauge symmetry breaking, A_μ gets a mass and

has three degrees of freedom. Since the would-be NG boson disappears from the theory, we have only one scalar degree of freedom. Therefore, the total degrees of freedom after symmetry breaking is also four. We may say that the would-be NG boson is eaten by the gauge boson and enjoys the longitudinal degree of freedom of the massive gauge boson.

There is another expression of the unitary gauge. Instead of $\Phi = \frac{1}{\sqrt{2}}(v + h + i\eta)$, we can express the Higgs field as

$$\Phi = \frac{1}{\sqrt{2}}(v + h)e^{i\frac{\chi}{v}}, \tag{4.25}$$

with χ a real scalar, corresponding to η. In this expression, $\Phi^\dagger\Phi = \frac{1}{2}(v+h)^2$ is independent of χ, and hence V is independent of χ. Consider the $U(1)$ gauge transformation,

$$\Phi' = e^{iQ\theta(x)}\Phi = \frac{1}{\sqrt{2}}(v + h)\exp\left[i\left(Q\theta(x) \quad \frac{\chi(x)}{v}\right)\right]. \tag{4.26}$$

This indicates that we can choose the gauge parameter to satisfy $Q\theta(x) \quad \frac{\chi(x)}{v} = 0$, so that the scalar χ disappears from the theory. This choice of $\theta(x)$ is nothing but the unitary gauge.

4.2.2 Spontaneous Symmetry Breaking in the SM

Electroweak Symmetry Breaking

The Higgs sector of SM Lagrangian is

$$\begin{aligned}
\mathcal{L}_{Higgs} &= (D^H_\mu H)^\dagger(D^{H\mu}H) \quad V(H^\dagger H), && (4.27)\\
\text{with } V &= \lambda\left(H^\dagger H \quad \frac{v^2}{2}\right)^2, && (4.28)\\
\text{and } D^H_\mu &= \partial_\mu \quad igA_\mu \quad ig'\frac{1}{2}B_\mu. && (4.29)
\end{aligned}$$

Here, g is the $SU(2)$ gauge coupling, A_μ is the $SU(2)$ gauge boson, g' is the $U(1)_Y$ gauge coupling, and B_μ is the $U(1)_Y$ gauge boson. The $SU(2)$ gauge boson is expressed as

$$A_\mu = A_\mu^a T^a, \tag{4.30}$$

$$T^a = \frac{1}{2}\sigma^a. \tag{4.31}$$

T^a is $SU(2)$ generator, and σ^a, with $a = 1, 2, 3$, are the Pauli matrices.

The potential minimum is at $H^\dagger H = \frac{v^2}{2}$, and we set

$$\langle H \rangle = \begin{pmatrix} 0 \\ v/\sqrt{2} \end{pmatrix}. \tag{4.32}$$

In the unitary gauge, we express H to be

$$H = \frac{1}{\sqrt{2}} \begin{pmatrix} 0 \\ \sqrt{2}(v + h + i\chi) \end{pmatrix}. \tag{4.33}$$

and the Higgs boson mass is found to be

$$V(H^\dagger H) \quad \lambda v^2 h^2 \quad \frac{1}{2} m_h^2 h^2, \tag{4.34}$$

with $m_h = \sqrt{2\lambda} v$.

Gauge Boson Mass Spectrum after Symmetry Breaking

There is

$$\mathcal{L}_{Higgs} \quad (D_\mu^H H)^\dagger (D^{H\mu} H), \tag{4.35}$$

with

$$\begin{aligned} D_\mu^H &= \partial_\mu \quad igA_\mu \quad ig'\left(\frac{1}{2}\right)B_\mu \\ &= \partial_\mu \quad \frac{1}{2}\begin{pmatrix} gA_\mu^3 + g'B_\mu & g(A_\mu^1 \quad iA_\mu^2) \\ g(A_\mu^1 + iA_\mu^2) & gA_\mu^3 + g'B_\mu \end{pmatrix}. \end{aligned} \tag{4.36}$$

Introduce W boson and Z boson,

$$W_\mu^+ = \frac{1}{\sqrt{2}}(A_\mu^1 \quad iA_\mu^2), \tag{4.37}$$

$$W_\mu^- = (W_\mu^+)^* = \frac{1}{2}(A_\mu^1 + iA_\mu^2)), \tag{4.38}$$

$$Z_\mu = \cos\theta_W A_\mu^3 \quad \sin\theta_W B_\mu, \tag{4.39}$$

where θ_W is the weak mixing angle, or Weinberg angle, which is defined as

$$\sin\theta_W = \frac{g'}{g_Z}, \tag{4.40}$$

$$\cos\theta_W = \frac{g}{g_Z}, \qquad \text{with} \tag{4.41}$$

$$g_Z \qquad \sqrt{g^2 + g'^2}. \tag{4.42}$$

Thus, we have

$$(D_\mu^H \langle H \rangle)^\dagger (D^{H\mu} \langle H \rangle) = \frac{1}{4}g^2v^2(W_\mu^+ W^{-\mu}) + \frac{1}{2}\left(\frac{1}{4}g_Z^2v^2\right)(Z_\mu Z^\mu), \tag{4.43}$$

and W bosons and Z boson get their masses as

$$W \text{ boson mass: } m_W = \frac{1}{2}gv, \tag{4.44}$$

$$Z \text{ boson mass: } m_Z = \frac{1}{2}g_Z v = \frac{1}{2}\sqrt{g^2 + g'^2}v = \frac{m_W}{\cos\theta_W}. \tag{4.45}$$

Since Z_μ is a linear combination of A^3_μ and B_μ, its orthogonal combination is

$$A^0_\mu = \sin\theta_W A^4_\mu + \cos\theta_W B_\mu, \tag{4.46}$$

which is photon, and has no mass. By the electroweak symmetry breaking, $SU(2)_L \quad U(1)_Y \;\; ! \;\; U(1)_{em}$, the original gauge bosons, $A^1_\mu, A^2_\mu, A^3_\mu$ and B_μ, are rearranged to get the mass eigenstates, $W^\pm_\mu$, Z_μ, and A^0_μ.

Fermion Mass

The Yukawa part of Lagrangian is

$$\mathcal{L}_{Yukawa} = \quad Y_e\overline{l_L}He_R \quad Y_d\overline{q_L}Hd_R \quad Y_u\overline{q_L}\tilde{H}u_R + H.c.. \tag{4.47}$$

Replace H with $\langle H \rangle$, it goes to

$$\frac{Y_e v}{\sqrt{2}}\overline{e_L}e_R \quad \frac{Y_d v}{\sqrt{2}}\overline{d_L}d_R \quad \frac{Y_u v}{\sqrt{2}}\overline{u_L}u_R + H.c.. \tag{4.48}$$

The electron mass, up quark mass, and down quark mass are given by

$$m_e = \frac{Y_e}{\sqrt{2}}v, \tag{4.49}$$

$$m_u = \frac{Y_u}{\sqrt{2}}v, \tag{4.50}$$

$$m_d = \frac{Y_d}{\sqrt{2}}v. \tag{4.51}$$

Gauge Interactions of Leptons

The covariant derivatives for leptons are

$$\begin{aligned} D_\mu^{l_L} &= \partial_\mu \quad igA_\mu \quad i\left(\quad \frac{1}{2}\right) g' B_\mu \\ &= \partial_\mu \quad \frac{i}{2}\begin{pmatrix} g_Z Z_\mu & \sqrt{2} g W_\mu^+ \\ \sqrt{2} g W_\mu^- & g_Z \cos 2\theta_W Z_\mu \quad g_Z \sin 2\theta_W A_\mu^0 \end{pmatrix}, \end{aligned} \tag{4.52}$$

and

$$\begin{aligned} D_\mu^{e_R} &= \partial_\mu \quad ig'(\quad 1) B_\mu \\ &= \partial_\mu \quad i(g_Z \sin^2\theta_W) Z_\mu \quad i(g_Z \sin\theta_W \cos\theta_W)(\quad 1) A_\mu^0. \end{aligned} \tag{4.53}$$

Thus, the lepton kinetic terms are expressed as

$$\begin{aligned} \mathcal{L}_{fermion} & \quad \overline{l_L} i\gamma^\mu D_\mu^{l_L} l_L + \overline{e_R} i\gamma^\mu D_\mu^{e_R} e_R \\ &= \overline{\nu_L} i\gamma^\mu \partial_\mu \nu_L + \overline{e_L} i\gamma^\mu \partial_\mu e_L + \overline{e_R} i\gamma^\mu \partial_\mu e_R \\ &+ \quad J_{CC}^{+\mu} W_\mu^- + J_{CC}^{-\mu} W_\mu^+ + J_{NC}^\mu Z_\mu + J_{em}^\mu A_\mu^0, \end{aligned} \tag{4.54}$$

with

$$\text{Charged current: } J_{CC}^{-\mu} = \frac{g}{\sqrt{2}} (\overline{\nu_L} \gamma^\mu e_L), \tag{4.55}$$

$$J_{CC}^{+\mu} = \frac{g}{\sqrt{2}} (\overline{e_L} \gamma^\mu \nu_L), \tag{4.56}$$

$$\begin{aligned} \text{Neutral current: } J_{NC}\mu &= \frac{1}{2} g_Z (\overline{\nu_L} \gamma_\mu \nu_L) \\ & \quad \frac{1}{2} g_Z (1 \quad 2\sin^2\theta_W)(\overline{e_L} \gamma^\mu e_L) \\ &+ \quad g_Z \sin^2\theta_W (\overline{e_R} \gamma^\mu e_R), \end{aligned} \tag{4.57}$$

$$\text{EM current: } J_{em}^\mu = \quad (g_Z \sin\theta_W \cos\theta_W)(\overline{e_L} \gamma^\mu e_L + \overline{e_R} \gamma^\mu e_R). \tag{4.58}$$

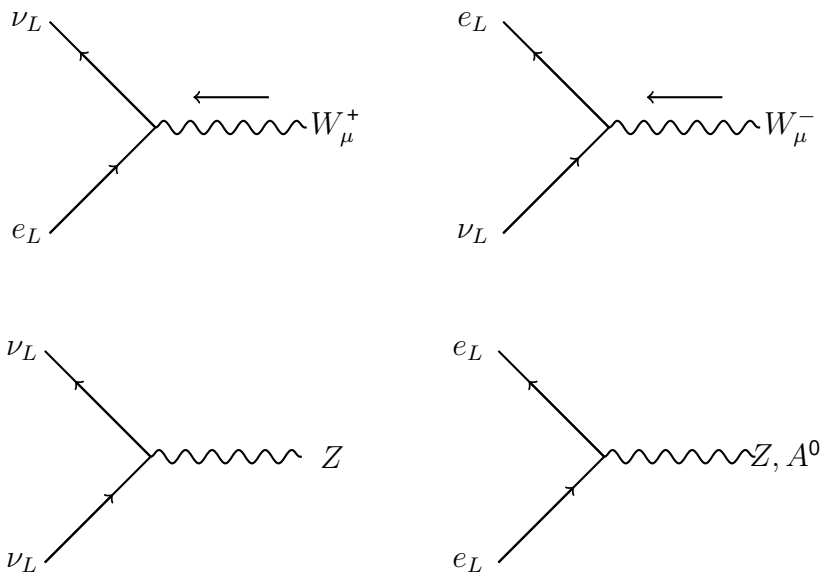

Figure 4.4: Interactions between leptons and gauge bosons.

The Feynman diagrams for The interactions of the leptons with the gauge bosons are shown in Fig. 4.4.

Interactions of Higgs Boson in Unitary Gauge

By the unitary gauge, the Higgs doublet is of the form,

$$H = \frac{1}{\sqrt{2}}\begin{pmatrix} 0 \\ v+h \end{pmatrix}, \tag{4.59}$$

and the kinetic term of the Higgs doublet is expressed as

$$\begin{aligned} (D_\mu^H)^\dagger (D^{H\mu} H) &= \frac{1}{2}(\partial\mu h)(\partial^\mu h) + m_W^2 \left(1 + 2\frac{h}{v} + \frac{h^2}{v^2}\right) W_\mu^+ W^{-\mu} \\ &+ \frac{1}{2} m_Z^2 \left(1 + 2\frac{h}{v} + \frac{h^2}{v^2}\right) Z_\mu^\mu, \end{aligned} \tag{4.60}$$

which includes the interaction terms,

$$m_W^2 (2\frac{h}{v} + \frac{h^2}{v^2}) W_\mu^+ W^{-\mu} + \frac{1}{2} m_Z^2 (2\frac{h}{v} + \frac{h^2}{v^2}) Z_\mu^\mu, \tag{4.61}$$

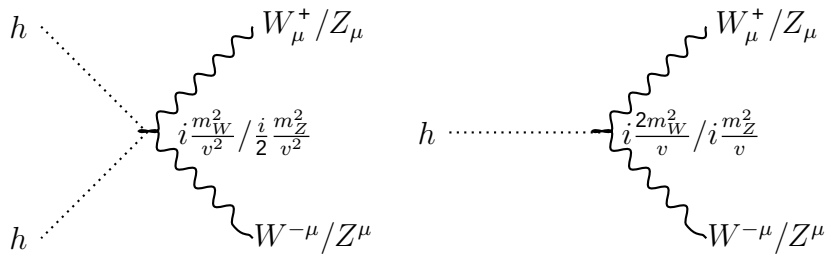

Figure 4.5: Interactions between Higgs boson and W/Z bosons.

as shown in Fig. 4.5.

The Higgs potential also includes the interaction terms,

$$V = \lambda \left(H^\dagger H \quad \frac{v^2}{2} \right)^2 \quad \frac{m_h^2}{2v} h^3 + \frac{m_h^2}{8v^2} h^4, \tag{4.62}$$

which are shown in Fig. 4.6.

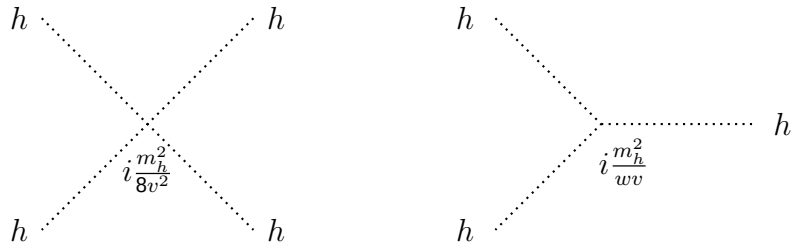

Figure 4.6: Interactions from Higgs potential.

Interactions from Yukawa terms

From eq. (4.47), we get Yukawa interactions,

$$\mathcal{L}_{Yukawa} \qquad m_e \frac{h}{v} \overline{e_L} e_R \quad m_d \frac{h}{v} \overline{d_L} d_R \quad m_u \frac{h}{v} \overline{u_L} u_R + H.c, \tag{4.63}$$

which is shown in Fig. 4.7.

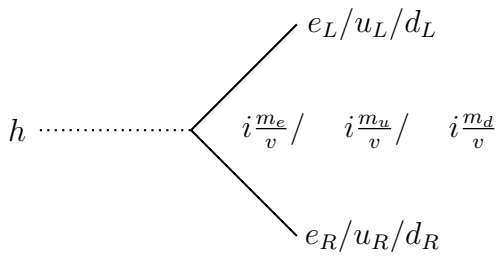

Figure 4.7: Interactions between Higgs boson and electrons and quarks.

Gauge Interactions of Quarks

The quark Lagrangian has kinetic terms as

$$\mathcal{L}^{kin}_{quark} = \overline{q_L} i\gamma^\mu D^{q_L}_\mu + \overline{u_R} i\gamma^\mu D^{u_R}_\mu u_R + \overline{d_R} i\gamma^\mu D^{d_R}_\mu d_R, \tag{4.64}$$

where the covariant derivatives are given by

$$D^{q_L}_\mu = \partial_\mu \quad ig_s G_\mu \quad igA_\mu \quad ig'\left(\frac{1}{6}\right) B_\mu, \tag{4.65}$$

$$D^{u_R}_\mu = \partial_\mu \quad ig_s G_\mu \quad ig'\left(\frac{2}{3}\right) B_\mu, \tag{4.66}$$

$$D^{d_R}_\mu = \partial_\mu \quad ig_s G_\mu \quad ig'\left(-\frac{1}{3}\right) B_\mu. \tag{4.67}$$

Here, g_s is the QCD gauge coupling, $G_\mu = G^a_\mu \lambda^a$ with $a = 1, 2, \quad 8$ are gluons, and λ^a are $SU(3)$ generators. Then, the QCD interaction is given by

$$\begin{aligned}
\mathcal{L}^{int}_{QCD} &= \overline{u_L} i\gamma^\mu(-ig_s G_\mu) u_L + \overline{u_R} i\gamma^\mu(-ig_s G_\mu) u_R \\
&+ \overline{d_L} i\gamma^\mu(-ig_s G_\mu) d_L + \overline{d_R} i\gamma^\mu(-ig_s G_\mu) d_R \\
&= g_s(\overline{u_L}\gamma^\mu \lambda^a u_L) G^a_\mu + g_s(\overline{u_R}\gamma^\mu \lambda^a u_R) G^a_\mu \\
&+ g_s(\overline{d_L}\gamma^\mu \lambda^a d_L) G^a_\mu + g_s(\overline{d_R}\gamma^\mu \lambda^a d_R) G^a_\mu.
\end{aligned} \tag{4.68}$$

In addition, there are the electroweak interactions:

$$\begin{aligned}
\mathcal{L}_{EW}^{int} &= \overline{q_L} i\gamma^\mu \left(\quad igA_\mu \quad ig' \left(\frac{1}{8}\right) B_\mu \right) q_L + \overline{u_R} i\gamma^\mu \left(\quad ig' \left(\frac{2}{3}\right) B_\mu \right) u_R \qquad (4.69)\\
&+ \overline{d_R} i\gamma^\mu \left(\quad ig' \left(\quad \frac{1}{3}\right) B_\mu \right) d_R \\
&= \overline{q_L}\gamma^\mu \left(gA_\mu + \frac{1}{6} g' B_\mu \right) q_L + \frac{2}{3} g' (\overline{u_R}\gamma^\mu u_R) B_\mu \\
&\quad \frac{1}{3} g' (\overline{d_R}\gamma^\mu d_R) B_\mu .
\end{aligned}$$

The first term can be rewritten as

$$\begin{aligned}
\mathcal{L}_{EW}^{int} &\quad \overline{q_L}\gamma^\mu (gA_\mu + \frac{1}{6} g' B_\mu) q_L \qquad (4.70)\\
&= \not{p} \frac{g}{\overline{2}} (\overline{u_L}\gamma^\mu d_L) W_\mu^+ + \not{p} \frac{g}{\overline{2}} (\overline{d_L}\gamma^\mu u_L) W_\mu^- \\
&+ g_Z (\frac{1}{2} \quad Q_u \sin^2\theta_W) (\overline{u_L}\gamma^\mu u_L) Z_\mu \\
&+ g_Z (\quad \frac{1}{2} \quad Q_d \sin^2\theta_W) (\overline{d_L}\gamma^\mu d_L Z_\mu \\
&+ eQ_u (\overline{u_L}\gamma^\mu u_L) A_\mu^0 + eQ_d (\overline{d_L}\gamma^\mu d_L) A_\mu^0 ,
\end{aligned}$$

where $e \quad g_Z \sin\theta_W \cos\theta_W = \not{p} \frac{g g'}{\overline{g^2 + g'^2}}$ is the QED coupling. The second and third terms are

$$\begin{aligned}
\mathcal{L}_{EW}^{int} &\quad \frac{2}{3} g' (\overline{u_R}\gamma^\mu u_R) B_\mu \quad \frac{1}{3} g' (\overline{d_R}\gamma^\mu d_R) B_\mu \qquad (4.71)\\
&= \quad g_Z Q_u \sin^2\theta_W (\overline{u_R}\gamma^\mu u_R) Z_\mu + eQ_u (\overline{u_R}\gamma^\mu u_R) A_\mu^0 \\
&+ \quad g_Z Q_d \sin^2\theta_W (\overline{d_R}\gamma^\mu d_R) Z_\mu + eQ_d (\overline{d_R}\gamma^\mu d_R) A_\mu^0 .
\end{aligned}$$

Hence, the interaction terms are expressed as

$$\mathcal{L}_{EW}^{int} = J_{CC}^{+\mu} W_\mu^- + J_{CC}^- W_\mu^+ + J_{NC}^\mu Z_\mu + J_{em}^\mu A_\mu^0 , \qquad (4.72)$$

with the charged current,

$$J_{CC}^{+\mu} = \frac{g}{\sqrt{2}}(\overline{u_L}\gamma^\mu d_L) = \frac{g}{\sqrt{2}}(\overline{u}\gamma^\mu P_L d), \tag{4.73}$$

$$J_{CC}^{-\mu} = \frac{g}{\sqrt{2}}(\overline{d_L}\gamma^\mu u_L) = \frac{g}{\sqrt{2}}(\overline{d}\gamma^\mu P_L u) = (J_{CC}^{+\mu})^\dagger, \tag{4.74}$$

neutral current,

$$\begin{aligned} J_{NC}^\mu &= g_Z(\frac{1}{2} \quad Q_u \sin^2\theta_W)(\overline{u_L}\gamma^m u u_L) \quad g_Z Q_u \sin^2\theta_W (u_R \gamma^\mu u_R) \\ &+ g_Z(\ \frac{1}{2} \quad Q_d \sin^2\theta_W)(\overline{d_L}\gamma^\mu d_L) \quad g_Z Q_d \sin^2\theta_W (\overline{d_R}\gamma^\mu d_R), \end{aligned} \tag{4.75}$$

and the EM current,

$$J_{em}^\mu = eQ_u(\overline{u_L}) + eQ_d(\overline{d_L}\gamma^\mu d_L) + L \ \ ! \ \ R \tag{4.76}$$

$$= eQ_u(\overline{u}\gamma^\mu u) + eQ_d(\overline{d}\gamma^\mu d). \tag{4.77}$$

Define

$$P_L = \begin{pmatrix} \mathbb{1} & 0 \\ 0 & 0 \end{pmatrix}, \tag{4.78}$$

$$P_R = \begin{pmatrix} 0 & 0 \\ 0 & \mathbb{1} \end{pmatrix}, \tag{4.79}$$

and

$$d = \begin{pmatrix} d_L \\ d_R \end{pmatrix}, \tag{4.80}$$

$$u = \begin{pmatrix} u_L \\ u_R \end{pmatrix}, \tag{4.81}$$

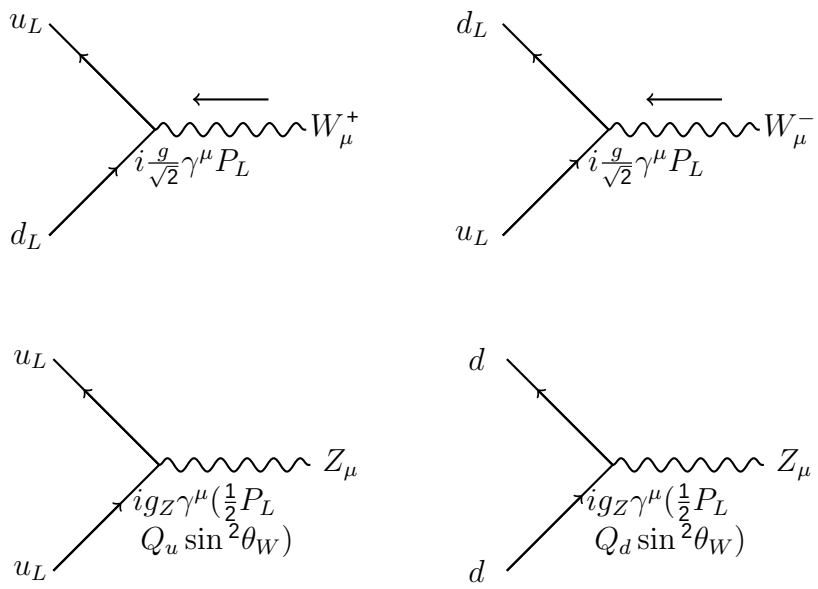

Figure 4.8: Interactions between quarks and bosons.

we express the charged and neutral currents as follows:

$$J^{+\mu}_{CC} = \frac{g}{2}(\overline{u}\gamma^\mu P_L d), \tag{4.82}$$

$$J^{-\mu}_{CC} = \frac{g}{2}(\overline{d}\gamma^\mu P_L u) = (J^{+\mu}_{CC})^\dagger, \tag{4.83}$$

and

$$\begin{aligned} J^\mu_{NC} &= g_Z \frac{1}{2}(\overline{u}\gamma^\mu P_L u) \quad g_Z Q_u \sin^2\theta_W (\overline{u}\gamma^\mu u) \\ &+ g_Z(\ -\frac{1}{2})(\overline{d}\gamma^\mu P_L d) \quad g_Z Q_d \sin^2\theta_W (\overline{d}\gamma^\mu d). \end{aligned} \tag{4.84}$$

These interactions are shown in Fig. 4.8.

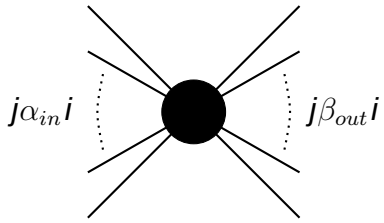

Figure 4.9: The scattering process.

4.3 The Scattering Process

4.3.1 S Matrix

A scattering process is shown in Fig. 4.9. Here, $|\alpha_{in}\rangle$ represents the state of in-coming particles for $x_0 \to -\infty$, and $|\beta_{out}\rangle$ represents the state of out-going particles for $x_0 \to +\infty$. Both in-state and out-state form the complete sets:

$$\sum_\gamma |\gamma_{in}\rangle\langle\gamma_{in}| = \sum_\gamma |\gamma_{out}\rangle\langle\gamma_{out}| = 1. \tag{4.85}$$

The S-matrix is defined as

$$S_{\beta\alpha} = \langle\beta_{out}|\alpha_{in}\rangle = \langle\beta_{out}|S|\alpha_{in}\rangle, \tag{4.86}$$

with $\langle\beta_{out}| = \langle\beta_{in}|S$. Since the S matrix is unitary, there is

$$\begin{aligned} \sum_\gamma S^\dagger_{\gamma\beta} S_{\gamma\alpha} &= \sum_\gamma \langle\gamma_{out}|\beta_{in}\rangle^\dagger \langle\gamma_{out}|\alpha_{in}\rangle \\ &= \langle\beta_{in}| \sum_\gamma |\gamma_{out}\rangle\langle\gamma_{out}| \alpha_{in}\rangle \\ &= \langle\beta_{in}|\alpha_{in}\rangle \\ &= \delta_{\beta\alpha}. \end{aligned} \tag{4.87}$$

Lehmann-Symanzik-Zimmermann (LSZ) Reduction Formula for Real Scalar

We consider the case that all the incoming and outgoing particles are scalars. When $x_0 \to \pm\infty$, all fields are free, and we express them as

$$\Phi_{\substack{\text{in}\\\text{out}}} = \int \frac{d^3p}{\sqrt{(2\pi)^3 2\omega_p}} (a_{\substack{\text{in}\\\text{out}}}(\vec{p})e^{-ipx} + a^\dagger_{\substack{\text{in}\\\text{out}}}(\vec{p})e^{ipx}), \tag{4.88}$$

since they satisfy the Klein-Gordon equation, $(\Box + m^2)\Phi_{\substack{\text{in}\\\text{out}}}(x) = 0$. Define $f_p(x) = \not{p}\frac{1}{\sqrt{(s\pi)^3 2\omega_p}}e^{-ipx}$, then the expression of the free field is $\Phi(x) = \int d^3p(a(\vec{p})f_p(x) + a^\dagger(\vec{P})f_p^*(x))$. From it, we get

$$a(\vec{p}) = i\int d^3x \overleftrightarrow{\partial_t}\Phi(x))f_p^*(x) \qquad \Phi(x)(\partial_t f_p^*(x)), \tag{4.89}$$

$$a^\dagger(\vec{p}) = i\int d^3x \overleftrightarrow{\Phi(x)(\partial_t f_p(x))} \qquad (\partial_t\Phi(x))f_p(x). \tag{4.90}$$

Suppose an incoming state includes a state with momentum p, then we can express it as $|\alpha\ p_{in}\rangle$. The S-matrix for this case is given by

$$\begin{aligned} S_{\beta,\alpha p} &= \langle\beta_{out}|\alpha\ p_{in}\rangle \\ &= \langle\beta_{out}|a^\dagger_{in}(\vec{p})|\alpha_{in}\rangle \\ &= \langle\beta_{out}|a^\dagger_{out}(\vec{p})|\alpha_{in}\rangle \qquad \langle\beta_{out}|\overleftrightarrow{a^\dagger_{out}(\vec{p})} \qquad a^\dagger_{in}(\vec{p})|\alpha_{in}\rangle. \end{aligned} \tag{4.91}$$

Note that $\langle\beta_{out}|a^\dagger_{out}(\vec{p})$ is non-vanishing only if the outgoing state includes the state with momentum p. This corresponds to the case that the initial state with momentum p appears in the final states as the same state and this state experiences no scattering. Since we are not interested in such a case (no scattering), we assume $\langle\beta_{out}|a^\dagger_{out}(\vec{p}) = 0$. Therefore,

$$S_{\beta,\alpha p} = \langle\beta_{out}|\overleftrightarrow{a^\dagger_{out}(\vec{p})} \qquad a^\dagger_{in}(\vec{p})|\alpha_{in}\rangle. \tag{4.92}$$

Since

$$a^{\dagger}_{in}(\vec{p}) = \lim_{x_0\to-\infty} \frac{i}{\sqrt{Z}} \int d^3x(\Phi(x)\partial_t f_p(x) \quad \partial_t\Phi(x) f_p(x)), \tag{4.93}$$

$$a^{\dagger}_{out}(\vec{p}) = \lim_{x_0\to+\infty} \frac{i}{\sqrt{Z}} \int d^3x(\Phi(x)\partial_t f_p(x) \quad \partial_t\Phi(x) f_p(x)), \tag{4.94}$$

where $\frac{i}{\sqrt{Z}}$ is the normalization factor,

$$\begin{aligned} S_{\beta,\alpha p} &= \frac{i}{\sqrt{Z}} \int d^3x \hbar\beta_{out}|[(\Phi(x)\partial_t f_p(x) \quad \partial_t\Phi(x) f_p(x))|_{x_0\to+\infty} \\ &\quad (\Phi(x)\partial_t f_p(x) \quad \partial_t\Phi(x) f_p(x))|_{x_0\to-\infty}]|\alpha_{in}\rangle \\ &= \frac{i}{Z} \int d^4x \partial_t \hbar\beta_{out}|\Phi(x)\partial_t f_p(x) \quad \partial_t\Phi(x) f_p(x)|\alpha_{in}\rangle \\ &= \frac{i}{\sqrt{Z}} \int d^4x \hbar\beta_{out}|\Phi(\partial_t^2 f_p) \quad (\partial_t^2\Phi) f_p|\alpha_{in}\rangle. \end{aligned} \tag{4.95}$$

Using the fact that $f(x)$ satisfies the Klein-Gordon equation, $(\quad + m^2) f_p(x) = 0$, $\partial_t^2 f_p = \vec{\nabla}^2 f_p \quad m^2 f_p$, and $\int d^4x\Phi(\partial_t^2 f_p) = \int d^4x[(\vec{\nabla}^2 \quad m^2)\Phi] f_p$, we get

$$S_{\beta,\alpha p} = \frac{i}{\sqrt{Z}} \int d^4x[(\quad + m^2)\hbar\beta_{out}|\Phi(x)|\alpha_{in}\rangle] f_p(x). \tag{4.96}$$

In the same way, we can easily derive

$$\begin{aligned} S_{\beta p',\alpha} &= \hbar\beta p'_{out}|\alpha_{in}\rangle \\ &= \frac{i}{\sqrt{Z}} \int d^4y(\quad_y + m^2)\hbar\beta_{out}|\Phi(y)|\alpha_{in}\rangle f^*_{p'}(y). \end{aligned} \tag{4.97}$$

Repeating the above calculations for a general case,

$$|\alpha_{in}\rangle = |q_1 q_2 \quad q_l\rangle_{in} = a^{\dagger}_{in}(q_1)a^{\dagger}_{in}(q_2) \quad a^{\dagger}_{in}(q_l)|0\rangle \tag{4.98}$$

$$\hbar\beta_{out}| = \hbar p_1 p_2 \quad p_m\rangle_{out}| = \hbar 0|a_{out}(p_1)a_{out}(P_2) \quad a_{out}(p_m), \tag{4.99}$$

we can derive

$$\begin{aligned} \langle p_1 p_2 \quad p_{m\ out}|q_1 q_2 \quad q_{l\ in}\rangle &= (\frac{1}{Z})^{m+l}\prod_{i=1}^{m}(i\int d^4y_i f^*_{p_i}(y_i)k_{y_i}) \\ &\prod_{j=1}^{l}(i\int d^4x_j f_{q_j}(x_j)k_{x_j}) \\ &\langle 0|T\Phi(y_1)\Phi(y_2) \quad \Phi(y_m)\Phi(x_1)\Phi(x_2) \quad \Phi(x_l)|0\rangle, \end{aligned} \tag{4.100}$$

where

$$k_z = \quad _z + m^2 = \eta^{\mu\nu}\frac{\partial}{\partial z^\mu}\frac{\partial}{\partial z^\nu} + m^2. \tag{4.101}$$

By the use of Green's function, there is

$$\begin{aligned} &\langle 0|T\Phi(y_1)\Phi(y_2) \quad \Phi(y_m)\Phi(x_1)\Phi(x_2) \quad \Phi(x_l)|0\rangle \\ &= G_{m+l}(y_1, y_2, \quad , y_m, x_1, x_2, \quad , x_l), \end{aligned} \tag{4.102}$$

with G the Green's function, and

$$\begin{aligned} &G_{m+l}(y_1, y_2, \quad , y_m, x_1, x_2, \quad , x_l) \\ &= \int \frac{d^4\tilde{p}_1}{(2\pi)^4}\frac{d^4\tilde{p}_2}{(2\pi)^4} \quad \frac{d^4\tilde{p}_l}{(2\pi)^4}\frac{d^4\tilde{q}_1}{(2\pi)^4}\frac{d^4\tilde{q}_2}{(2\pi)^4} \quad \frac{d^4\tilde{q}_m}{(2\pi)^4} \\ &e^{-ip_1y_1}e^{-ip_2y_2} \quad e^{-ip_ly_l}e^{+iq_1x_1}e^{+iq_2x_2} \quad e^{+iq_mx_m} \\ &(2\pi)^4\delta^4(\sum_{j=1}^{l}\tilde{p}_j \quad \sum_{k=1}^{m}\tilde{q}_k)\tilde{G}_{l+m}(\tilde{p}_1\tilde{p}_2 \quad \tilde{p}_l\tilde{q}_1\tilde{q}_2 \quad \tilde{q}_m). \end{aligned} \tag{4.103}$$

Considering that

$$(i\int d^4y_j f^*_{p_j}(y_j)(\quad _{y_j} + m^2))\int \frac{d^4\tilde{p}_j}{(2\pi)^4}e^{-ip_jy_j} = \frac{1}{\sqrt{(2\pi)^3 2p_j^0}}(\quad i)(p_j^2 \quad m^2) \tag{4.104}$$

and

$$(i\int d^4x_k f_{q_k}(x_k)(\quad_{x_k}+m^2))\int\frac{d^4\tilde{q}_k}{(2\pi)^4}e^{+iq_kx_k}=\frac{1}{\sqrt{(2\pi)^3 2q_k^0}}(\quad i)(q_k^2\quad m^2), \tag{4.105}$$

there is

$$\begin{aligned}\langle p_1p_2\quad p_{m\ out}|q_1q_2\quad q_{l\ in}\rangle &= (\frac{1}{\not{p}-\not{z}})^{m+l}(2\pi)^4\delta^4(\sum_{i=1}^{m}p_i\quad\sum_{i=1}^{l}q_i)\\ &\prod_{i=1}^{m}\frac{1}{\sqrt{(2\pi)^3 2p_i^0}}\prod_{i=1}^{l}\frac{1}{\sqrt{(2\pi)^3 2q_i^0}}\\ &i\tilde{\Gamma}_{m+l}(p_1,p_2,\quad,p_m,q_1,q_2,\quad,q_l),\end{aligned} \tag{4.106}$$

where $\tilde{\Gamma}_{m+l}$ is $m+l$ 1-PI function in momentum space,

$$\begin{aligned}i\tilde{\Gamma}_{m+l} &= \tilde{G}_{m+l}(\quad i)^{m+l}(p_1^2\quad m^2)(p_2^2\quad m^2)\quad(p_m^2\quad m^2)\\ &(q_1^2\quad m^2)(q_2^2\quad m^2)\quad(q_l^2\quad m^2).\end{aligned} \tag{4.107}$$

LSZ Reduction Formula for Fermions

We consider the situation that both the initial and the final states have only fermions. The initial and the final states should be free states, which are expressed as

$$\Psi_{\substack{\text{in}\\\text{out}}}=\int d^3p\sum_{s=\pm}(b(\not{p}\ ,s)u(\not{p}\ ,s)f_p(x)+d^\dagger(\not{p}\ ,s)v(\not{p}\ ,s)f_p^*(x)), \tag{4.108}$$

where $b(\not{p}\ ,s)$ is the annihilation operator of particle, $d^\dagger(\not{p}\ ,s)$ is the creation operator of anti-particle, $u(\not{p}\ ,s)$ is the wave function of particle that obeys $(\not{p}\quad m)u(\not{p}\ ,s)=0$, and $v(\not{p}\ ,s)$ is the wave function of anti-particle that obeys $(\not{p}+m)v(\not{p}\ ,s)=0$. The annihilation and creation

operators are expressed by

$$b(\vec{p},s) = \int d^3x f_p^*(x)\overline{u}(\vec{p},s)\gamma^0\Psi(x) \tag{4.109}$$

$$d^\dagger(\vec{p},s) = \int d^3x f_p(x)\overline{v}(\vec{p},s)\gamma^0\Psi(x), \tag{4.110}$$

with $f_p(x) = \not{p}\frac{1}{\sqrt{(2\pi)^3 2p^0}}e^{-ipx}$. We calculate the following S-matrix,

$$\begin{aligned} S_{\beta p,\alpha} &= \langle\beta + p_{out}|\alpha_{in}\rangle \\ &= \langle\beta_{out}|b_{out}(\vec{P},s)|\alpha_{in}\rangle \\ &= \langle\beta_{out}|b_{in}(\vec{p},s)|\alpha_{in}\rangle + \langle\beta_{out}|b_{out}(\vec{p},s) \quad b_{in}(\vec{p},s)|\alpha_{in}\rangle \end{aligned} \tag{4.111}$$

Like in the scalar case, we consider the case that the first term is zero, and hence

$$\begin{aligned} S_{\beta p,\alpha} &= \langle\beta_{out}|b_{out}(\vec{p},s) \quad b_{in}(\vec{p},s)|\alpha_{in}\rangle \\ &= \not{p}\frac{1}{z}\int d^3x\langle\beta_{out}|f_p^*(x)\overline{u}(\vec{p},s)\gamma^0\Psi(x)|_{x^0\to-\infty}^{x^0\to+\infty}|\alpha_{in}\rangle \\ &= \not{p}\frac{1}{z}\int d^4x\langle\beta_{out}|\partial_0(f_P^*(x)\overline{u}(\vec{p},s)\gamma^0\Psi(x))|\alpha_{in}\rangle. \end{aligned} \tag{4.112}$$

After straightforward calculations, we arrive at

$$\begin{aligned} S_{\beta p,\alpha} &= \not{p}\frac{1}{z}(\quad i)\int d^4x\langle\beta_{out}|f_p^*(x)\overline{u}(i\gamma^\mu\partial_\mu \quad m)\Psi(x)|\alpha_{in}\rangle \\ &= \not{p}\frac{1}{z}(\quad i)\int d^4x f_p^*(x)\overline{u}(\vec{p},x)D_x\langle\beta_{out}|\Psi(x)|\alpha_{in}\rangle. \end{aligned} \tag{4.113}$$

Compared with the scalar case, $f_p^*(x)\overline{u}(\not{p}, s)D_x$ appears in S, just as $f_p^*(x)k_x$ as shown in eq. (4.101) for the scalar case. For the general case, we can get

$$\begin{aligned} \langle p_1^{s_1'} p_2^{s_2'} \quad p_{m\ out}^{s_m'} | q_1^{s_1} q_2^{s_2} \quad q_{l\ in}^{s_l} \rangle &= (\frac{1}{\overline{Z}})^{m+l} \prod_{i=1}^{m} (i \int d^4 y_i f_{p_i}^*(y_i) \overline{u}(\not{p}_i, s_i') D_{y_i}) \\ &\prod_{j=1}^{l} (i \int d^4 x_j f_{q_j}(x_j) v(\not{q}_j, s_j) D_{x_j}) \\ &\langle 0 | T \Psi^\dagger(y_1) \Psi^\dagger(y_2) \quad \Psi^\dagger(y_m) \Psi(x_1) \Psi(x_2) \quad \Psi(x_l) | 0 \rangle. \end{aligned} \tag{4.114}$$

LSZ reduction formula for gauge bosons

A free gauge boson is expanded as

$$A^\mu = \int d^3 p \sum_{\lambda=\pm 1} (\epsilon_\lambda^\mu a_\lambda(\not{p}) f_p(x) + \epsilon_\lambda^{\mu *} a_\lambda^\dagger(\not{p}) f_p^*(x)), \tag{4.115}$$

with a polarization vector ϵ_λ^μ for a helicity λ. After calculations similar to the scalar and the fermion cases, we arrive at

$$\begin{aligned} \langle p_1^{\lambda_1'} p_2^{\lambda_2'} \quad p_{m\ out}^{\lambda_m'} | q_1^{\lambda_1} q_2^{\lambda_2} \quad q_{l\ in}^{\lambda_l} \rangle &= (\frac{1}{\overline{Z}})^{m+l} \prod_{i=1}^{m} (i \int d^4 y_i f_{p_i}^*(y_i) (\epsilon_{\lambda_i'}^{\mu_i})^* D_{y_i}) \\ &\prod_{j=1}^{l} (i \int d^4 x_j f_{q_j}(x_j) \epsilon_{\lambda_j}^{\nu_j} D_{x_j}) \\ &\langle 0 | T A_{\mu 1}^\dagger(y_1) A_{\mu 2}^\dagger(y_2) \quad A_{\mu m}^\dagger(y_m) A_{\nu 1}(x_1) A_{\nu 2}(x_2) \quad A_{\nu l}(x_l) | 0 \rangle. \end{aligned} \tag{4.116}$$

4.3.2 Scattering Cross Section

Number of Collisions

Consider a scattering process with two beams of particles of relative velocity $\overline{v}_{rel}$ and interaction cross section σ. Suppose one beam is composed of particle 1 with number density n_1 and the other is composed of particle 2 with number density n_2. From Fig. 2.3, for a particle 2 at rest,

the number of collisions in time period T is

$$N_2 = (\overline{v}_{rel}T) \quad \sigma \quad n_1. \tag{4.117}$$

Since the particle density of beam 2 is n_2, in volume V and time period T, the number of collision is

$$N_{total} = VTn_1n_2\overline{v}_{rel}\sigma. \tag{4.118}$$

Relative Velocity

For the relative velocity $\overline{v}_{rel}$, consider

$$p_1^\mu = \begin{pmatrix} p_1^0 \\ \vec{p}_1 \end{pmatrix}, \tag{4.119}$$

$$p_2^\mu = \begin{pmatrix} p_2^0 \\ \vec{p}_2 \end{pmatrix}. \tag{4.120}$$

For the head-on collision,

$$\overline{v}_{rel} = \vec{j}\vec{v}_1 \quad \vec{v}_2\vec{j} = \begin{vmatrix} \vec{p}_1 & \vec{p}_2 \\ p_1^0 & P_2^0 \end{vmatrix}. \tag{4.121}$$

In the general frame, we find

$$\overline{v}_{rel} = \frac{\sqrt{(p_1 \ \ p_2)^2 \quad m_1^2 \ \ m_2^2}}{p_1^0 \ \ p_2^0}. \tag{4.122}$$

Scattering Amplitude for a $q_1q_2 \;!\; p_1p_2 \quad p_m$ Process

Corresponding to the normalization of the complete set, $\int \frac{d^3p}{(2\pi)^3 2p_0} |p\rangle\langle p| = 1$, the number of collisions for the final state with a momentum $\vec{p}$ between $\vec{p}_j$ and $\vec{p}_j + d\vec{p}_j$ is

$$\begin{aligned} dN &= \prod_{i=1}^{m} \frac{d^3p_i}{(2\pi)^3 2p_i^0} \langle\alpha|S^\dagger|p_1p_2 \quad p_m\rangle\langle p_1p_2 \quad p_m|S|\alpha\rangle \qquad (4.123) \\ &= \prod_{i=1}^{m} \frac{d^3p_i}{(2\pi)^3 s p_i^0} |M_{\beta\alpha}|^2 [(2\pi)^4\delta^4(\sum_{i=1}^{m} p_i \quad q_1 \quad q_2)]^2 \\ &= \prod_{i=1}^{m} \frac{d^3p_i}{(2\pi)^3 2p_i^0} |M_{\beta\alpha}|^2 (2\pi)^4\delta^4(\sum_{i=1}^{m} p_i \quad q_1 \quad q_2)(2\pi)^4\delta^4(0). \end{aligned}$$

Using

$$\begin{aligned} (2\pi)\delta(0) &= \int_{-\infty}^{\infty} dt = T \qquad (4.124) \\ (2\pi)^3\delta^3(0) = \int d^3x &= V, \qquad (4.125) \end{aligned}$$

we get

$$\begin{aligned} dN &= VT \prod_{i=1}^{m} \frac{d^3p}{(2\pi)^3 2p_i^0} |M_{\beta\alpha}|^2 (2\pi)^4\delta^4(\sum_{i=1}^{m} p_i \quad q_1 \quad q_2) \qquad (4.126) \\ &= VT n_1 n_2 \overline{v}_{rel} d\sigma. \qquad (4.127) \end{aligned}$$

The normalization condition

$$\begin{aligned} \langle p|q\rangle &= (2\pi)^3 2p_0 \delta^3(\vec{p} \quad \vec{q}) \qquad (4.128) \\ \Rightarrow \quad \langle p|p\rangle &= 2p_0(2\pi)^3\delta^3(0) = 2p_0 V = \text{the number of } p\text{-states}, \qquad (4.129) \end{aligned}$$

means that $2p^0$ is the number density. Thus,

$$n_1 n_2 \overline{v}_{rel} = (2q_1^0)(2q_2^0) \frac{\sqrt{(q_1q_2)^2 \quad m_1^2m_2^2}}{q_1^0 q_2^0} = 4\sqrt{(q_1q_2)^2 \quad m_1^2m_2^2}, \qquad (4.130)$$

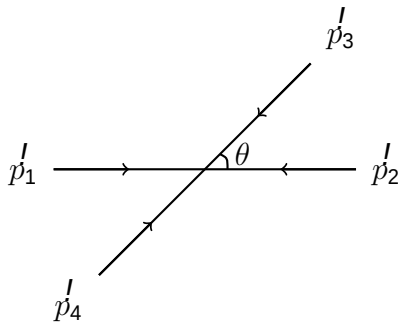

Figure 4.10: The 2 by 2 scattering process.

we find the cross-section formula for the scattering process as

$$d\sigma = \prod_{i=1}^{m} \frac{d^3p_i}{(2\pi)^3 2p_0} \frac{jM^2_{\beta\alpha}}{4\sqrt{(q_1q_2)^2 \quad m_1^2m_2^2}} (2\pi)^4\delta^4(\sum_{i=1}^{m} p_i \quad q_1 \quad q_2). \tag{4.131}$$

Cross Section for a 2-by-2 Scattering

We consider a 2-by-2 scattering in the center-of-mass (C.O.M) frame. Set the momentum for the initial two particles and the final two particles as (see Fig. 4.10)

$$p_i^\mu = \begin{pmatrix} p_i^0 \\ p_i' \end{pmatrix}. \tag{4.132}$$

For the initial particles, $i = 1,\ 2$, while for the final particles, $i = 3,\ 4$. In C.O.M. frame, the 4 momentum conservation is expressed as

$$p_1^0 + p_2^0 = p_3^0 + p_4^0, \tag{4.133}$$

$$p_1' + p_2' = p_3' + p_4' = 0. \tag{4.134}$$

The scattering cross-section is given by

$$\sigma = \int \frac{d^3p_3}{(2\pi)^3 sp_3^0} \frac{d^3p_4}{(2\pi)^3 2p_4^0} \frac{jM_{\alpha\beta}j^2}{4\sqrt{(p_1p_2)^2 \quad m_1^2m_2^2}} (2\pi)^4\delta(p_3 + p_4 \quad p_1 \quad p_2) \tag{4.135}$$

phase space integral $jM_{\beta\alpha}j^2$.

The phase integral can be calculated as

$$\begin{aligned} & \int \frac{d^3p_3}{(2\pi)^3 2p_3^0}\frac{d^3p_4}{(2\pi)^3 2p_4^0}\frac{1}{4\sqrt{(p_1p_2)^2 \quad m_1^2m_2^2}}(2\pi)^4\delta(p_3+p_4 \quad p_1 \quad p_2) \qquad (4.136)\\ = & \int \frac{d^3p_3}{(2\pi)^3 2p_3^0}\frac{1}{2p_4^0}\frac{1}{4\sqrt{(p_1p_2)^2 \quad m_1^2m_2^2}}(2\pi)\delta(p_3+p_4 \quad p_1 \quad p_2). \end{aligned}$$

For $i = 3, 4$,

$$\begin{aligned} (p_i^0)^2 = \mathbf{j}\mathbf{\dot{p}}_i\mathbf{j}^2 + m_i^2 \quad & \mathbf{)} \quad p_i^0\ dp_i^0 = \mathbf{j}\mathbf{\dot{p}}_i\mathbf{j}\ d\mathbf{j}\mathbf{\dot{p}}_i\mathbf{j} = \mathbf{j}\mathbf{\dot{p}}'\mathbf{j}\ d\mathbf{j}\mathbf{\dot{p}}'\mathbf{j} \qquad (4.137)\\ & \mathbf{)} \quad d^3p_3 = \mathbf{j}\mathbf{\dot{p}}_3\mathbf{j}^2\ d\mathbf{j}\mathbf{\dot{p}}_3\mathbf{j}\ d\Omega = \mathbf{j}\mathbf{\dot{p}}_3\mathbf{j}p_3^0\ dp_3^0\ d\Omega, \end{aligned}$$

where $\mathbf{\dot{p}}_3 = \quad \mathbf{\dot{p}}_4 = \mathbf{\dot{p}}'$. Considering the following identity,

$$\frac{p_3^0p_4^0\ d(p_3^0+p_4^0)}{p_3^0+p_4^0} = \frac{p_3^0p_4^0\ dp_3^0 + p_3^0p_4^0\ dp_4^0 (= (p_3^0)^2 dp_3^0)}{p_3^0+p_4^0} = p_3^0\ dp_3^0, \qquad (4.138)$$

we have

$$d^3p_3 = \mathbf{j}\mathbf{\dot{p}}'\mathbf{j}\frac{p_3^0p_4^0\ d(p_3^0+p_4^0)}{p_3^0+p_4^0}d\Omega. \qquad (4.139)$$

Finally, the phase space integral becomes

$$\frac{1}{64\pi^2}\int d\Omega\frac{\mathbf{j}\mathbf{\dot{p}}'\mathbf{j}}{(p_1^0+p_2^0)\sqrt{(p_1p_2)^2 \quad m_1^2m_2^2}}. \qquad (4.140)$$

The relative velocity in a general frame can be transformed into the C.O.M frame as

$$\begin{aligned} \overline{v}_{rel} \quad = \quad & \frac{\sqrt{(p_1p_2)^2 \quad m_1^2m_2^2}}{p_1^0p_2^0} \text{ in general frame} \qquad (4.141)\\ ! \quad & \left|\frac{\mathbf{\dot{p}}}{p_1^0} \quad \frac{(\quad \mathbf{\dot{p}}\ )}{p_2^0}\right| = \frac{p_1^0+p_2^0}{p_1^0p_2^0}\mathbf{j}\mathbf{\dot{p}}\mathbf{j} \text{ in C.O.M frame.} \end{aligned}$$

We introduce Mandelstam's variables:

$$s = (p_1 + p_2)^2, \tag{4.142}$$

$$t = (p_1 \quad p_2)^2, \tag{4.143}$$

$$u = (p_1 \quad p_4)^2. \tag{4.144}$$

Since in the C.O.M frame

$$s = (p_1 + p_2)^2 = (p_1^0 + p_2^0)^2, \tag{4.145}$$

we get the final form of the cross-section formula:

$$\sigma = \frac{1}{64\pi^2 s} \int d\Omega \, \frac{|\vec{p}'|}{|\vec{p}|} |M_{\beta\alpha}^2|. \tag{4.146}$$

Differential Cross Section

In a $2 \to 2$ scattering, $|M_{\beta\alpha}|^2$ is independent of ϕ, and thus $d\Omega = \sin\theta \, d\theta d\phi = 2\pi \sin\theta \, d\theta = 2\pi \, d\cos\theta$ for $0 \quad \theta \quad \pi$. Hence, the differential cross section is given by

$$\frac{d\sigma}{d\cos\theta} = \frac{1}{32\pi s} \frac{|\vec{p}'|}{|\vec{p}|} |M_{\beta\alpha}|^2. \tag{4.147}$$

Decay width

Let us consider the decay of a particle at rest into several particles. The initial state four-momentum is given by

$$p_0^\mu = \begin{pmatrix} m \\ \vec{0} \end{pmatrix}, \tag{4.148}$$

and we define the four-momentum of a final state i by

$$p_i^\mu = \begin{pmatrix} p_i^0 \\ \vec{p}_i \end{pmatrix}. \tag{4.149}$$

From the energy-momentum conservation, there are

$$\sum_{i=1} p_i^0 = m, \tag{4.150}$$

$$\sum_{i=1} \vec{p}_i = 0. \tag{4.151}$$

Define the decay width Γ as the probability of the decay per particle per second, which has mass dimension 1. The number of initial particles is $\langle p_0 | p_0 \rangle = s p_0^0 (2\pi)^3 \delta^3(0) = 2mV$, then,

$$\begin{aligned} d\Gamma &= \frac{dN_{decay}}{T(2mV)} \\ &= \prod_{j=1} \frac{d^3 p_j}{(2\pi)^3 2p_j^0} \frac{|M|^2}{2m} (2\pi)^4 \delta(\sum_{i=1} p_i - p_0). \end{aligned} \tag{4.152}$$

CHAPTER 5

HIGGS-PORTAL DM MODEL

One shortcoming of SM is that it does not include DM. A DM candidate should fit three conditions:

1. Electrically neutral
2. Stable
3. Cold dark matter (CDM)

It should be electrically neutral because until now, DM has not been detected optically, which means it can not interact with the electromagnetic field. It should be stable because the DM particles exist in the present universe, so its age should be no less than the age of the universe. Also, a DM particle weakly interacts with the SM particles, and except for its interaction with gravity, there is no direct evidence of its existence. It should be cold, which means at the time of structure formation, DM particles are sufficiently non-relativistic.

5.1 Particle Content

In the Higgs-portal DM model ([23, 24, 25]) the DM particles interact with the SM particles only through the Higgs bosons. The particle content of the Higgs-portal DM model is shown in Table 5.1, where S is a real scalar particle, which is the DM candidate added to the SM. Also, a new symmetry Z_2 is added, under which S is odd, while others are positive. Imposing the conservation of Z_2 symmetry to the Lagrangian, a single S can not interact with other particles

	$SU(3)_C$	$SU(2)_L$	$U(1)_Y$	Z_2
q_L^i	3	2	1/6	+
u_R^i	3	1	2/3	+
d_R^i	3	1	1/3	+
l_L^i	1	2	1/2	+
e_R^i	1	1	1	+
H	1	2	1/2	+
S	1	1	0	

Table 5.1: Higgs-portal DM model particles content

directly. Also, Z_2 symmetry forbids the linear and cubic terms of S. It has a vanishing VEV, which ensures its stability. The Lagrangian of the model is given by

$$\mathcal{L} = \mathcal{L}_{SM} + \frac{1}{2}(\partial_\mu S)(\partial^\mu S) \quad \frac{m_0^2}{2}S^2 \quad \frac{\lambda_S}{4}S^4 \quad \lambda S^2 H^\dagger H. \tag{5.1}$$

Here, $\mathcal{L}_{SM}$ is the SM Lagrangian discussed in the previous chapter. The second term is the kinetic term of the DM S, which is followed by the mass term and the four-point interaction term. The last term is the interaction between S and the Higgs doublet. The self-interaction, $\lambda_S S^4$, since is just an interaction among DM particles themselves and can not produce SM particles, is not important for DM physics, and we ignore it by assuming it is very small.

After spontaneous symmetry breaking of the $SU(2)_L \quad U(1)_Y$ symmetry and with the help of the unitary gauge,

$$H = \frac{1}{\sqrt{2}}\begin{pmatrix} 0 \\ v+h \end{pmatrix}, \tag{5.2}$$

the Lagrangian becomes

$$\mathcal{L} = \mathcal{L}_{SM} + \frac{1}{2}(\partial_\mu S)(\partial^\mu S) \quad \frac{1}{2}m_D^2 S^2 \quad \lambda v h S^2 \quad \frac{1}{2}\lambda h^2 S^2, \tag{5.3}$$

with $m_D^2 = m_0^2 + \lambda v^2$ and $v = 246$ GeV. The Higgs-portal DM physics is controlled by only two

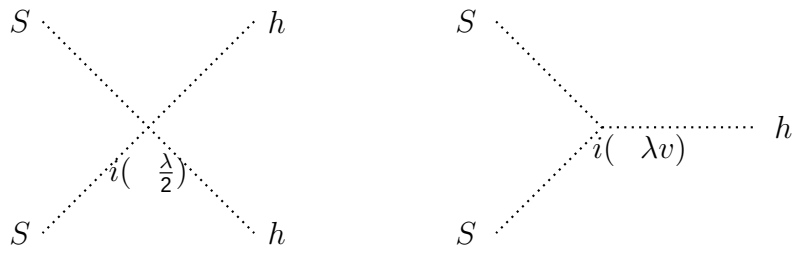

Figure 5.1: The couplings between S and h.

free parameters: the mass of DM m_D and the mixed-quartic coupling λ. The most important terms for the Higgs-portal DM physics are the last two terms through which the Higgs-portal DM interacts with the SM particles, as shown in Fig. 5.1.

5.2 DM Particles' Annihilation Cross-Sections

5.2.1 $SS \; ! \; hh$ process

The processes of DM particles annihilating to produce two Higgs bosons are shown in Fig. 5.2. Here, q_1, q_2 are the incoming 4 momenta, p_1, p_2 are the outgoing 4 momenta, and s, t, and u are Mandelstam's variables. We have

$$iM_4 = i(\ 2\lambda) \text{ for figure 2,} \tag{5.4}$$

$$iM_s = i\frac{12\lambda^2 v^2}{s\ \ m_h^2} \text{ for figure 1,} \tag{5.5}$$

$$iM_t = i\frac{4\lambda^2 v^2}{t\ \ m_s^2} \text{ for figure 3,} \tag{5.6}$$

$$iM_u = i\frac{4\lambda^2 v^2}{u\ \ m_s^2} \text{ for figure 4.} \tag{5.7}$$

So, for the process of $S + S \; ! \; h + h$,

$$iM_{hh} = iM_4 + iM_s + iM_t + iM_u. \tag{5.8}$$

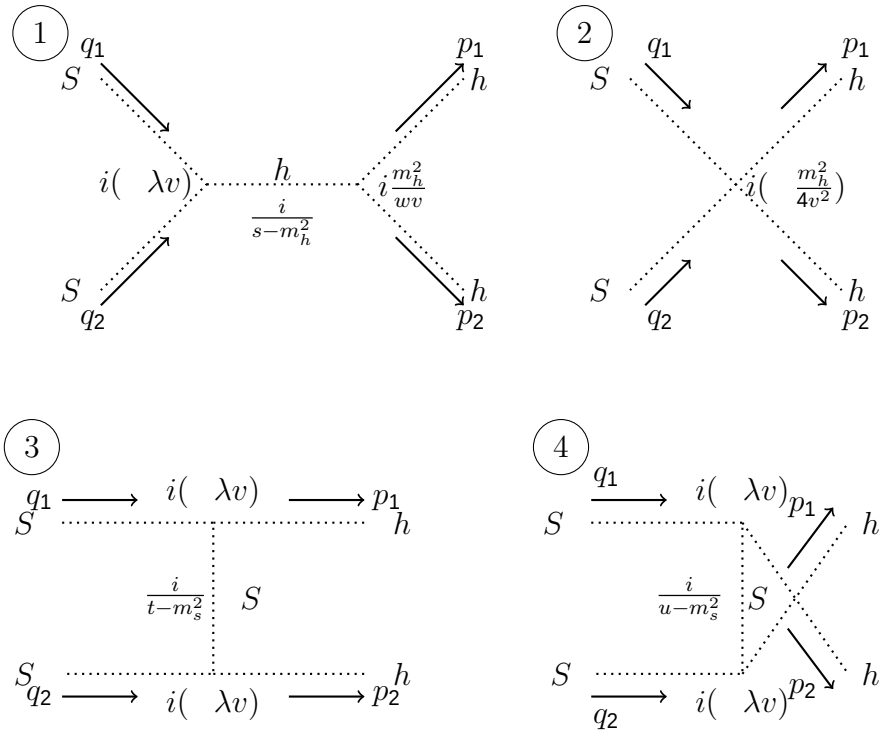

Figure 5.2: DM pair annihilation processes to a pair of Higgs bosons.

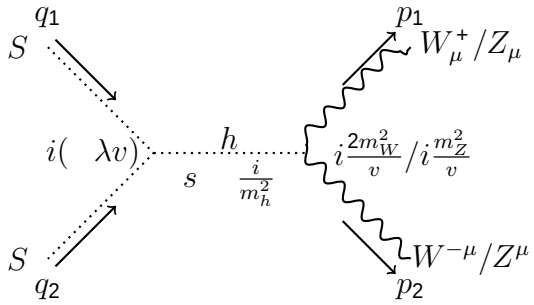

Figure 5.3: DM pair annihilation processes to W and Z bosons.

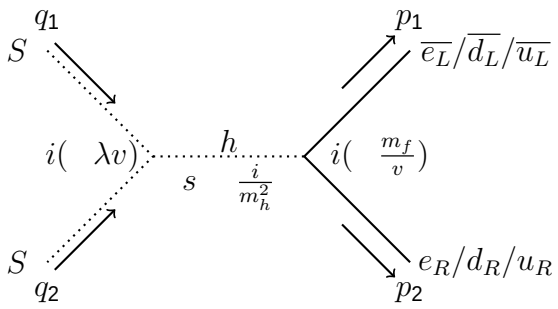

Figure 5.4: DM pair annihilation processes to fermions.

5.2.2 $SS \quad W^+W^-, ZZ$ process

This process is shown in Fig. 5.3. When the final states are W bosons,

$$\begin{aligned} iM_{WW} &= 2i(\quad \lambda v)\frac{i}{s \quad m_h^2} i\frac{2m_W^2}{v}\epsilon_{\alpha_1}^{*\mu}\epsilon_{\alpha_2\mu}^{*} \\ &= i4\lambda\frac{m_W^2}{s \quad m_h^2}\epsilon_{\alpha_1}^{*\mu}\epsilon_{\alpha_2\mu}^{*}, \end{aligned} \tag{5.9}$$

where ϵ_α^μ and $\epsilon_{\alpha\mu}$ are wave functions of the bosons with helicity α, For the squared amplitude, $M^\dagger M$, all helicities are summed.

When the final states are Z bosons,

$$\begin{aligned} iM_{ZZ} &= 4i(\quad \lambda v)\frac{i}{s \quad m_h^2} i\frac{m_z^2}{v}\epsilon_{\alpha_1}^{*\mu}\epsilon_{\alpha_2\mu}^{*} \\ &= i4\lambda\frac{m_Z^2}{s \quad m_h^2}\epsilon_{\alpha_1}^{*\mu}\epsilon_{\alpha_2\mu}^{*}. \end{aligned} \tag{5.10}$$

5.2.3 $SS \; ! \; f\overline{f}$ process

f represents an SM fermion, such as electron e, electron-type neutirno ν, up quark u, down quark d, and corresponding fermions in the other generations. In Fig. 5.4, m_f is the mass of

the fermion we consider here. The scattering amplitude is given by

$$\begin{aligned} iM_{ff} &= i(\quad \lambda v)\frac{i}{s \quad m_h^2} i(\quad \frac{m_f}{v})\overline{u_f} v_f \\ &= i\lambda \frac{m_f}{s \quad m_h^2}\overline{u_f} v_f, \end{aligned} \tag{5.11}$$

where u_f and v_f are the fermion and anti-fermion wave functions, respectively.

5.2.4 Thermal Average of the Product of Interaction-cross Section and Relative Velocity $\langle\sigma v\rangle$

We calculate the thermally averaged cross section times the relative velocity $\langle\sigma v\rangle$ for the DM pair annihilation processes [26]. For a pair of particles, their relative velocity is expressed as

$$v_{ij} = \frac{\sqrt{(p_i p_j)^2 \quad m_i^2 m_j^2}}{E_i E_j}, \tag{5.12}$$

with p_i and E_i the four-momentum and the energy of particle i, respectively. At equilibrium, the number density is

$$n_i^{eq} = \frac{g_i}{(2\pi)^3}\int d^3 p_i f_i, \tag{5.13}$$

where p_i is the three-momentum of particle i, and f_i is the equilibrium distribution function. Since we study DM particles at decoupling, they should be non-relativistic, so we can use the Maxwell-Boltzmann approximation and calculate the thermal average as

$$\langle\sigma_{ij} v_{ij}\rangle = \frac{\int d^3 p_i d^3 p_j f_i f_j \sigma_{ij} v_{ij}}{\int d^3 p_i d^3 p_j f_i f_j}, \tag{5.14}$$

with

$$f_i = e^{-E_i/T}. \tag{5.15}$$

We define $\langle\sigma v\rangle$ as

$$\langle\sigma v\rangle = \sum_{ij} \langle\sigma_{ij} v_{ij}\rangle \frac{n_i^{eq}}{n_{eq}} \frac{n_j^{eq}}{n_{eq}} = \frac{A}{n_{eq}^2}, \tag{5.16}$$

with $n_{eq} = \sum_i n_i^{eq}$ and

$$n_i^{eq} = \frac{g_i}{(2\pi)^3} \int d^3p_i e^{-E_i/T} = \frac{T}{s\pi^2} g_i m_i^2 K_2\left(\frac{m_i}{T}\right), \tag{5.17}$$

where K_2 is the modified Bessel function of the second kind of order 2. We calculate A in the $\langle\sigma v\rangle$ as

$$\begin{aligned} A &= \sum_{ij} \langle\sigma_{ij} v_{ij}\rangle n_i^{eq} n_j^{eq} = \sum_{ij} \frac{g_i g_j}{(2\pi)^6} \int d^3p_i d^3p_j f_i f_j \sigma_{ij} v_{ij} \\ &= \sum_{ij} \int W_{ij} \frac{g_i f_i d^3p_i}{(2\pi)^3 2E_i} \frac{g_j f_j d^3p_j}{(2\pi)^3 2E_j}. \end{aligned} \tag{5.18}$$

Here, W_{ij} is a dimensionless Lorentz invariant,

$$W_{ij} = 4p_{ij}\sqrt{s}\sigma_{ij} = 4\sigma_{ij}\sqrt{(p_i p_j)^2 \quad m_i^2 m_j^2} = 4E_i E_j \sigma_{ij} v_{ij}, \tag{5.19}$$

and

$$p_{ij} = \frac{[s \quad (m_i + m_j)^2]^{1/2}[s \quad (m_i \quad m_j)^2]^{1/2}}{2\sqrt{s}} \tag{5.20}$$

is the momentum of particle i in the center of mass frame of the particle pair i and j. Thus, we have

$$A = \sum_{ij} \int g_i g_j W_{ij} e^{-E_i/T} e^{-E_j/T} \frac{d^3p_i}{(2\pi)^3 2E_i} \frac{d^3p_j}{(2\pi)^3 2E_j}, \tag{5.21}$$

where p_i and p_j are the three-momenta and E_i and E_j are the energies of the incoming particles. It is easy to prove that

$$d^3p_i d^3p_j = 4\pi \mathbf{j} \mathbf{p}_i' \mathbf{j} E_i dE_i 4\pi \mathbf{j} \mathbf{p}_j' \mathbf{j} E_j dE_j \frac{1}{2} d\cos\theta, \tag{5.22}$$

with θ the angle between p_i and p_j, as shown in Fig. 4.10. Defining the new variables as

$$E_+ = E_i + E_j, \tag{5.23}$$

$$E_- = E_i \quad E_j, \tag{5.24}$$

$$s = m_i^2 + m_j^2 + 2E_iE_j \quad 2\mathbf{j}\mathbf{p}_i'\mathbf{j}\mathbf{j}\mathbf{p}_j'\mathbf{j}\cos\theta, \tag{5.25}$$

we get

$$\frac{d^3p_i}{(2\pi)^3 2E_i}\frac{d^3p_j}{(2\pi)^3 2E_j} = \frac{1}{(2\pi)^4}\frac{dE_+ dE_- ds}{8}. \tag{5.26}$$

The integration regions $E_i \quad m_i, E_j \quad m_j$, and $\mathbf{j}\cos\theta\mathbf{j} \quad 1$ are expressed as

$$s \quad (m_i + m_j)^2, \tag{5.27}$$

$$E_+ \quad \mathbf{p}_{\overline{s}}, \tag{5.28}$$

$$\left| E_- \quad E_+ \frac{m_j^2 \quad m_i^2}{s} \right| \quad 2p_{ij}\sqrt{\frac{E_+^2 \quad s}{s}}. \tag{5.29}$$

In the integration of A, the term $e^{-E_i/T}e^{-E_j/T}$ is related to E_+, while W_{ij} is related to s. Therefore the integration over E_- can be integrated out as

$$\int dE_- = 4p_{ij}\sqrt{\frac{E_+^2 \quad s}{s}}. \tag{5.30}$$

Hence,

$$\frac{d^3p_i}{(2\pi)^3 2E_i}\frac{d^3p_j}{(2\pi)^3 2E_j} = \frac{1}{(2\pi)^4}\frac{p_{ij}}{2}\sqrt{\frac{E_+^2 \quad s}{s}}dE_+ ds. \tag{5.31}$$

Under this condition, A has the form

$$A = \frac{T}{32\pi^4}\sum_{ij}\int_{(m_i+m_j)^2}^{\infty} ds g_i g_j p_{ij} W_{ij} K_1\left(\frac{p_{\bar{s}}}{T}\right), \tag{5.32}$$

with K_1 the modified Bessel function of the second kind of order 1.

Since we are considering the pair annihilation process of DM particles, $g_i = g_j = 1$ and $m_i = m_j = m_D$. Hence,

$$\begin{aligned} p_{ij} &= \frac{[s \quad (m_i+m_j)^2]^{1/2}[s \quad (m_i \quad m_j)^2]^{1/2}}{2p_{\bar{s}}} \\ &= \frac{\sqrt{s \quad 4m_D^2}}{2}, \end{aligned} \tag{5.33}$$

The thermal averaged cross section is given by

$$\langle\sigma v\rangle = \frac{1}{n_{eq}^2}\frac{m_D}{64\pi^4 x}\int_{4m_D^2}^{\infty}\hat{\sigma}(s)p_{\bar{s}}K_1\left(\frac{x p_{\bar{s}}}{m_D}\right)ds, \tag{5.34}$$

where

$$x = \frac{m_D}{T}, \tag{5.35}$$

$$\begin{aligned} n_{eq} &= \frac{g_i}{2\pi^2}\frac{m_D^2}{x}K_2(x) \\ &= \frac{1}{2\pi^2}\frac{m_D^2}{x}K_2(x), \end{aligned} \tag{5.36}$$

$$\begin{aligned} \hat{\sigma}(s) &= 4E_1E_2\sigma v g_i^2\sqrt{1 \quad \frac{4m_D^2}{s}} \\ &= \hat{\sigma}g_i^2\sqrt{1 \quad \frac{4m_D^2}{s}}. \end{aligned} \tag{5.37}$$

Here, $g_i = 1$ is the internal degree of freedom for this scalar DM model, and $\hat{\sigma} = 4E_1E_2\sigma v$, with σ being the summation of pair annihilation cross sections for all possible final states ([23], [27]): $\hat{\sigma} = \hat{\sigma}_{ff} + \hat{\sigma}_{ZZ} + \hat{\sigma}_{WW} + \hat{\sigma}_{hh}$, where

$$\hat{\sigma}_{ff} = \sum_f \frac{\lambda^2 m_f^2}{\pi} \frac{1}{(s \quad m_h^2)^2 + m_h^2\Gamma_h^2} \frac{(s \quad 4m_f^2)^{1.5}}{p\overline{s}}, \tag{5.38}$$

$$\hat{\sigma}_{ZZ} = \frac{\lambda^2}{4\pi} \frac{s^2}{(s \quad m_h^2)^2 + m_h^2\Gamma_h^2} \sqrt{1 \quad \frac{4m_Z^2}{s}} \left(1 \quad \frac{4m_Z^2}{s} + \frac{12m_Z^4}{s^2}\right), \tag{5.39}$$

$$\hat{\sigma}_{WW} = \frac{\lambda^2}{2\pi} \frac{s^2}{(s \quad m_h^2)^2 + m_h^2\Sigma_h^2} \sqrt{1 \quad \frac{4m_W^2}{s}} \left(1 \quad \frac{4m_W^2}{s} + \frac{12m_W^4}{s^2}\right), \tag{5.40}$$

$$\begin{aligned} \hat{\sigma}_{hh} &= \frac{\lambda^2}{4\pi} \sqrt{1 \quad \frac{4m_h^2}{s}} \left[\left(\frac{s + 2m_h^2}{s \quad m_h^2} \right)^2 \quad \frac{16\lambda v^2}{s \quad 2m_h^2} \frac{s + 2m_h^2}{s \quad m_h^2} F(\xi) \right. \\ &+ \left. \frac{32\lambda^2 v^4}{(s \quad 2m_h^2)^2} \left(\frac{1}{1 \quad \xi^2} + F(\xi) \right) \right], \end{aligned} \tag{5.41}$$

with $F(\xi) \quad \text{arctanh}(\xi)/\xi$ and $\xi \quad \sqrt{(s \quad 4m_h^J 2)(s \quad 4m_D)^2}/(s \quad 2m_h^2)$. The Higgs boson decay width is $\Gamma_h = 4.07 \quad 10^{-3}$.

5.3 DM Relic Density

We now solve the Boltzmann equation to evaluate the DM relic density. In the standard BBC,

$$\frac{dY_D}{dx} = \quad \lambda_0 \frac{h\sigma v i}{x^2} (Y_D^2 \quad (Y_D^{eq})^2), \tag{5.42}$$

$\lambda_0 = \frac{s(T=m_D)}{H(T=m_D)}$. Since the DM particles were in thermal equilibrium at high temperatures, we set the initial condition to be $Y_D(x) = Y_D^{eq}(x)$ for $x \quad 1$. The DM yield at present is evaluated by $Y_D(x \;!\; 1)$. Then, the DM energy density parameter at present is given by

$$\Omega_D h^2 = \frac{m_D Y_D(x \;!\; 1) s_0}{\rho_{crit}^0/h^2}, \tag{5.43}$$

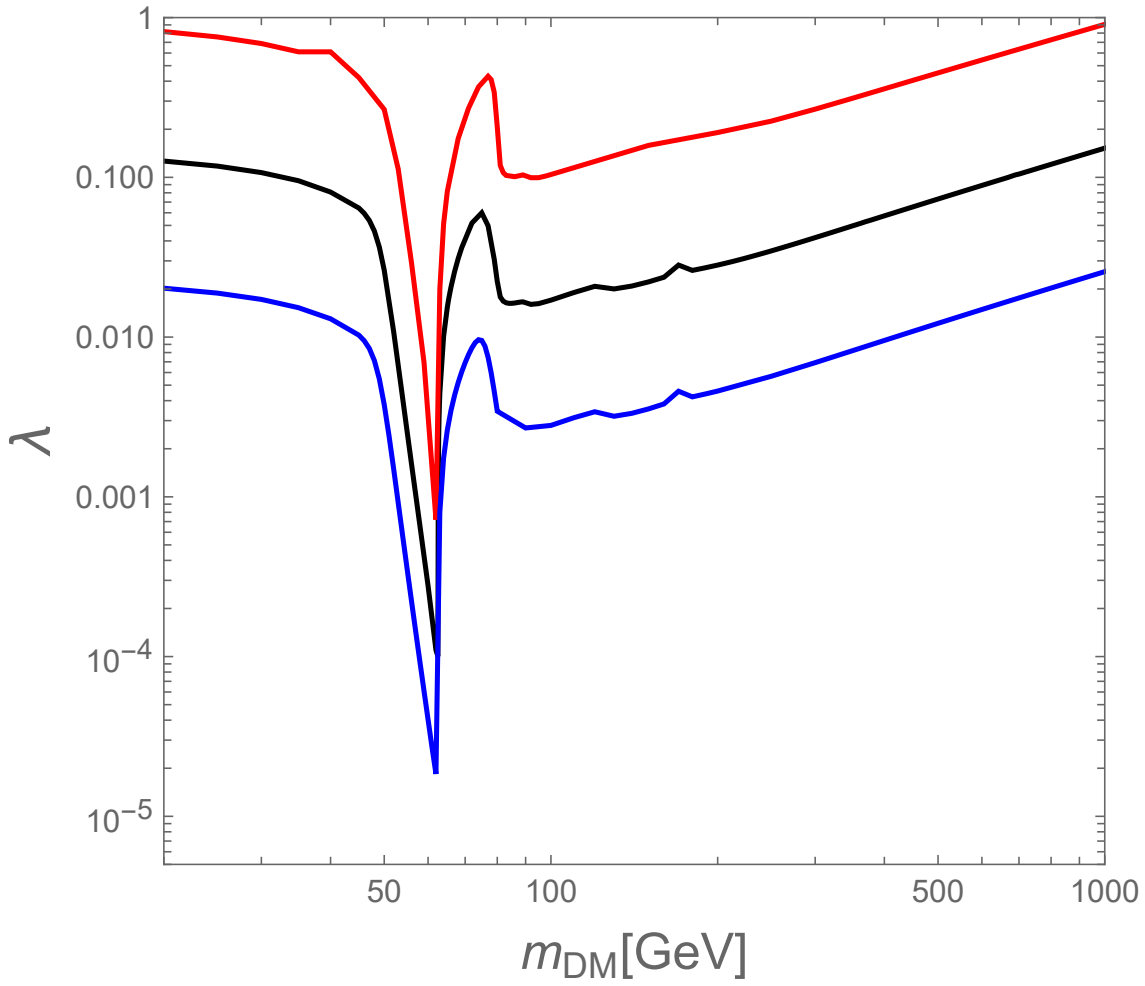

Figure 5.5: λ m_D relations that fit for the observed DM relic density. The curves from top to bottom show the relations in the RS brane cosmology with $x_t = 500$, the 4 dimensional Big Bang cosmology, and the GB brane cosmology with $x_t = 10000$.

where s_0 ' 2.89 10^3[cm^{-3}] is the entropy density of the present Universe, ρ^0_{crit} ' $1.05h^2$ 10^{-5}[GeV/cm^3] is the critical density of the present Universe, and $h = H_0/(100\text{km/s/Mpc})$ is the normalized Hubble constant. As we have discussed, the Higgs-portal DM model has only two free parameters, the DM mass m_D and the DM-Higgs interaction coupling λ, and thus the DM energy density of Eq. (5.43) is a function of λ and m_D. In order to reproduce the observed DM relic density determined the Planck 2018 observation [28], $\Omega_D h^2 = 0.12$, the coupling λ is determined as a function of m_D.

In the 5 dimensional brane-world cosmologies, the Boltzmann equation becomes Eq. (3.22)

with the condition Eq. (3.21):

$$\frac{dY_D}{dx} = \quad \frac{\lambda_0}{x^2}\frac{\hbar\sigma v i}{(x_t/x)^\gamma}(Y_D^2 \quad (Y_D^{eq})^2). \tag{5.44}$$

Here, the parameter $\gamma = 2$ represents the RS brane-world cosmology, while $\gamma = \quad 2/3$ represents the GB brane-world cosmology. As discussed before, x_t is a free parameter as long as the BBN constraint $T_t > 1$ MeV. As a benchmark, we set $x_t = 500$ for the RS cosmology, while $x_t = 10000$ for the GB cosmology. Repeating the same analysis as in the 4-dimensional case, we determine λ as a function of m_D.

We show our results in Fig. 5.5. The black solid curve depicts the result in the BBC, while the red (top) and blue (bottom) curves correspond to the results in the RS and GB cosmologies, respectively. The RS and GB brane-world cosmological effects shift the result in the BBC upward and downward, respectively. The difference between the results in the Big Bang and brane-world cosmologies becomes wider as x_t gets larger. Since $T_t = \frac{m_D}{x_t}$, we find $m_D[\text{GeV}] \gtrsim 10^{-3} x_t$ from the BBN bound of $T_t \gtrsim 1$ MeV. The choice of $x_t = 10000$ is consistent with the BBN bound for the DM mass range ($m_D \quad 20$ GeV) shown in Fig. 5.5.

5.4 DM Direct and Indirect Detection

There are three ways to detect DM: making DM in accelerators, direct DM detection in terrestrial labs, and indirect DM detection through cosmic rays created by DM annihilations and late-time decays. In this section, we consider the direct and indirect DM detections to identify the allowed parameter regions from the experimental constraints.

5.4.1 DM Direct Detection

Since the halo of our Milky Way Galaxy is filled with DM particles and the Earth is moving in the halo, we should have a flux of the DM particles. There have been lots of efforts to detect WIMP DMs on Earth directly by different kinds of detectors, such as cryogenic crystal

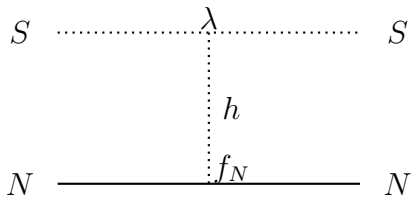

Figure 5.6: Feynman diagram for DM elastic scattering off with a nucleon (N).

detectors, noble gas scintillators, crystal scintillators, and bubble chambers. The Cryogenic Rare Event Search with Superconducting Thermometers (CRESST) [29] is an example of a cryogenic crystal detector. The XENON [30] series and the LUX-ZEPLIN (LZ) [31] are noble gas scintillators. The DAMA/LIBRA [32] experiment is an example of the crystal scintillator experiment. As for bubble chambers, one example is PICO. [33]

The Higgs-portal DM can be detected through its elastic scattering off with nucleon. See Fig. 5.6 for the Feynman diagram of the process. Here, a DM particle collides with a nucleon and then departs it. In the XENON series [30] and LZ [31] experiments, the detector consists of a tank of liquid xenon. The dark matter particle interacts with Xenon atoms, generates primary scintillation and electrons. These electrons are then drifted into the gas phase, produce secondary scintillation through electroluminescence. Until now, no evidence of colliding DM particles has been observed, so that the direct DM detection experiments provide us with the upper bounds of the spin-independent cross-section of the Higgs-portal DM as a function of DM mass. In the model, the scattering cross-section is given by (see, for example, [34])

$$\sigma_N^{SI}(\lambda, m_D) = \frac{\lambda^2}{4m_h^4}\left(\frac{m_N}{m_D + m_N}\right)^2 \frac{f_N^2}{\pi}, \tag{5.45}$$

with an effective Higgs-nucleon coupling $f_N = 0.250$ GeV and nucleon mass m_N.

5.4.2 DM Indirect Detection

DM indirect detection experiments have been searching for an excess of cosmic rays originating from DM annihilations or decay into SM particles. Experiments of this type include the Fermi Large Area Telescope (Fermi-LAT), [35] IceCube, [36] MAGIC Cherenkov telescopes,

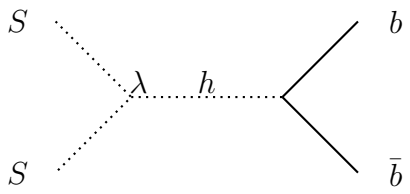

Figure 5.7: DM pair annihilation process relevant to DM indirect detection.

[37] etc. The most severe constraints have been obtained by the search results from Milky Way Dwarf Spheroidal Galaxies ([35]), which excludes a WIMP DM scenario for a DM mass less than 100 GeV if the main DM pair annihilation mode is into a bottom quark pair ($b\bar{b}$).

We calculate the cross section of the process that the Higgs-portal DM pair annihilate into $b\bar{b}$ (see Fig. 5.7 for the process diagram), which is given by

$$\langle\sigma v\rangle_0 = \frac{g_D^2}{(n_D^{eq})^2}\frac{m_D}{64\pi^4 x}\int_{4m_D^2} ds\ \sigma_{bb}(s)\,2(s \quad 4m_D^2)\sqrt{s}K_1\left(\frac{x\sqrt{s}}{m_D}\right), \tag{5.46}$$

where $\sigma_{bb}(s)$ is the DM pair annihilation cross-section into the bottom quark pair. This cross section is essentially the same as $\sigma_{bb}(s)v$ with $s = 4m_D^4$ and $v \ ! \ 0$.

5.4.3 Constraints from Direct and Indirect DM Detection Experiments

Imposing the observed DM relic density condition, we have obtained λ as a function of m_D in the Big Bang and brane-world cosmologies as shown in Fig. 5.5. Using this relation, we can calculate the cross sections in Eqs. (5.45) and (5.46) as a function of m_D and compare the resultant cross-sections with the experimental results.

Constraints from the Direct DM Detection Experiment

Along the plots shown in Fig. 5.5, we calculate the spin-independent elastic cross-section with a nucleon, and show our results in Fig. 5.8, along with the upper bound from the LZ experiment [38]. The panels from left to right correspond to the situations in the standard BBC, the RS brane-world cosmology with $x_t = 500$, and the GB brane-world cosmology with $x_t = 10000$, respectively. The regions in red are excluded since the predicted cross sections exceed the LZ

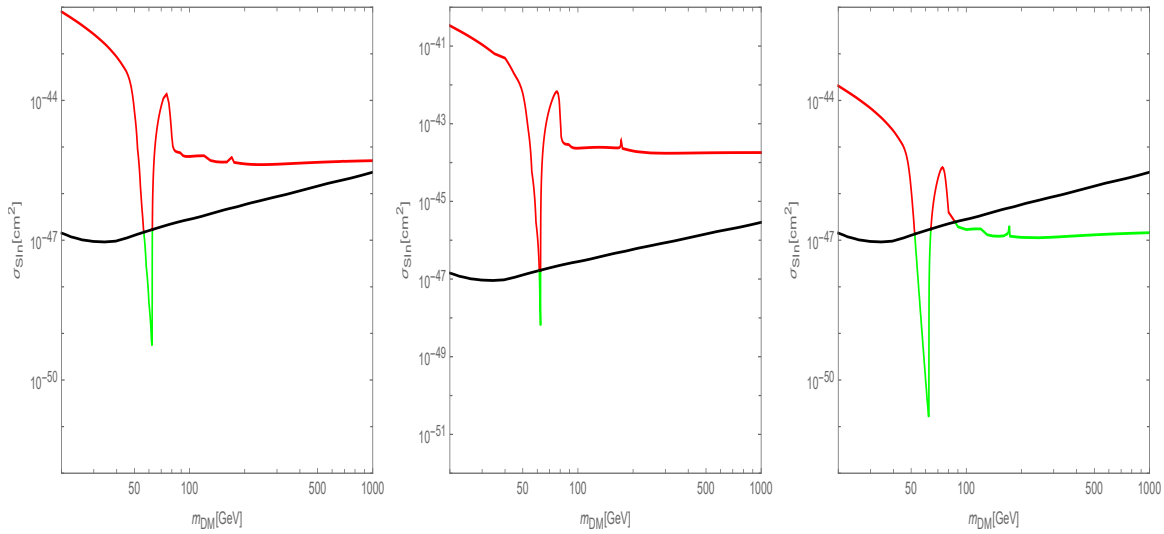

Figure 5.8: The DM-nucleon elastic scattering cross section as a function of DM mass for the standard Big Bang (left) and brane cosmologies: RS with $x_t = 500$ (middle) and GB with $x_t = 10000$ (right). The observed DM relic density of $\Omega_{DM}h^2 = 0.12$ is reproduced along the curves. In each panel, the upper bound on the cross-section from the LZ experiment is depicted by the black solid curve. The green regions are allowed.

bound (black horizontal lines). As well-known, the allowed parameter region for the Higgs-portal DM model in the standard Big Bang cosmology is very severely constrained. We have found that the allowed parameter region becomes more severely constrained in the RS brane-world cosmology. As we raise x_t further, the allowed region eventually disappears. The result in the GB brane-world cosmology is probably more interesting since this effect enlarges the allowed region and only the regions of $m_D \; . \; m_h/2$ and $m_D \; ' \; m_W$ are excluded.

Constraints from the Indirect DM Detection Experiment

Along the plots shown in Fig. 5.5, we calculate the DM pair annihilation cross-section to $b\bar{b}$ and show our results in Fig. 5.9, along with the indirect DM detection constraint from the Fermi-LAT result [39]. The panels from left to right correspond to the situations in standard BBC, the RS brane-world cosmology with $x_t = 500$, and the GB brane-world cosmology with $x_t = 10000$, respectively. Similar to the result from the direct DM detection constraint, the parameter region in the RS brane-world cosmology is more severely constrained than in the

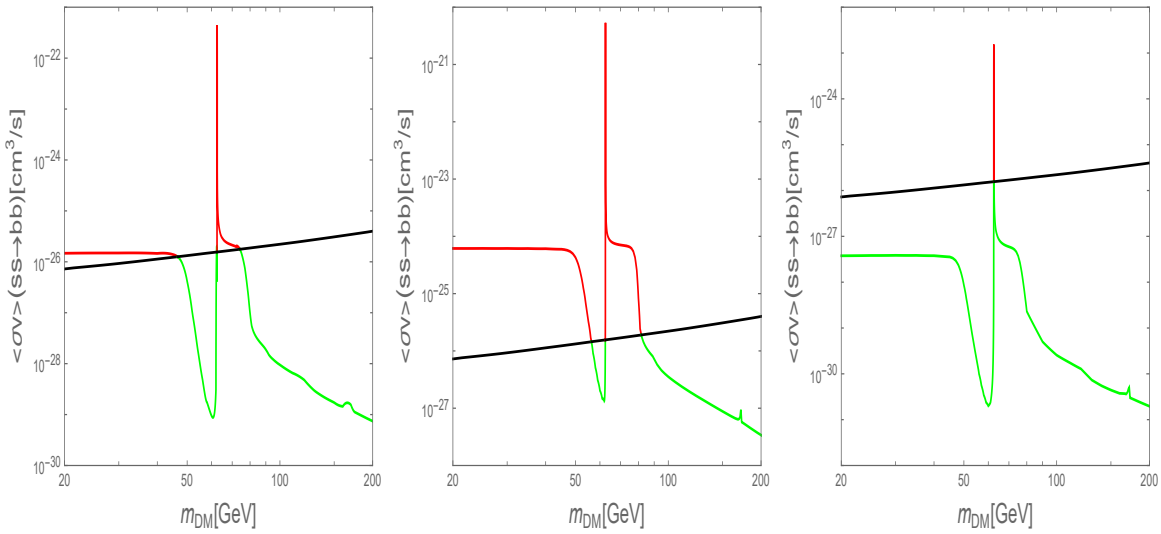

Figure 5.9: The DM pair annihilation cross-section to $b\bar{b}$ as a function of DM mass for the standard Big Bang (left) and brane cosmologies: RS with $x_t = 500$ (middle) and GB with $x_t = 10000$ (right). The observed DM relic density of $\Omega_{DM}h^2 = 0.12$ is reproduced along the curves. In each panel, the upper bound on the cross-section from the Fermi-LAT experiment is depicted by the black solid curve. The green regions are allowed.

standard BBC case, while the indirect detection experiment provides (almost) no constraint on the GB case.

5.4.4 Combined Results

Finally, we combine the results shown in Figs. 5.8 and 5.9 and show the allowed region in (λ, m_D)-plane in Fig. 5.10 [40]. The Three curves from top to bottom correspond to the results from the RS brane-world cosmology with $x_t = 500$, the standard BBC, and the GB brane-world cosmology with $x_t = 10000$, respectively. As we have already discussed, the observed DM density is reproduced along the curves from the corresponding cosmologies. The direct and indirect DM search results only allow the regions displayed in green. We have found very narrow allowed regions for the RS and the standard Big Bang cosmologies while in the GB brane-world cosmology, the large portion of the parameter space for m_D & $m_h/2$ is still allowed. For $m_D < m_h/2$, the Higgs boson can invisibly decay to a pair of the Higgs-portal DMs. Thus, the Higgs-portal DM model is also constrained by the (null) results from the search for invisible decays of the Higgs boson at the Large Hadron Collider (LHC). Since this constraint is much

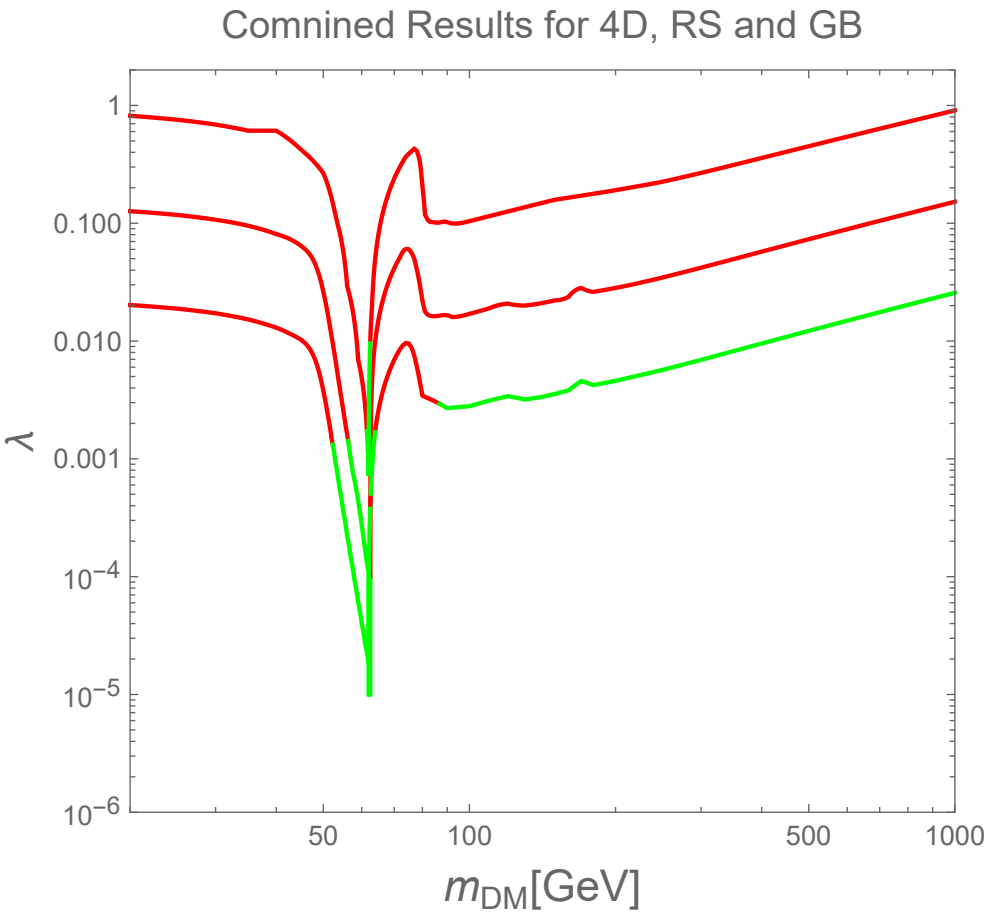

Figure 5.10: Allowed parameter region in (m_D, λ)-plane for the standard Big Bang (middle) and brane cosmologies: RS with $x_t = 500$ (top) and GB with $x_t = 10000$ (bottom). The observed DM relic density of $\Omega_{DM}h^2 = 0.12$ is reproduced along the curves. The green regions depict the allowed regions for the three cases after imposing the direct and indirect DM detection constraints.

weaker than the one from the LZ experiment for the range of $m_D > 20$ GeV [41], we don't show it. However, the LHC results provide us with the most severe constraints for m_D . 5 GeV.

CHAPTER 6

$B \quad L$ Z' PORTAL DARK MATTER MODEL

Besides the missing candidate of DM, how the neutrinos get mass is another enigma in the SM. The extension of the SM is also required to incorporate the neutrino masses. In this section, we discuss a $B \quad L$ extension of the SM [4, 5, 6, 7], where B means baryon number, and L means lepton number.

The SM Lagrangian at the tree level is invariant under the global $U(1)_B$ and $U(1)_L$ transformations:

$$\psi \quad ! \quad \psi' = e^{iQ_B\theta_B}\psi \tag{6.1}$$

$$\psi \quad ! \quad \psi' = e^{iQ_L\theta_L}\psi, \tag{6.2}$$

where θ_B and θ_L are constant and Q_B and Q_L are charges equal to baryon number B and lepton number L of the fermion ψ, respectively. A quark (anti-quark) has a baryon number $1/3$ ($1/3$), while a lepton has a baryon number 0. A lepton (anti-lepton) has a lepton number 1 (1), while a quark has 0. Both of the global symmetries are anomalous, but the difference between them, $B \quad L$, is anomaly-free. The global $U(1)_{B-L}$ transformation for a field ψ is given by

$$\psi \;\; ! \;\; \psi' = e^{i(Q_B-Q_L)\theta_B \;\; {}_L}\psi, \tag{6.3}$$

under which the SM Lagrangian is invariant.

	$SU(3)_C$	$SU(2)_L$	$U(1)_Y$	$U(1)_{B-L}$
q_L^i	3	2	1/6	1/3
u_R^i	3	1	2/3	1/3
d_R^i	3	1	1/3	1/3
l_L^i	1	2	1/2	1
N_R^i	1	1	0	1
ψ	1	1	0	$Q_\psi = 1$
e_R^i	1	1	1	1
H	1	2	1/2	0
ϕ	1	1	0	$Q_\phi = 2$

Table 6.1: B L model particles content

6.1 Particle Content of the Gauged B L Model with a Dirac Fermion DM

The global B L symmetry can be gauged, along with 3 generations of right-handed neutrinos which makes the model free from all gauge and mixed gauge-gravitational anomalies. We can add a Dirac fermion with an arbitrary B L charge to the model, which is the DM candidate. The particle content is shown in Table 6.1. In addition to the SM particle content, three right-handed neutrinos N_R^i $(i = 1, 2, 3)$, an SM-gauge singlet Higgs ϕ with $U(1)_{B-L}$ charge $Q_\phi = 2$, and a Dirac fermion ψ with $U(1)_{B-L}$ charge Q_ψ are introduced. For simplicity, we set $Q_\psi = 1$. More precisely, Q_ψ is almost 1, but not exactly 1. This choice makes the Dirac fermion stable and hence the DM candidate of the model. The B L gauge symmetry is spontaneously broken by VEV of ϕ, which generates the B L gauge boson (Z') mass and the Majorana mass of the right-handed neutrinos. After the electroweak symmetry and the B L gauge symmetry breaking, tiny neutrino masses are generated by the seesaw mechanism.

6.2 The Related Lagrangian Terms

The part of Lagrangian related to the $U(1)_{B-L}$ symmetry and the new particles are

$$\mathcal{L} \quad \mathcal{L}_{fermion}^{B-L} + \mathcal{L}_{Higgs}^{B-L} \tag{6.4}$$

with

$$\mathcal{L}^{B-L}_{fermion} = \overline{\psi} i\gamma^{\mu}(\partial_{\mu} \quad igQ_{\psi}Z'_{\mu})\psi \quad m_{\psi}\overline{\psi}\psi + \overline{f} i\gamma^{\mu}(\partial_{\mu} \quad igQ_{f}Z'_{\mu})f, \tag{6.5}$$

$$\mathcal{L}^{B-L}_{Higgs} = (\partial_{\mu} + igQ_{\phi}Z'_{\mu})\phi^{\dagger}(\partial^{\mu} \quad igQ_{\phi}Z'^{\mu})\phi \quad \lambda\left(\phi^{\dagger}\phi \quad \frac{v_{\phi}^{2}}{2}\right)^{2}. \tag{6.6}$$

where f represents the SM fermions with $Q_f = 1/3$ for quarks and $Q_f = \quad 1$ for leptons, and Z' is the $U(1)_{B-L}$ gauge boson. The $U(1)_{B-L}$ symmetry is spontaneously broken by $\langle\phi\rangle = v_{\phi}/\sqrt{2}$. The DM physics of this model is controlled by only three parameters, the $B \quad L$ gauge coupling (g), the Z' boson mass ($m_{Z'}$) and the DM mass (m_{ψ}). In the following analysis, we set $m_{Z'} = 4000$ GeV for simplicity, and neglect all fermion masses.

6.3 $U(1)_{B-L}$ Symmetry Breaking and Z' Boson Mass Generation

With the replacement $\phi \; ! \; \langle\phi\rangle = v_{\phi}/\sqrt{2}$ in the kinetic term of ϕ,

$$\begin{aligned}\mathcal{L}^{B-L}_{Higgs} &\quad (\quad igQ_{\phi}Z'_{\mu}\phi)^{\dagger}(\quad igQ_{\phi}Z'^{\mu}\phi) \\ &! \quad g^{2}Q_{\phi}^{2}\frac{v_{\phi}^{2}}{2}Z'_{\mu}Z'^{\mu} \\ &= 2g^{2}v_{\phi}^{2}Z'_{\mu}Z'^{\mu},\end{aligned} \tag{6.7}$$

which is the mass term of Z'_{μ} boson with $m_{Z'} = 2gv_{\phi}$.

6.3.1 Seesaw Mechanism and Neutrino Mass Generation

The Yukawa sector of the SM is extended to include

$$\mathcal{L}^{B-L}_{Yukawa} = \quad \sum_{i=1}^{3}\sum_{j=1}^{3} Y_{D}^{ij}\bar{l}_{L}^{i}HN_{R}^{j} \quad \frac{1}{2}\sum_{k=1}^{3} Y_{N}^{k}\phi\overline{N}_{R}^{kc}N_{R}^{k} + h.c., \tag{6.8}$$

where Y_D^{ij} is the Dirac Yukawa coupling matrix, and Y_N^k is the Majorana Yukawa coupling matrix, which is taken to be diagonal without loss of generality. By the replacement $\phi \; ! \; \langle\phi\rangle =$

$\frac{v_\phi}{\sqrt{2}}$ and $H \;!\; \langle H \rangle = \frac{1}{\sqrt{2}} \begin{pmatrix} v_H \\ 0 \end{pmatrix}$,

$$\begin{aligned} \mathcal{L}^{B-L}_{Yukawa} \;!\; & \sum_{i=1}^{3}\sum_{j=1}^{3} Y_D^{ij} \bar{l}_L^i \tilde{\Phi} \frac{1}{\sqrt{2}} \begin{pmatrix} v_H \\ 0 \end{pmatrix} N_R^j \quad \frac{1}{2}\sum_{k=1}^{3} Y_N^k \frac{v}{\sqrt{2}} \overline{N}_R^{kc} N_R^k + h.c. \\ = \quad & \frac{1}{2}\sum_{i=1}^{3}\sum_{j=1}^{3} \begin{pmatrix} \bar{\nu}_L^i & \bar{N}_R^j \end{pmatrix} \begin{pmatrix} 0 & m_D^{ij} \\ m_D^{ijT} & M^{ij} \end{pmatrix} \begin{pmatrix} \nu_L^i \\ N_R^j \end{pmatrix} + h.c., \end{aligned} \tag{6.9}$$

with $m_D^{ij} = \frac{Y_D^{ij}}{\sqrt{2}} v_H$ and $M^{ij} = \frac{Y_N^{ij}}{\sqrt{2}} v_\phi$. Assuming that $|m_D^{ij}| \ll M^k$, we can approximately diagonalize the mass matrix as

$$\begin{pmatrix} 0 & m_D \\ m_D^T & M \end{pmatrix} \;!\; \begin{pmatrix} m_D^T M^{-1} m^D & 0 \\ 0 & M \end{pmatrix}. \tag{6.10}$$

For one generation case, two mass eigenvalues are given by

$$m_{\nu_l} \;'\; \frac{m_D^2}{M} = m_D \frac{m_D}{M} \ll m_D, \tag{6.11}$$

$$m_{\nu_h} \;'\; M, \tag{6.12}$$

with ν_l the light neutrino eigenstate and ν_h the heavy neutrino eigenstate. In this way, the seesaw mechanism naturally derives the tiny neutrino mass.

6.4 The Total Decay Width of Z' to Fermions

Through the gauge interaction,

$$\begin{aligned} \mathcal{L}^{B-L}_{fermion} & \bar{\Psi} i\gamma^\mu (\partial_\mu - igQ_\Psi Z'_\mu \Psi) + \bar{f} i\gamma^\mu (\partial_\mu - igQ_f Z'_\mu f) \\ = \; & gQ_\Psi \bar{\Psi}\gamma^\mu Z'_\mu \Psi + gQ_f \bar{f}\gamma^\mu Z'_\mu f, \end{aligned} \tag{6.13}$$

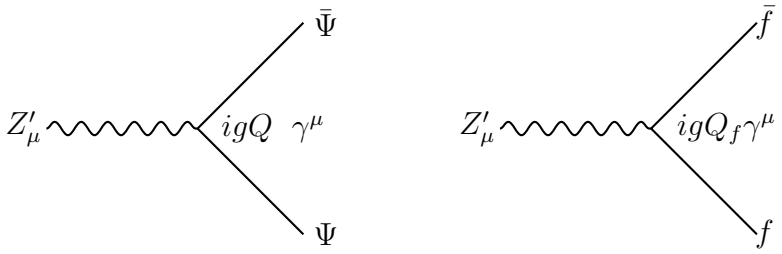

Figure 6.1: Z' boson decay processes

the Z' boson decays to the SM fermion pair and DM fermion pair if kinematically allowed (see Fig. 6.1 for the diagram).

For the $Z' \ ! \ \overline{\psi}\psi$ process, we find

$$\Gamma_{Z^0\rightarrow} \quad = \frac{g^2Q^2\, m_{Z^0}}{12\pi}\left(1+2\frac{m^2}{m^2_{Z^0}}\right)\sqrt{1 \quad 4\frac{m^2}{m^2_{Z^0}}}, \tag{6.14}$$

while for the $Z' \ ! \ \overline{f}f$ process,

$$\Gamma_{Z^0\rightarrow ff,\ m_f\sim 0} = \frac{g^2Q_f^2 m_{Z^0}}{12\pi}. \tag{6.15}$$

Here, we have neglected the SM fermion masses. The total decay width for $m_{Z^0} > 2m_\psi$ is given by

$$\Gamma_{Z^0\rightarrow SM+DM} \quad = \Gamma_{Z^0\rightarrow} \quad + \Gamma_{Z^0\rightarrow ff,\ m_f\sim 0}. \tag{6.16}$$

If $m_{Z^0} \quad 2m_\psi$,

$$\Gamma_{Z^0\rightarrow SM} \quad = \Gamma_{Z^0\rightarrow ff,\ m_f\sim 0}. \tag{6.17}$$

The Feynman diagrams for $Z' \ ! \ \overline{f}f$ are shown in Fig. 6.2, and the decay width for the $Z' \ !$

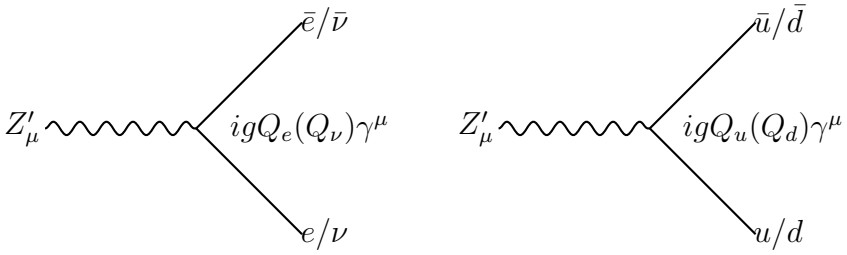

Figure 6.2: Z' decay to fermions

leptons process is given by

$$\Gamma_{Z^0\to e_R e_R/e_L e_L/\nu\nu} = \frac{1}{2}\frac{g^2(\quad 1)^2}{12\pi} m_{Z^0}. \tag{6.18}$$

For the Z' ! quarks process, we have

$$\Gamma_{Z^0\to u_L u_L/u_R u_R/d_L d_L/d_R d_R} = \frac{3}{2}\frac{g^2(\frac{1}{3})^2}{12\pi} m_{Z^0}. \tag{6.19}$$

Then, the decay width for Z' ! SM particles is given by

$$\begin{aligned}\Gamma_{Z^0\to SM} &= \frac{g^2}{12\pi} m_{Z^0}\left(\frac{3}{2}\left(\frac{1}{3}\right)^2 \quad 4 + \frac{1}{2}(\quad 1)^2 \quad 3\right) \quad 3 \\ &= \frac{g^2}{12\pi} \quad \frac{13}{2} m_{Z^0}.\end{aligned} \tag{6.20}$$

Now we calculate the annihilation-cross section of a DM pair to create SM fermion pairs. The Feynman diagram for this process is shown in Fig. 6.3. The annihilation cross-section is given by

$$\sigma \quad _{\to ff} = \frac{g^4}{12\pi} s\left(1 \quad \frac{4m^2}{s}\right)^{-\frac{1}{2}} \frac{Q_f^2 Q^2}{(s \quad m_{Z^0})^2 + m_{Z^0}^2\Gamma_{Z^0\to SM}^2}. \tag{6.21}$$

Here, if $m_{Z^0} > 2m_\psi$, $\Gamma_{Z^0\to SM}$ should be replaced by $\Gamma_{Z^0\to SM+DM}$.

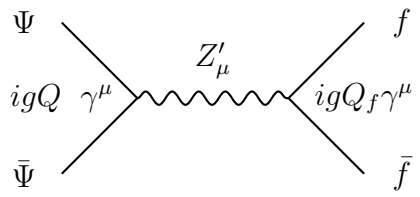

Figure 6.3: Z' portal DM annihilation

6.5 Relic Density of B L Z'-portal DM

To evaluate the relic density of the B L Z'-portal DM, We repeat what we did in the Higgs-portal DM model: we first calculate $\hbar\sigma v i$, then solve the Boltzmann equation to get $Y(x\ !\ 1)$. As previously mentioned, we set $m_{Z^0} = 4000$ GeV in our analysis, so that the DM physics is controlled by only g and m_{DM}. Imposing the observed relic density condition, $\Omega h^2 = 0.12$, we get a relation between m_{DM} and g and express g as a function of m_{DM}. This relation in (m_{DM}, g)-plane is shown in Fig. 6.4. The lines from top to bottom correspond to the results in the RS cosmology with $x_t = 50$, the BBC, and the GB cosmology with $x_t = 25000$, respectively. The observed DM relic density of $\Omega h^2 = 0.12$ is reproduced along the lines. Similar to the Higgs-portal DM, the RS and GB brane-world cosmological effects shift the result in the BBC upward and downward, respectively. The difference between the results in the Big Bang and brane-world cosmologies becomes wider as xt gets larger. For the DM mass range shown in this figure, the BBN constraint of $T_t \ \& \ 1$ MeV is satisfied.

6.6 Direct Detection Constraints

The Z'-portal DM can scatter off with a nucleon through Z' mediated process, shown in Fig. 6.5. This spin-independent cross-section is calculated as

$$\sigma_{SI} = \frac{1}{\pi} Q^2\, g^4 \frac{\mu^2{}_N}{m^4_{Z^0}}, \tag{6.22}$$

with $\mu_N = \frac{m_\Psi m_N}{m_\Psi + m_n}$ being the reduced mass for DM-nucleon system, and $m_N = 0.983$ GeV.

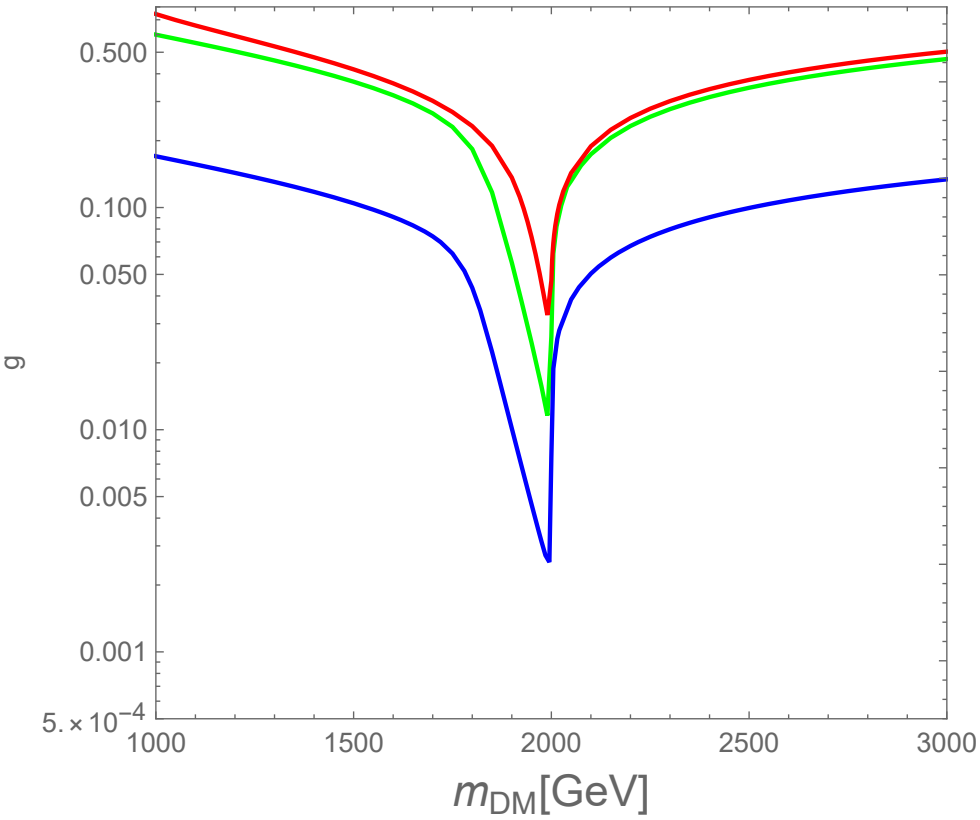

Figure 6.4: The relation between m_{DM} and g to fit the observed DM relic density. The lines from top to bottom correspond to the results in the RS cosmology with $x_t = 50$, the Big Bang cosmology, and the GB cosmology with $x_t = 25000$, respectively.

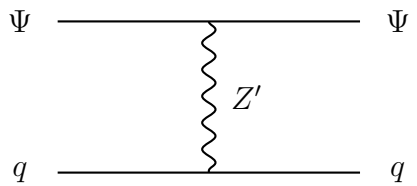

Figure 6.5: The DM scatters off with a nucleon.

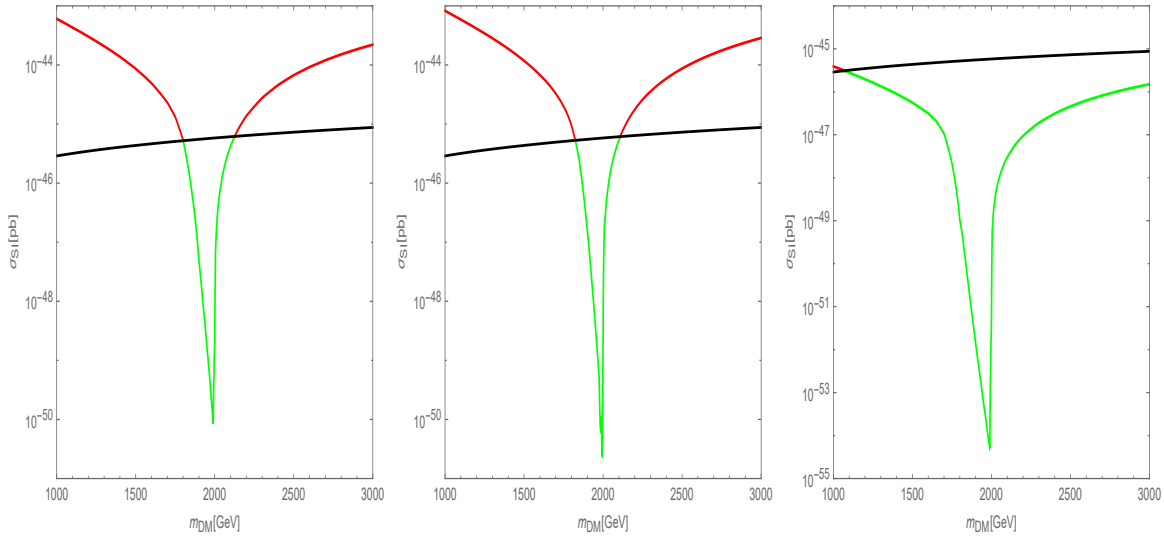

Figure 6.6: The DM-nucleon elastic scattering cross section as a function of DM mass for the standard Big Bang (left) and brane cosmologies: RS with $x_t = 50$ (middle) and GB with $x_t = 25000$ (right). The observed DM relic density of $\Omega_{DM}h^2 = 0.12$ is reproduced along the curves. In each panel, the upper bound on the cross-section from the LZ experiment is depicted by the black solid curve. The green regions are allowed.

Under the relation to reproduce the observed relic density shown in Fig. 6.4, this spin-independent elastic scattering cross section is determined as a function of m_{DM}, which is subject to the LZ constraint. We show our results in Fig. 6.6. The panels from left to right show the results in the RS brane-world cosmology with $x_t = 50$, the BBC, and the GB brane-world cosmology with $x_t = 25000$, respectively. Along the solid curves, $\Omega_D h^2 = 0.12$ is satisfied. The black solid lines depict the upper bound on the DM-nucleon elastic scattering cross-section from the LZ result, and the regions above the lines are excluded.

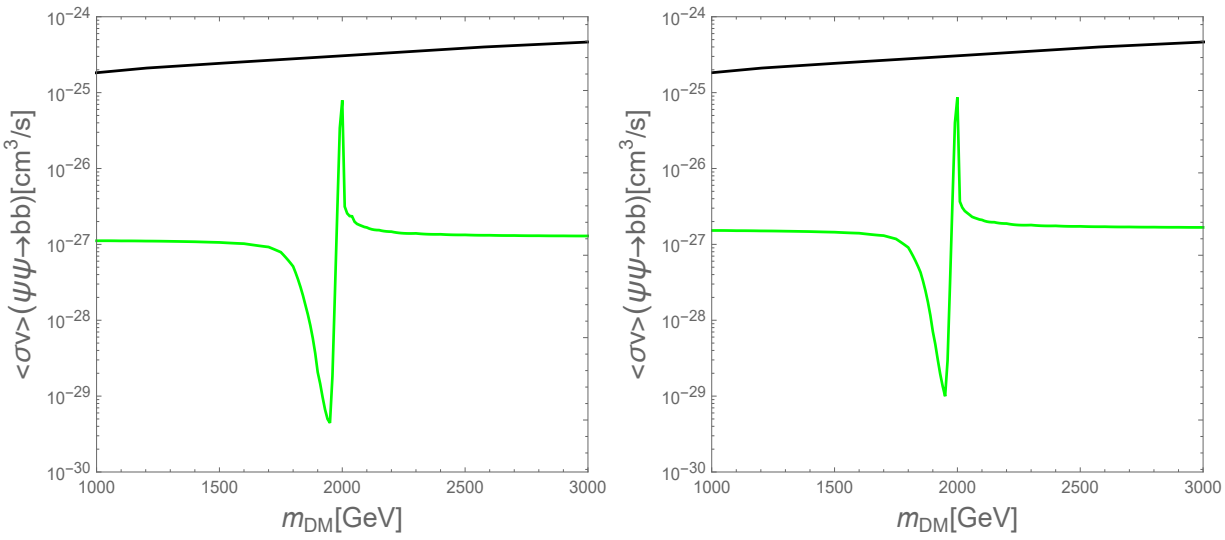

Figure 6.7: The DM pair annihilation cross-section to $b\bar{b}$ as a function of DM mass for the standard Big Bang (left) and the RS cosmology with $x_t = 50$ (right). The observed DM relic density of $\Omega_{DM}h^2 = 0.12$ is reproduced along the curves. In each panel, the upper bound on the cross-section from the Fermi-LAT experiment is depicted by the black solid curve. The whole regions shown are allowed.

6.7 Indirect Detection Constraints

We calculate the DM pair annihilation process into a bottom quark pair at present:

$$\begin{aligned} h\sigma\ -_{\to b\bar{b}}v\,ij_{v\to 0}\ '\ \sigma\ -_{\to b\bar{b}}v\,j_{v\to 0} \\ = \frac{g^4}{6\pi}\frac{Q_b^2 Q^2}{(4m^2\quad m_{Z^0}{}^2)^2 + m_{Z^0}^2\Gamma_{Z^0}^2} \\ (4m^2\ + 2m^2\ )\quad 3. \end{aligned}$$

Under the relation to reproduce the observed relic density shown in Fig. 6.4, this cross-section is determined as a function of m_{DM}, which is subject to the Fermi-LAT constraint. We show our results in Fig. 6.7. The left and right panels show the results in the BBC and the RS brane-world cosmology with $x_t = 50$, respectively. Along the solid curves, $\Omega_D h^2 = 0.12$ is satisfied. The black solid lines depict the upper bound on the annihilation cross-section from the Fermi-LAT result. We see that the indirect DM detection constraints are all satisfied. Here,

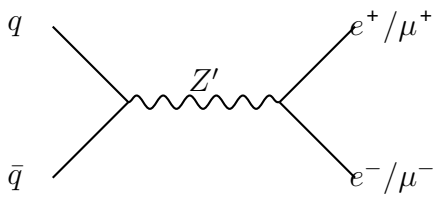

Figure 6.8: Resonant Z' production at the LHC, decaying to di-lepton final states.

we do not show the result in the GB cosmology since the whole region is clearly allowed.

6.8 Collider Constraints form the Search for Z' Resonance at the LHC

The ATLAS and CMS collaborations have been searching for a Z' boson resonance at the LHC. The most severe constraints on the $B \quad L$ Z' gauge boson is from the (null) search results with di-lepton ($e^+e^-/\mu^+\mu^-$) final states (see Fig. 6.8 for the process). The LHC Run-2 final results provide the upper bound on Z' boson production cross-section, which means the upper bound on g as a function of m_{Z^0} in our $B \quad L$ model. We adopt the results given in [42] for the upper bound on g as a function of m_{Z^0}: $g < 0.132$ for $m_{Z^0} = 4$ TeV.

6.9 Combined Results

Finally, we combine the results shown in Figs. 6.6 and 6.7. and show the allowed region in (g, m_{DM})-plane in Fig. 6.9. The three curves from top to bottom correspond to the results in the RS brane-world cosmology with $x_t = 50$, the standard BBC, and the GB brane-world cosmology with $x_t = 25000$, respectively. As we have already discussed, the observed DM density is reproduced along the curves for the corresponding cosmologies. The direct and indirect DM search results only allow the regions displayed in green and red. The horizontal line in blue is the LHC upper bound on g, and the region above this line is excluded. Combining all the constraints, we find the allowed region in green. Similar to the Higgs-portal DM model, the allowed region in the RS cosmology is more severely constrained than the Big Bang cosmology, while the GB cosmological effect significantly enlarges the allowed parameter region.

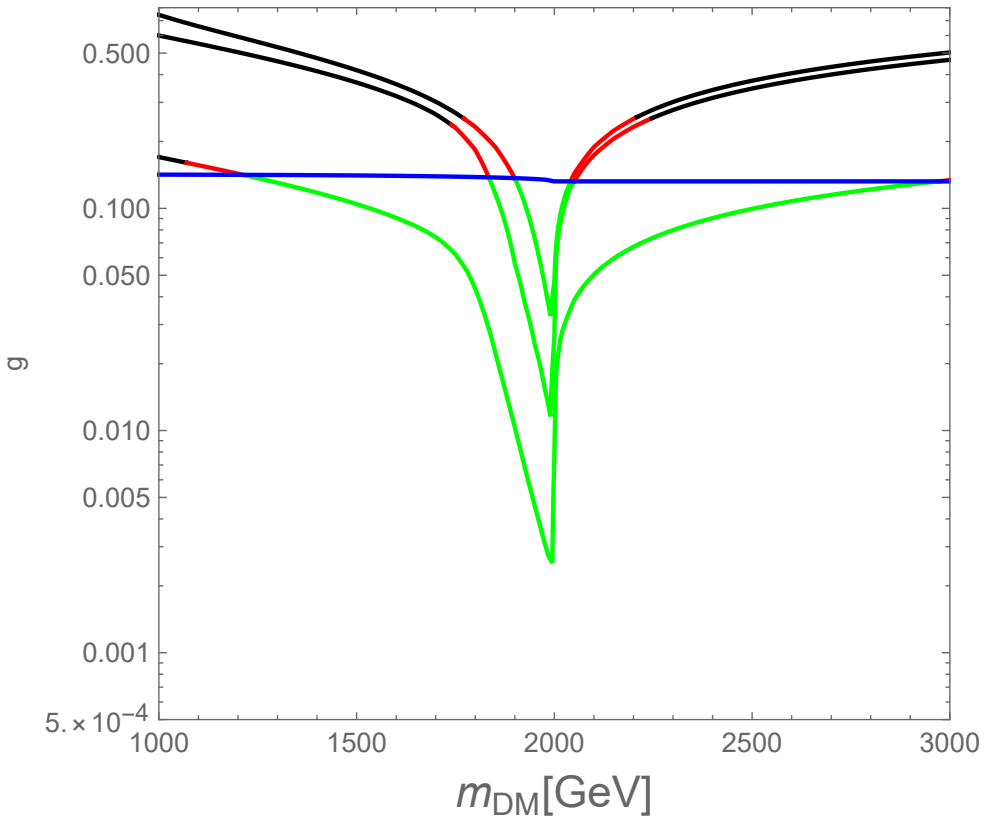

Figure 6.9: Allowed parameter regions in (m_D, g) plane. The three curves from top to bottom correspond to the results in the RS brane-world cosmology with $x_t = 50$, the standard BBC, and the GB brane-world cosmology with $x_t = 25000$, respectively. The observed DM density is reproduced along the curves for the corresponding cosmologies. The direct and indirect DM search results only allow the regions displayed in green and red. The horizontal line in blue is the LHC upper bound on g, and the region above this line is excluded. Combining all the constraints, the allowed regions are shown in green.

CHAPTER 7

CONCLUSIONS

According to various astrophysical and cosmological observations, the DM constitutes about 26.8% of the energy density of the Universe. However, no viable DM particle candidate exists within the SM. The WIMP DM scenario from physics beyond the SM remains an attractive candidate for DM. In this dissertation, we have considered two well-motivated and simple WIMP DM models, the Higgs-portal scalar DM model and the $B \quad L$ Z' portal DM model. These models have been well-studied in the standard BBC. We have investigated them in two well known 5-dimensional brane-world cosmologies, the RS and the GB cosmologies, which reproduce the standard BBC at low energies. In contrast, at high energies, the evolution of the universe was significantly altered in the brane-world cosmologies. We have examined brane-world cosmological effects on the two DM models.

We have first considered the Higgs-portal DM model. This is a simple extension of the SM to supplement the SM with a real scalar DM, which communicates with the SM particles through the Higgs boson. This DM physics is controlled by only two free parameters, the DM mass (m_D) and the mixed quartic coupling between the DM scalar and the SM Higgs doublet (λ). We have calculated the DM pair annihilation cross-sections for various final states, and with the cross-section formula, we have solved the Boltzmann equation to evaluate the DM relic density. To reproduce the observed DM relic density, we have found a relation between m_D and λ, so that λ is expressed as a function of m_D. Using this relation, we have calculated the spin-independent cross-section of the elastic scattering of the DM particle off nuclei, which is severely constrained by the direct DM search experiments. We have also calculated the DM

pair annihilation cross-section into the bottom quark pair in the present Universe. This cross-section is also constrained by the indirect DM search experiments through the observation of cosmic ray excess originating from the DM pair annihilation. In the Big Bang cosmology, it is well-known that only DM mass in the vicinity of half the Higgs boson mass is allowed in the Higgs-portal scalar DM model. We have investigated how the brane-world cosmological effects change this conclusion when the DM particle decouples from the SM thermal plasma at the decoupling temperature higher than the transition temperature. We have found that the resultant DM relic density can be significantly altered from the one in the standard BBC. The difference becomes wider as the transition temperature decreases. We have found that the allowed parameter region becomes more severely constrained and even disappears in the RS cosmology, while the GB cosmological effect significantly enlarges the allowed parameter region. Among various constraints on the WIMP DM scenario, the direct DM detection constraints are the most severe. This fact may indicate that future direct detection experiments have a high potential to discover WIMP DM soon. Once discovered, we can determine the transition temperature in the GB brane-world cosmology.

The second WIMP DM model we have considered is the $B \quad L$ Z'-portal DM model, which is a slight extension of the minimal $B \quad L$ model by introducing an SM-gauge singlet Dirac fermion with an arbitrary $B \quad L$ charge. The $B \quad L$ gauge invariance ensures the stability of this fermion. Although the minimal $B \quad L$ model is a well-motivated model beyond the SM to incorporate the neutrino masses naturally into the SM, the DM candidate is missing. We supplement the minimal $B \quad L$ model with the Dirac fermion DM. In the model, the DM particle interacts with the SM particles through the $B \quad L$ gauge boson Z', and the DM physics is controlled by only three free parameters, the DM mass (m_D), the $B \quad L$ gauge coupling (g), and the Z' boson mass ($m_{Z'}$). We have calculated the DM pair annihilation cross-section for various SM particle final states, and with the cross-section formula, we have solved the Boltzmann equation to estimate the DM relic density at present. For a fixed $m_{Z'}$, we have determined the $B \quad L$ gauge coupling as a function of the DM mass by imposing the observed

DM relic density condition. Using this relation, we have calculated the spin-independent cross-section of the elastic scattering of the DM particle off nuclei and the DM pair annihilation cross-section into the bottom quark pair in the present universe, and compared our results with the constraints from the direct and indirect DM detection experiments. In addition to these constraints, we have also considered the upper bound on the $B \quad L$ gauge coupling from the LHC results of the search for the Z' boson resonance for a fixed $m_{Z'}$. Combining all constraints, we have found that the allowed DM mass appears only in the vicinity of half the Z' boson mass. The constraints from the direct DM detection and LHC experiments are comparable and the most severe. We have investigated how much the results in the BBC can be altered by the brane-world cosmological effects. Similar to the case of the Higgs-portal model, we have found that the allowed parameter region becomes more severely constrained in the RS cosmology, while the GB cosmological effect significantly enlarges the allowed parameter region. There is an interesting prospect for future direct DM detection and LHC experiments: The Z'-portal DM may be discovered by future direct DM detection experiments with a mass m_{DM}, while the future LHC experiment may discover the Z' boson with mass $m_{Z'} \quad 2m_{DM}$.

REFERENCES

[1] K. Freese, "Status of Dark Matter in the Universe," Int. J. Mod. Phys. **1** (2017) no. 06, 325–355, arXiv:1701.01840 [astro-ph.CO].

[2] **Planck** Collaboration, N. Aghanim *et al.*, "Planck 2018 results. VI. Cosmological parameters," Astron. Astrophys. **641** (2020) A6, arXiv:1807.06209 [astro-ph.CO]. [Erratum: Astron.Astrophys. 652, C4 (2021)].

[3] J. McDonald, "Gauge singlet scalars as cold dark matter," Phys. Rev. D **50** (1994) 3637–3649, arXiv:hep-ph/0702143.

[4] R. N. Mohapatra and N. Okada, "Dark Matter Constraints on Low Mass and Weakly Coupled B-L Gauge Boson," Phys. Rev. D **102** (2020) no. 3, 035028, arXiv:1908.11325 [hep-ph].

[5] A. Alves, A. Berlin, S. Profumo, and F. S. Queiroz, "Dark Matter Complementarity and the Z′ Portal," Phys. Rev. D **92** (2015) no. 8, 083004, arXiv:1501.03490 [hep-ph].

[6] A. Alves, A. Berlin, S. Profumo, and F. S. Queiroz, "Dirac-fermionic dark matter in $U(1)_X$ models," JHEP **10** (2015) 076, arXiv:1506.06767 [hep-ph].

[7] S. Okada, Dark Matter in the Minimal U (1) X Extended Standard Model. PhD thesis, YAMAGATA UNIVERSITY, 2018.

[8] L. Randall and R. Sundrum, "An Alternative to compactification," Phys. Rev. Lett. **83** (1999) 4690–4693, arXiv:hep-th/9906064.

[9] J. E. Lidsey and N. J. Nunes, "Inflation in Gauss-Bonnet brane cosmology," Phys. Rev. D **67** (2003) 103510, arXiv:astro-ph/0303168.

[10] D. Langlois, "Brane cosmology: An Introduction," Prog. Theor. Phys. Suppl. **148** (2003) 181–212, arXiv:hep-th/0209261.

[11] P. Binetruy, C. Deffayet, and D. Langlois, "Nonconventional cosmology from a brane universe," Nucl. Phys. B **565** (2000) 269–287, arXiv:hep-th/9905012.

[12] P. Binetruy, C. Deffayet, U. Ellwanger, and D. Langlois, "Brane cosmological evolution in a bulk with cosmological constant," Phys. Lett. B **477** (2000) 285–291, arXiv:hep-th/9910219.

[13] T. Shiromizu, K.-i. Maeda, and M. Sasaki, "The Einstein equation on the 3-brane world," Phys. Rev. D **62** (2000) 024012, arXiv:gr-qc/9910076.

[14] D. Ida, "Brane world cosmology," JHEP **09** (2000) 014, arXiv:gr-qc/9912002.

[15] J. E. Kim, B. Kyae, and H. M. Lee, "Various modified solutions of the Randall-Sundrum model with the Gauss-Bonnet interaction," Nucl. Phys. B **582** (2000) 296–312, arXiv:hep-th/0004005. [Erratum: Nucl.Phys.B 591, 587–587 (2000)].

[16] S. Nojiri, S. D. Odintsov, and S. Ogushi, "Friedmann-Robertson-Walker brane cosmological equations from the five-dimensional bulk (A)dS black hole," Int. J. Mod. Phys. A **17** (2002) 4809–4870, arXiv:hep-th/0205187.

[17] J. E. Lidsey, S. Nojiri, and S. D. Odintsov, "Brane world cosmology in (anti)-de Sitter Einstein-Gauss-Bonnet-Maxwell gravity," JHEP **06** (2002) 026, arXiv:hep-th/0202198.

[18] C. Charmousis and J.-F. Dufaux, "General Gauss-Bonnet brane cosmology," Class. Quant. Grav. **19** (2002) 4671–4682, arXiv:hep-th/0202107.

[19] K.-i. Maeda and T. Torii, "Covariant gravitational equations on brane world with Gauss-Bonnet term," Phys. Rev. D **69** (2004) 024002, arXiv:hep-th/0309152.

[20] L. Randall and R. Sundrum, "A Large mass hierarchy from a small extra dimension," Phys. Rev. Lett. **83** (1999) 3370–3373, arXiv:hep-ph/9905221.

[21] N. Okada and S. Okada, "Gauss-Bonnet braneworld cosmological effect on relic density of dark matter," Phys. Rev. D **79** (2009) 103528, arXiv:0903.2384 [hep-ph].

[22] K. Ichiki, M. Yahiro, T. Kajino, M. Orito, and G. J. Mathews, "Observational constraints on dark radiation in brane cosmology," Phys. Rev. D **66** (2002) 043521, arXiv:astro-ph/0203272.

[23] W.-L. Guo and Y.-L. Wu, "The Real singlet scalar dark matter model," JHEP **10** (2010) 083, arXiv:1006.2518 [hep-ph].

[24] J. McDonald, "Gauge singlet scalars as cold dark matter," Phys. Rev. D **50** (1994) 3637–3649, arXiv:hep-ph/0702143.

[25] G. Arcadi, A. Djouadi, and M. Raidal, "Dark Matter through the Higgs portal," Phys. Rept. **842** (2020) 1–180, arXiv:1903.03616 [hep-ph].

[26] J. Edsjo and P. Gondolo, "Neutralino relic density including coannihilations," Phys. Rev. D **56** (1997) 1879–1894, arXiv:hep-ph/9704361.

[27] H. Wu and S. Zheng, "Scalar Dark Matter: Real vs Complex," JHEP **03** (2017) 142, arXiv:1610.06292 [hep-ph].

[28] **Planck** Collaboration, N. Aghanim *et al.*, "Planck 2018 results. VI. Cosmological parameters," Astron. Astrophys. **641** (2020) A6, arXiv:1807.06209 [astro-ph.CO]. [Erratum: Astron.Astrophys. 652, C4 (2021)].

[29] **CRESST** Collaboration, A. H. Abdelhameed *et al.*, "First results from the CRESST-III low-mass dark matter program," Phys. Rev. D **100** (2019) no. 10, 102002, arXiv:1904.00498 [astro-ph.CO].

[30] **XENON** Collaboration, E. Aprile *et al.*, "Search for New Physics in Electronic Recoil Data from XENONnT," Phys. Rev. Lett. **129** (2022) no. 16, 161805, arXiv:2207.11330 [hep-ex].

[31] **LZ** Collaboration, J. Aalbers *et al.*, "First Dark Matter Search Results from the LUX-ZEPLIN (LZ) Experiment," Phys. Rev. Lett. **131** (2023) no. 4, 041002, arXiv:2207.03764 [hep-ex].

[32] R. Bernabei *et al.*, "First model independent results from DAMA/LIBRA-phase2," Nucl. Phys. Atom. Energy **19** (2018) no. 4, 307–325, arXiv:1805.10486 [hep-ex].

[33] **PICO** Collaboration, C. Amole *et al.*, "Dark Matter Search Results from the PICO-60 C_3F_8 Bubble Chamber," Phys. Rev. Lett. **118** (2017) no. 25, 251301, arXiv:1702.07666 [astro-ph.CO].

[34] S. Kanemura, S. Matsumoto, T. Nabeshima, and N. Okada, "Can WIMP Dark Matter overcome the Nightmare Scenario?," Phys. Rev. D **82** (2010) 055026, arXiv:1005.5651 [hep-ph].

[35] **Fermi-LAT** Collaboration, M. Ackermann *et al.*, "Searching for Dark Matter Annihilation from Milky Way Dwarf Spheroidal Galaxies with Six Years of Fermi Large Area Telescope Data," Phys. Rev. Lett. **115** (2015) no. 23, 231301, arXiv:1503.02641 [astro-ph.HE].

[36] **IceCube, Fermi-LAT, MAGIC, AGILE, ASAS-SN, HAWC, H.E.S.S., INTEGRAL, Kanata, Kiso, Kapteyn, Liverpool Telescope, Subaru, Swift NuSTAR, VERITAS, VLA/17B-403** Collaboration, M. G. Aartsen *et al.*, "Multimessenger observations of a flaring blazar coincident with high-energy neutrino IceCube-170922A," Science **361** (2018) no. 6398, eaat1378, arXiv:1807.08816 [astro-ph.HE].

[37] **MAGIC** Collaboration, J. Aleksić *et al.*, "The major upgrade of the MAGIC telescopes, Part II: A performance study using observations of the Crab Nebula," Astropart. Phys. **72** (2016) 76–94, arXiv:1409.5594 [astro-ph.IM].

[38] **LZ** Collaboration, J. Aalbers *et al.*, "First Dark Matter Search Results from the LUX-ZEPLIN (LZ) Experiment," Phys. Rev. Lett. **131** (2023) no. 4, 041002, arXiv:2207.03764 [hep-ex].

[39] **Fermi-LAT** Collaboration, M. Ackermann *et al.*, "Searching for Dark Matter Annihilation from Milky Way Dwarf Spheroidal Galaxies with Six Years of Fermi Large Area Telescope Data," Phys. Rev. Lett. **115** (2015) no. 23, 231301, arXiv:1503.02641 [astro-ph.HE].

[40] T. Liu, N. Okada, and D. Raut, "Higgs-Portal Dark Matter in Brane-World Cosmology," arXiv:2309.16625 [hep-ph].

[41] **ATLAS** Collaboration, "Combination of searches for invisible decays of the Higgs boson using 139 fb 1 of proton-proton collision data at s=13 TeV collected with the ATLAS experiment," Phys. Lett. B **842** (2023) 137963, arXiv:2301.10731 [hep-ex].

[42] A. Das, P. S. B. Dev, and N. Okada, "Long-lived TeV-scale right-handed neutrino production at the LHC in gauged $U(1)_X$ model," Phys. Lett. B **799** (2019) 135052, arXiv:1906.04132 [hep-ph].